Navigation of an Autonomous Tractor Using Multiple Sensors

January 2006

Tofael AHAMED

Navigation of an Autonomous Tractor Using Multiple Sensors

A Dissertation Submitted to
the Graduate School of Life and Environmental Sciences,
the University of Tsukuba
in Partial Fulfillment of the Requirements
for the Degree of Doctor of Philosophy in Agricultural Science
(Doctoral Program in Biosphere Resource Science and Technology)

Tofael AHAMED

Abstract

Autonomous systems composed of multiple sensors potentially have significant importance in applications while one sensor is not suffice due to interference of signals, limitations in angular range, and malfunctions of sensors in the navigation scheme. Besides the failure of sensors, it is prerequisite to switch the sensor for approaching to the target object from absolute to relative positional sensor. The core work of this thesis concerns the coordination and switching of sensors for essential approaching using landmark for agricultural operations. To accomplish the elusive project of approaching using multiple sensors, four major experiments were conducted: the discrimination and localization of landmark using Laser Range Finder (LRF), navigation of tractor to the implement's position using landmark, approaching to the implement composed of multiple-segment, and parking of tractor inside the yard comprising switching of sensors and coordinate-based path. In addition, automatic coupling of implement with the tractor is introduced. First, the basic experiment was conducted in a 20 m x 20 m grid to discriminate and localize different shape of reflectors, which could functions as artificial landmark in the environment. Least square algorithm was used to fit line, circle, and geometrical shape of the reflector to localize the position of the reflector on the x-y coordinate. Flat reflectors had the better template fitting advantages at the longer distance, and positional error of reflectors were less than 5 cm until 15 m distance from the LRF. Second, the LRF was used to develop the positioning method for the discriminated landmark. In the experiment, a computer-controlled four-wheel drive 15.4 kW tractor was modified for autonomous control using a programmable logic controller and relay switches as its executive control regulating hydraulic actuators based on data measured by sensors. A computer, LRF, GPS, fiber-optic gyroscope, linear encoder, and two incremental rotary encoders were used in the experimental tractor. The results of the field experiments showed

that the autonomous tractor could approach to the implement's position within a final lateral error of less than 2 cm and directional error of 1˚, for the single reflector positioning method and two-reflector positioning method, both on the concrete surface and on the field covered with grasses. Third, the combination of dead reckoning and LRF was used for approaching an implement with forward and backward movements of an autonomous tractor, while the reflector is out of the angular range of the LRF. It was confirmed by experiments that the autonomous tractor could switch the sensors and track multiple-segment paths. Experimental results during two-segment navigation (Cartesian to Cartesian) showed that the final lateral error was 2 cm and directional error was 1˚ at the goal position. Finally, experiment was conducted to park the tractor inside the yard using dead reckoning sensors and LRF while GPS was not receiving the signals due to the yard. Two-segment navigation (Polar to Cartesian) for parking a tractor in a yard showed a final lateral error of 1 cm and directional error of 1˚. The experiment was conducted to hitch the implement with the autonomous tractor. The preliminary trails were successfully hitched the implement with the tractor. The results confirmed that the automatic coupling could also enable with modification of the quick coupler with more flexible errors at the top link position of the implement. Furthermore, proximity sensors can be implemented to detect the top link without any contact prior of coupling. Thus, multi-sensor system could be used for different operational aspects, while one is not suffice other could provide the positional information of the vehicle or the implement. The integration of sensors and switching with another according to field condition could ensure the reliability in navigation for autonomous vehicle.

List of Contents

Nomenclature

a, b, c, d, e, f	coefficients of polynomial function
a_M, b_M, r_M	circle parameter in least square method
A, B, C, D, E, F	statistical parameter for least square method in circle fitting
c_{sl}	speed of the light
d_t	distance of target
e_e	eccentricity of the earth ellipsoid
D	vehicle displacement along the path
D_1	wave traveling distance of FOG in time t_1, m
D_2	wave traveling distance of FOG in time t_2, m
f_1, f_2	feedback control gains in Polar coordinates
f_{mf}	modulation frequency
F	applied force, N
F_o	transmitted frequency
F_D	Doppler shift frequency, Hz
g_1, g_2	vector fields
h_x, h_y	horizontal and vertical distances between the center of the rear axle and the LRF, m
i	integer number
k_1, k_2	feedback control gains in Cartesian coordinates
l	wheel base of the tractor, m
l_1, l_2, l_3	the distances from the reflector to the LRF, m
l′, l″, l‴	lengths of the reflector plate, m
l_m	distance from the midpoint of two reflectors to the LRF, m
l_s	distance from the reflector to the LRF, m
l_t	distance from the LRF to the rear axle of the tractor, m
LMS_k	set of scan data points for LRF
m, c	straight line parameter, slop e and intercept
m_a, c_a	mass and damper of accelerometer
n	number of sampled coordinates
P	scan data point for LRF
q	position vector
r	radius or distance between the center and the center of the rear axle of the tractor, m
r_y	yaw angular velocity, deg/s
R	path of radius, m

S_1, S_2, S_3	segmented clusters for laser scan data
S_{est}	standard error of estimate, m
t_1, t_2	transit time to cover the distances of D_1 and D_2
u_i	control variables
v_{c1}	driving velocity input for car
v_{c2}	steering velocity input for car
v_{t1}	velocity control input for tractor
v_{t2}	steering angle control input for tractor
v_{w1}	linear velocity control input of the wheel
v_{w2}	angular velocity control input around the vertical axis of wheel
V	vehicle traveling speed, m/s
V_A	actual ground velocity along the path, m/s
V_D	measured Doppler velocity, m/s
$w_1(q)$	constraint vector
x_1, y_1	position of the first reflector from the LRF, m
x_2, y_2	position of the second reflector from the LRF, m
x, y	position in Cartesian coordinates, m
x', y'	intersecting points of first and second reflectors
x'', y''	intersecting points of second and third reflectors
x_{dp}	distance corresponding to the differential phase, m
x_e, y_e, z_e	position of the ECEF coordinates, m
x_f, y_f	final position of the vehicle in local coordinates, m
x_m, y_m	midpoint of the reflector, m
x_o, y_o	position of the reflector at the x-y coordinates, m
x_r, y_r	position of the vehicle at the current point in local coordinates, m
x_{sv}	state vector
y_{bs}	base vector
X_{gf}, Y_{gf}	final position of the vehicle in global coordinates, m
X_{gi}, Y_{gi}	initial position of the vehicle on the map in global coordinates, m
X_{gr}, Y_{gr}	current position of the vehicle on the map in global coordinates, m
X_o, Y_o	position of the reflector from the rear wheel of the vehicle, m
z_{fb}	fiber vector

Greek Symbol

θ_{rx}	geometrical angle between the reflector and the *x* axis, deg
α	angle of declination, deg

ω	rotational speed, deg/s
ζ	output of the linear system consisting chains of integrators
δ	steering angle, deg
λ	modulation wave length
θ	turning angle with respect to the center, deg
ϕ	angle between a tangent and the running direction of the vehicle, deg
ν	inclination angle of the reflector, deg
η	orientation angle of the reflector with respect to LRF, deg
ψ	vehicle heading or yaw angle of vehicle, deg
$\Re^n$	open subset of control variables
χ, ε, h	latitude, longitude, and altitude
η_1, η_2	orientation angles of the two reflectors with respect to LRF, deg
ψ_f	yaw angle of vehicle at the final position in local coordinates, deg
ψ_g	yaw angle of vehicle in global coordinates, deg
ψ_{gf}	yaw angle of vehicle at the final position in the global coordinates, deg
ψ_r	yaw angle of vehicle at the current position in the local coordinates, deg
Δl	distance between the object and the rear wheel center of the tractor at the target position, m
ϕ_{lt}	angle between the LRF and the center line of the tractor, deg
β_m	orientation of the trapezoidal reflector, deg
ψ_o	initial yaw angle of vehicle in global coordinate, deg
ϕ_{ps}	phase shift, deg
ϕ_{sf}	phase shift at particular frequency, deg

Subscript

o	position at origin of the coordinates
f	final condition
i	initial condition
r	rear axle of the tractor
x	component in x direction
y	component in y direction
g	global coordinates
lt	laser- tractor geometrical relation
rx	reflector-x coordinate geometrical relation

sv	state vector
bv	base vector
fb	fiber vector
sf	shift frequency
c	car
w	wheel
t	tractor
m	midpoint
M	modified least square
k	set of LRF scan data

Abbreviation

DGPS	Differential Global Positioning System
ECEF	Earth Center Earth Fixed Coordinates
FOG	Fiber Optic Gyroscope
GPS	Global Positioning System
GDS	Geomagnetic Direction Sensor
LMS	Laser Measurement System
LRF	Laser Range Finder
RTK-GPS	Real Time Kinematic Global Positioning System
TOF	Time of Flight
VRS	Virtual Reference System
WGS	World Geodetic Survey

List of Tables

List of Figures

Chapter 1

Introduction

Agricultural operation demands high accuracy and improved productivity. Position and information technologies are changing the farmer's relationship with the land all over the world. Researchers and manufacturers are emphasizing machine control systems to minimize the time required for operation and the drudgery associated with field operations. Intelligent systems are one of the promising means for minimizing human involvement in agriculture while achieving high accuracy and improved productivity. This system includes a navigation controller, actuators for driving control, positioning of the vehicle by GPS, and sensors for environmental recognition. The application of intelligent system in the industrial application is vast from the very beginning in comparison with agriculture. Application of intelligent systems in outdoor application had a difficult journey due to many factors like wheel slippage, undulation of land, natural constraints, rain, and fogs. However, efforts are being continued in the last few decades, for the development of sensors to overcome these constraints and the improvement of navigation controller for agricultural vehicles in the challenging environment.

1.1 Navigation and Sensors for Autonomous Operation

1.1.1 Concerns for Navigation

Navigation can be defined as the process of determining and controlling the position of a vehicle. In many cases, the purpose of navigation is to travel to given destination. The choice of course is a major concern for the navigator, but the path traveled doesn't affect the quality of the task except in terms of the cost of travel. In agricultural operations, the traveled course becomes a plowed or planted area; hence, the accuracy of navigation directly influences operational accuracy and efficiency. In addition, agricultural operation

requires not only movement to a specified position but also required sub-tasks accompanying the navigation. For example, in order to accomplish fertilizer application in a specified field, the autonomous vehicle must perform some sub-tasks such as movement to the field, application of fertilizer, refilling the applicator with fertilizer when the hopper is empty, and returning to the yard. Requested control and positioning in sub-tasks somewhat differ from one another. In traveling to the field for applying fertilizer, a vehicle can conduct tasks by following paths given on a map, in which case absolute positional information must be given. On the contrary, when the vehicle is approaching the fertilizer supplier, the relative position of the vehicle with respect to the supplier is requisite.

1.1.2 Sensors for Navigation

Accurate navigation systems are essential for autonomous system. The navigation system must provide measurements of absolute and relative position, velocity, and acceleration to the autonomous vehicle. The system will eventually use inertial measurements, map matching, satellite positioning, or landmarks, and the sensors provide the information such as posture, velocity, and heading of vehicle. Many uncertain influences may add noise to sensor readings, or cause of total malfunction of the sensor. To avert this effects we have use multiple sensors for the reliable navigation. Switching of sensor is required based on operational aspect, and the integrity of the sensors is essential for the reliable navigation. Reliability concerns with minimizing the failures. However, no matter how reliable the autonomous system, failure may occur. The integrity of sensors addresses the issue of ensuring the use of sensors in the appropriate operations substitute the sensors while one malfunction or does not receive signal due to interface of obstacles. For example, GPS receiver does not get any signal near the building or trees. In such case, need to replace the other sensor for absolute positioning. In other cases, the laser scanner has the limitations of angular range to recognize the landmark while the landmark is not observable, and needs

to replace another sensor to continue navigation process for reliable navigation. Again, in the approach navigation, the position system needs to change in relative positioning mode. Absolute positioning sensor does not give any orientation of the object, and while approaching the object absolute positioning sensor also needs to switch with the relative positioning sensor. Thus, the integrity and switching of sensors ensures the reliability in the navigation system of autonomous vehicle operation.

1.2 Motivations

The potential scope of implementing autonomous agricultural machines is immense in the Japanese agricultural scenario; farmers are increasingly demanding sophistication in agricultural operations. Recently, there has been a great change in the scenario of the Japanese agricultural labor force. In rural areas, the labor force has been rapidly decreasing, by the 2010s more than half the persons exclusively engaged in farming are expected to be 65 or older, and half the farmers will be women (Sasaki, 2002). In real farming operation, it requires skill ness and autonomous approaching to the implement position could reduce the drudgery in continuous watching to the back to take the tractor at the nearest position of top link with satisfactory accuracy. Our vision was to develop the essential approaching using multiple sensors in the real farming operations. For example, approach the implements, refilling of fertilizer, loading and unloading of containers, follow-up a vehicle. In these above consideration, we carried out the field experiments to approach a farm implement. Once an approach has been made with satisfactory accuracy to determine the implements position; hitching maneuvers can be performed with minimum human involvement and ensures safety during the coupling.

It is frequently observed that some of the sensors like GPS are unable to give the signal in the indoor environment, and laser sensor has the limitations of angular range to detect the landmark. In case of the path planning, the coordinate transformation, and switching of

path planning mode is required for turning and approaching. Thus, switching of sensors and coordinates transformation for reactive path planning is important in the navigation scheme. While one sensor could not give the information, then the another sensor could be used for the positional information.

1.3 Objectives

This study addresses the issues of reliable navigation using multiple sensors for essential operation in the autonomous agricultural vehicle. The goal of this thesis is to develop a navigation scheme for essential approaching and complete the navigational project from yard to field with outfitted the farm implement autonomously.

The objectives of this thesis in order to reach this goal are:

- To understand the contemporary navigation systems and vehicle motion planning to design navigation project with the absolute and relative positional information.

- To develop a robust method to discriminate the landmark from the environment, and localization of landmark in the field.

- To develop a positioning method to navigate an autonomous tractor to approach the implement's position using reflector as artificial landmark.

- To develop the navigation system composed of multiple segments with reactive path planning.

- To enable the automatic hitching of the farm implement with the autonomous tractor.

1.4 The Structure of this Thesis

The work in this thesis describes the progress of using multiple sensors for the navigation of autonomous tractor in the outdoor and indoor environment. In this chapter, discussed the nature of the problems: navigation and sensors for autonomous operation in section 1.1; the scope of this research and highlights the application of multiple sensors in approaching is discussed in the section 1.2; section 1.3 covers the objectives of this research; section 1.4

presents the structure of the thesis; and section 1.5 discusses the originality and the contribution of this thesis in the application of the autonomous operation.

The rest of the thesis is composed as follows:

- Chapter 2 is the description of the contemporary navigation systems and vehicle motion planning including nonholonomic constraints for the wheeled mobile robot.

- Chapter 3 covers the major work contributed in the autonomous agricultural vehicles. The uses of sensors to develop the guidance system for the autonomous agricultural vehicle will be reviewed in this chapter.

- Chapter 4 introduces the dynamics of the tractor including path planning for trajectory control and feedback algorithm for the sensors and steering controller.

- Chapter 5 discusses the installation of sensors in the experimental autonomous tractor and the sensors specifications will be described, which were used to navigate the tractor.

- Chapter 6 describes the discrimination and localization of the landmark for approach navigation. The method to discriminate the landmark from other object of the environment will be addressed. The template-fitting algorithm will be discussed for the different shape of reflectors that were used as artificial landmark.

- Chapter 7 describes the navigation to approach the implement using reflector as artificial landmark. The template fitting was applied to develop the positioning method for the reflector in approaching the implement. Experiments to navigate the tractor to the implements position are presented.

- Chapter 8 describes the navigation to approach composed of multiple paths. Switching of multiple sensors is presented to complete the particular operation in the field and yard.

- Chapter 9 introduces the automatic coupling of the implement with the tractor in some limited conditions using reflectors as landmark. Some of the recommendations will be reported for automatic coupling of the implement.

- Chapter 10 concludes the thesis with the summary of contributions to achieve the goal and recommendations for future research.

1.5 Contribution of this Research

This thesis is a part of wider project aimed to develop the complete autonomous system for the agricultural operations starts from the yard, and then outfitted the farm implement, enable the road navigation until field, and broadcast the fertilizer or cultivate the land; finally in the same way the autonomous tractor will return to the yard. Under this umbrella of this wide project, the main contributions of this thesis are:

1. The development of the algorithm for the robust discrimination of the land mark using reflectors from other objects in environment.

2. The development of the positioning method using a Laser Range Finder (LRF) to navigate an autonomous vehicle to the implement's position using reflectors as artificial landmark.

3. The developed positioning method with combination of dead reckoning sensor was used for navigation of tractor in forward–backward approach of tractor towards the implement. The positioning method could switch with operational mode. The approaching to the implement and parking inside the yard have been done with combination of two sensors.

4. Coordinate transformation in globally on map is discussed. Cartesian to Cartesian and polar to Cartesian coordinates based navigation is performed. Feedback control in polar coordinates has been introduced for from 90° to 360° turn.

5. In agricultural operation, one of most challenging automation is the automatic hitching of implement, which ensures the safety and drudgery of the human operators. In this compelling research, the automatic hitching of the implement with the tractor will be introduced.

Chapter 2

Contemporary Navigation Systems and Motion Planning

This chapter gives an overview of the contemporary navigation systems and motion planning related to vehicle navigation. The concept of navigation for mobile robots is a broad topic, covering a large spectrum of different technologies and applications. It draws on some very ancient techniques, as well as some of the most advanced space science and engineering. Any autonomous device must be able to determine its position to a resolution within at least its own dimensions, in order to be able to navigate and interact with its environment correctly.

The motion planning and issues related with motion planning tasks of autonomous vehicles is discussed. The control or the kinematic model obtained for such vehicles involves the concept of nonholonomy. It will be seen that the vehicles are nonlinear and under actuated in nature because of non-holonomic constraints on their generalized velocities. Some example of motion planning will be cited.

2.1 Navigation Reference

The two terms used here are, understandably, absolute and relative. In terms of position fixing, absolute implies finding ones position relative to an absolute origin; a fixed stationary point common to all position fixes across the range of navigation. Hence, in global navigation, there should be one such point on the planet, which all fixes are relative. In local navigation, the absolute origin is some fixed point in the robot's environment, and in personal navigation, the origin can be viewed as the centre of the robot itself.

A relative position fix when navigating globally, taken relative to some other reference point (environment-relative), is analogous to the absolute position fix in local navigation. Likewise, a position fix taken relative to the same robot's own position at some other point

in time (self-relative), is like the personal absolute position fix. Through knowledge of the absolute reference frame (typically using a map), absolute position fixes in one navigation domain, and can be transformed into position fixes in another. Indeed, almost all, global absolute position fixing is carried out by finding either an environment- or a self- relative position fix, and then converting this into a global position.

2.2 Sensors for Navigation

2.2.1 Satellite based GPS Sensors

The global positioning system is a satellite-based navigation system consisting of a network of 24 orbiting satellites that are orbiting in space eleven thousands miles from earth. The satellites are constantly moving, making two complete orbits around the every 24 hours. Once the GPS receiver looks on to four or more of these satellites, it can triangulate its location from the known positions of the satellites. A single receiver GPS is capable to provide a horizontal accuracy of 20 meters or better. The errors in range determination can be significantly reduced with the use of another station placed at a known fixed location. This station processes the information from all satellites available in the region and determines the errors in range information. These errors are then broadcast with a radio modem and used by the mobile receivers (rovers). This is called differential GPS (DGPS) and is shown in Fig. 2.1. It eliminates almost all the errors due to atmospheric and ionspheric delays and to a great extent the ones due to SA. Due to the latency involved in the correction the effect of SA cannot be eliminated in real time implementations. DGPS relies on the concept that the errors in the position at one location are similar to those for all locations within a given area. By applying corrections in real time, the accuracy of DGPS for instantaneous positioning is typically reduced to 1 m.
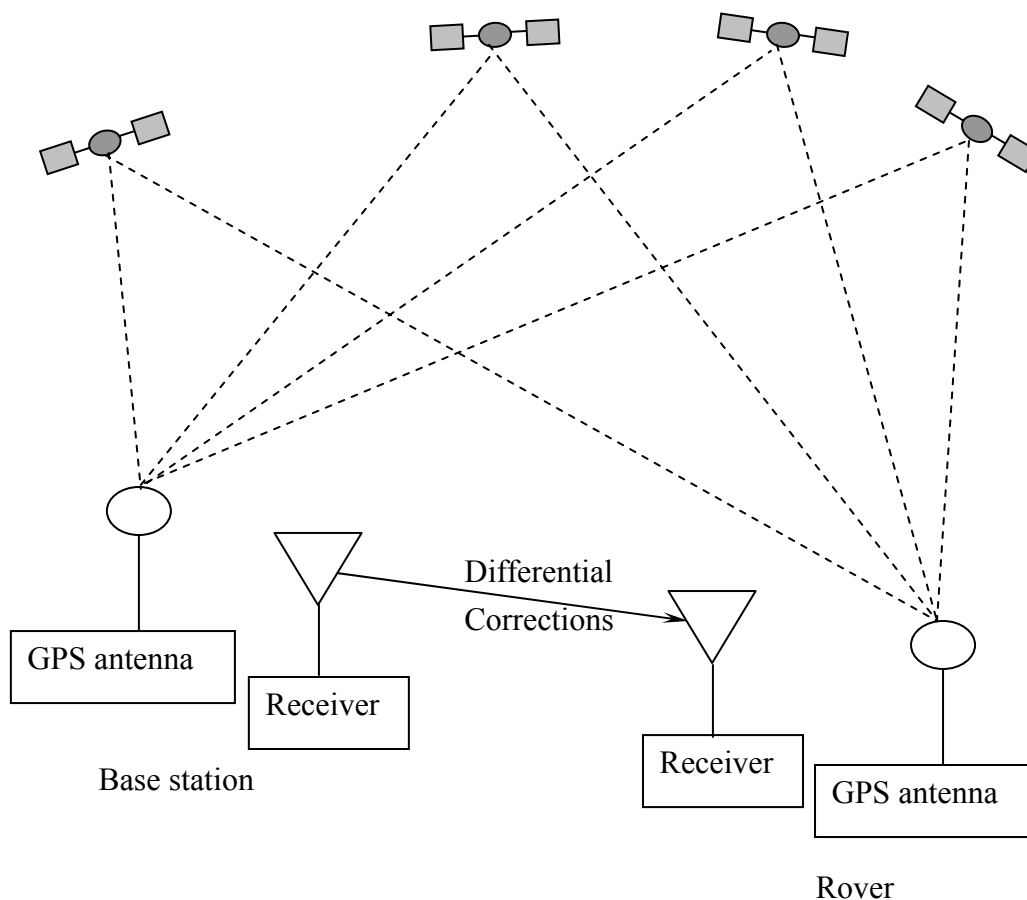
Fig. 2.1 Differential implementation of GPS

There are a few restrictions on the situations were it can be used however; the following problems can greatly reduces DGPS (or GPS) usability, periodic signal blockage due to obstruction, multi-path interference from large reflective surfaces in the vicinity, because of both of the above, it will not work indoors. For the certain precision agricultural applications such as row-crop bed preparation and planting or topographic map generation, sub meter DGPS accuracy is not enough. That's why centimeter level solutions using Real-Time-Kinematic GPS. With RTK, needs a based station on a known, surveyed point, and one or more mobile receivers within a ten kilometers range of the base station. The base station transmits corrections via the radio to the mobile receivers in the field. A typical radio link required for RTK is in the UHF, VHF, or spread spectrum radio band. Radios operate within line of sight or with a repeater. The GPS receivers used in the RTK

10

systems are generally duel-frequency receivers. Duel frequency receivers have high accuracy applications, such as precise guidance along the crop rows or collecting GPS elevation data for topography mapping.

2.2.1.1 Difference between DGPS and RTK

It can be difficult to distinguish the operation principles between RTK and DGPS. Some of the quick reviews regarding the differences between DGPS and RTK is given below:

- To initialize RTK GPS needs a minimum of five satellites. After that, RTK can operate with four satellites. On the hand, DGPS needs a minimum of three satellites, though at least four are required for sub meter accuracy.

- For RTK, a duel frequency GPS receiver is required. Single frequency receivers are sufficient for DGPS.

- RTK GPS receiver must be capable of On-the-Fly initialization (obtaining centimeter accuracy while moving). For DGPS this is not necessary.

- With RTK, it takes one minute to initialize. DGPS receiver initialize immediately.

- We can expect accuracy of a few centimeters in all three dimensions using RTK. Using DGPS we can achieve sub meter accuracy in horizontal position only.

- To obtain GPS corrections for RTK, needs own base station that is no more than ten kilometers from the field. DGPS can be used own base station, a correction service provider, or use the free radio beacon broadcasts in many regions.

The satellite-based GPS sensors are widely practiced for mobile robot localization, object and human tracking. The absolute position of the GPS receiver is determined using through simple triangulation technique based on time of flight radio signals that uniquely coded from the satellites. The main problem of GPS systems include: i)time synchronization between satellite and the receiver, ii) precise real time location of satellites, iii) difficult to measure the signal propagation time iv) electromagnetic noise and other influences like

periodic signal blockage by trees and buildings when the testing platform travels under or near trees or buildings. Another major draw back of GPS is the degradation of signals while the number of satellites from which the signals could be received is less then four or when interference occurred. This problem occurs for short distances in traveling course of the vehicle. In such a situation, a reliable sensor can be substituted for the short traveling.

2.2.2 Dead Reckoning Sensors

Dead reckoning is one of the reliable sensors for mobile robot for short traveling. It (derived from "deduced reckoning" from sailing) is a simple mathematical procedure for determining the present location of a vehicle by advancing some previous position through known course and velocity information over a given length of time. The simplest form of dead reckoning is often termed as odometry. This implies that the vehicle displacement along the path of travel is directly derived from some on-board "odometer."

2.2.2.1 Encoders

These are the most common sensors used to measure the velocity or position of a rotating device. Encoders are typically attached to a shaft to measure their rotational velocity. The frequency characteristics of these sensors are band-pass. To perform dead reckoning, wheel rate encoders and steer angle encoders are passed through the vehicle's forward kinematic equations in order to obtain a prediction of the position and orientations. The most popular type of rotary encoder for mobile robots is the incremental or absolute optical encoder.

(a) Incremental Optical Encoders

The single-channel tachometer encoder is the simplest type of incremental encoder. It is a mechanical light chopper that produces a certain number of pulses per shaft revolution. Increasing the number of pulses per revolution increases the resolution (and cost) of the encoder. These devices are especially suited as velocity feedback sensors in medium-to

high-speed control systems. However, they run into noise and stability problems at very slow velocities due to quantization errors. In addition to these instabilities, the single-channel tachometer encoder is incapable of detecting the direction of rotation and can not be used as a position sensor. Since the output signal of these encoders is incremental in nature, any resolution of angular position can only be relative to some specific reference, as opposed to absolute. For applications involving continuous 360° rotation, such a reference is provided by a third channel as a special index output that goes high once for each revolution of the shaft. Intermediate positions are then specified as a displacement from the index position.

(b) Absolute Optical Encoders

Absolute optical encoders are typically used for slower rotational applications that do not tolerate loss of positional information when there is a temporary power interruption. These encoders are best suited for slow and/or infrequent rotations such as steering angle encoding, as opposed to measuring high-speed continuous rotation required for calculating displacement along the path of travel. A potential disadvantage of absolute encoders is their parallel data output, which requires more complex interface due to the large number of electrical leads.

2.2.2.2 Potentiometers

This type of sensor is based on variable resistor whose value changes according to the position of its shaft. There are many types of potentiometers available including single and multiple turns. The position is sensed measuring the analog voltage between the moving contact and one of the extremes of the potentiometer. The resolution of these sensors depends on the quality of the device, the electronic noise level present and the number of digit used by the analog to digital converter. These devices are in general categorized as

low precision sensors are used in low most applications or two preposition incremental high-resolution sensors.

The rotational displacement sensors derive navigation data from wheel rotation. They are inherently subject to problems arising from wheel slippage, tread wear, and/or improper tire inflation. Doppler and inertial navigation techniques are sometimes employed to reduce the effects of such error sources.

2.2.2.3 Doppler Sensors

The rotational displacement sensors discussed above derive navigation data directly from wheel rotation. This means that they are inherently subject to problems arising from wheel slippage, tread wear, and/or improper tire inflation. Doppler and inertial navigation techniques are sometimes employed to reduce the effects of such error sources. The principle of operation is based on the Doppler shift in frequency observed when radiated energy reflects off a surface that is moving with respect to the emitter. Most implementations used for robots employ a single forward-looking transducer to measure ground speed in the direction of travel. An example of this is taken from the agricultural industry, where wheel slippage in soft freshly plowed fields can seriously interfere with the need to release seed at a rate proportional to vehicle advance. A typical implementation uses a microwave radar sensor, which is aimed downward (usually 45 degrees) to sense ground movement as shown in Fig. 2.2. The actual ground velocity can be expressed as:

$$V_A = \frac{V_D}{\cos\alpha} = \frac{c_{sl}F_D}{2F_o \cos\alpha} \qquad (2\text{-}1)$$

where V_A is the actual ground velocity along the path, V_D measured Doppler velocity, α is the angle of declination, c_{sl} is the speed of light, F_D is the observed Doppler shift frequency, and F_0 is the transmitted frequency.
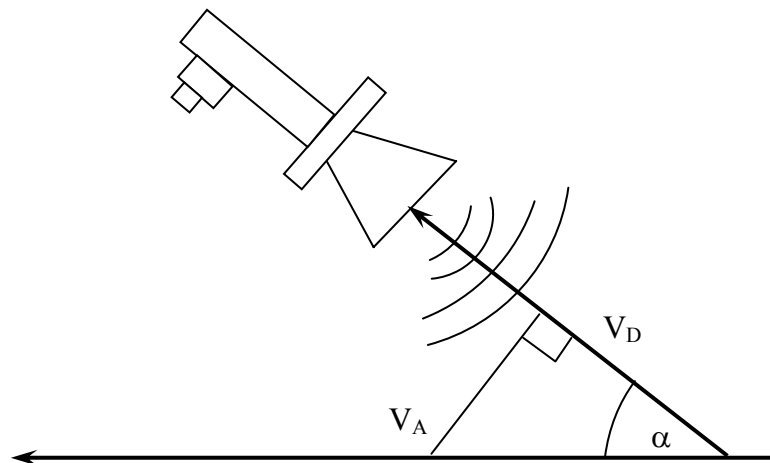
Fig. 2.2 A Doppler ground-speed sensor inclined at an angle α as shown measure the velocity component V_D of true ground speed V_A (Schultz, 1993)

2.2.3 Inertial Sensors

Inertial sensors make measurements of the internal state of the vehicle. A major advantage of inertial sensors is that they are non-radiating and non-jammable and may be packaged and sealed from the environment. This makes them potentially robust in harsh environmental conditions. Historically, Inertial Navigation Systems (INS) has been used in aerospace vehicles, military applications such as ships, submarines, missiles, and to a much lesser extent, in land vehicle applications. Only a few years ago, the application of inertial sensing was limited to high performance high cost aerospace and military applications. However, motivated by requirements for the automotive industry, whole varieties of low cost inertial systems have now become available in diverse applications involving heading and attitude determination.

The most common types of inertial sensors are accelerometers and gyroscopes. Accelerometers measure acceleration with respect to an inertial reference frame. This includes gravitational and rotational acceleration as well as linear acceleration. Gyroscopes measure the rate of rotation independent of the coordinate frame. They can

also provide 3-D position information and unlike encoders, have the potential of observing wheel slip. The most common application of inertial sensors is in the use of a heading gyro. Integration of the gyro rate information provides the orientation of the vehicle. A good quality gyro will have zero or constant bias, and small noise variance. Another application of inertial sensors is the use of accelerometers to measure the attitude of the vehicle. The inclination of a platform can be evaluated with two orthogonal accelerometers.

2.2.3.1 Accelerometers

The accelerometers measure the inertia force generated when a mass is affected by change in velocity. This force may change the tension of a string or cause a deflection of beam or may even change the vibrating frequency of a mass. The accelerometers are composed of three main elements: a mass, a suspension mechanism that positions the mass and a sensing element that returns an observation proportional to the acceleration of the mass. Some devices include an additional servo loop that generates an apposite force to improve the linearity of the sensor. A basic one-degree of freedom accelerometer is shown in Fig. 2.3.
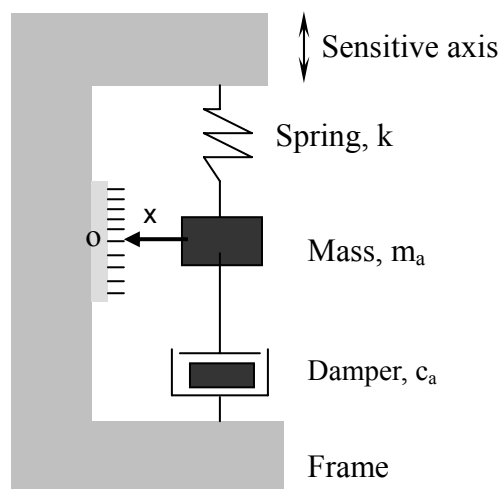
Fig. 2.3 Basic components of an open loop accelerometer

16

This accelerometer is usually referred to as an open loop since the acceleration is indicated by the displacement of the mass. The accelerometer described in this example can be modeled with a second order equation:

$$F = m_a \frac{d^2 x}{d^2 t} + c_a \frac{dx}{dt} + kx \qquad (2\text{-}2)$$

where F is the applied force to be measured. The damping can be adjusted to obtain fast responses without oscillatory behavior. Many of the actual commercial accelerometers are based on the pendulum principle. They are built with a proof mass, a spring hinge, and sensing device. These accelerometers are usually constructed with a feedback loop to constrain the movement of the mass and avoid cross coupling accelerations. One important specification of the accelerometers is the minimum acceleration that can be measured. This is of fundamental importance when working with large machines, where the acceleration expected is usually in the range of 0.1-0.3 g. Figure 2.3 shows the acceleration measured when traveling with a car at low speed. A standard accelerometer for such applications is usually capable of measuring acceleration of less than 500 μ g. The dependence of the bias with temperature and the linearity of the device are also important specifications.

2.2.3.2 Gyroscopes

These devices return an output proportional to the rotational velocity. There are large varieties of gyroscopes that are based on different principles. The price and quality of these sensors varies significantly. The following sections present some of the most common types of gyroscopes available for industrial applications.

(a) Vibratory Gyroscopes

These types of gyroscopes can be manufactured in very different forms but they are all based on a basic principle. The device can be modeled by a simple mass-spring system as shown in Fig. 2.4. The purpose of the gyroscope is to measure the angular velocity of the

particle that is supposed to be rotating about the axis OZ. With this design, it is necessary to make the particle vibrate with constant amplitude along the axis OX. This motion is usually referred to as primary motion and is controlled by an embedded circuit that maintains the oscillation at constant amplitude. Under rotation the mass will experience a coriolis inertia force that will be proportional to the applied rate of turn and
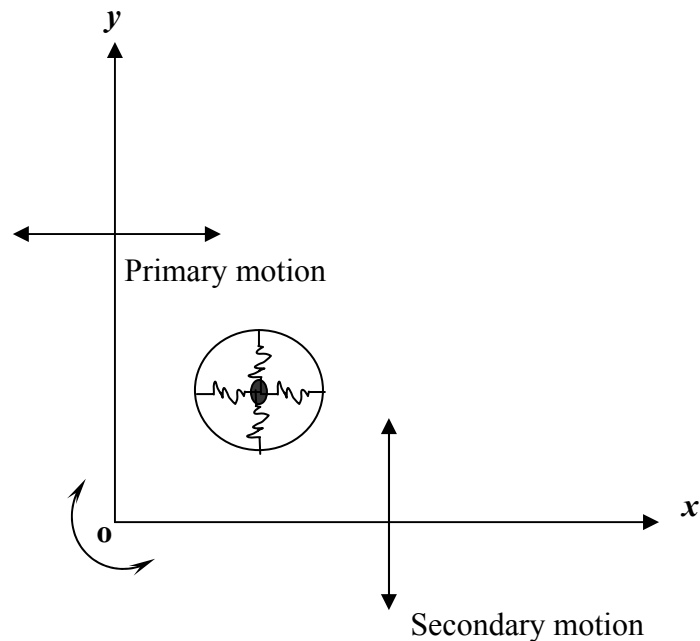
Fig. 2.4 Mass spring model for a vibratory gyroscope

will have a direction parallel to the OY axis. This motion is referred to as secondary motion and its amplitude is measured to provide information proportional to the angular rotation.

(b) Fiber Optic Gyros

The fiber optic gyros are based on the Sagnac effect discovered by Georges Sagnac in 1913. This effect can be easily explained assuming two waves of light circulating in apposite direction around a path of radius R. If the source is rotating at speed ω, the light traveling in the opposite direction will reach the source sooner than the wave traveling in the same direction, as shown in Fig. 2.5.
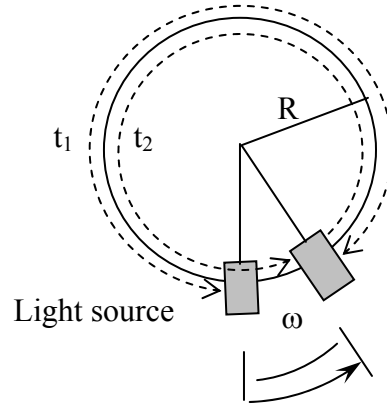
Fig. 2.5 Transmission time difference for fiber optic gyroscope

The wave traveling with the rotation will covers a distance D_1 in a transit time t_1, while the other signal covers a distance D_2 in a time t_2.

$$D_1 = 2\pi R - R\omega t_1 \tag{2-3}$$

$$D_2 = 2\pi R + R\omega t_2 \tag{2-4}$$

Making the waves travel the N times, the difference in transit time becomes:

$$\Delta t = N(t_2 - t_1) = \frac{4\pi n R^2 \omega}{c^2} \tag{2-5}$$

It is important to relate the time difference with a phase shift at particular frequency.

$$\phi_{sf} = 2\pi \Delta t f \tag{2-6}$$

For a given rotation ω the phase shift will be

$$\Delta\phi_{sf} = \frac{8\pi^2 R N}{c}\omega \tag{2-7}$$

Most low cost implements of these devices work in an open loop manner. The maximum phase shift that can be evaluated without ambiguities is 90°. There are commercial laser gyros such as the Andrew model 2030 and Autogyro, which are capable of drifts as low as 0.036° and 0.12° per minute respectively. Closed loop optical gyros are also available but they are more expensive

The accelerometers and gyroscope suffer extensive drift, and they are sensitive to uneven

grounds, because any disturbance from a perfectly horizontal position will cause the sensor to detect the gravitational acceleration. The main problems with the gyroscope are very expensive, drifts, and need to mount on a very stable platform. The dead reckoning and inertial sensors usually gives the absolute information on the map. Some times in operation needs to recognize the plant and relative distance of vehicle and plant. The relative sensors are required and it could able to give the geometrical disposition between the object and the vehicle in real time operation.

2.2.4 Vision-based Sensors

Vision-based sensors are one of the relative positioning sensors that are widely used in the mobile robots to recognize the objects. Vision-based navigation sensors mimic our human eyes and can provide huge amount of information, and one of the most powerful sensors in the mobile robots. However, visual information obtained from a vision sensor needs three processing stages: image transformation, image segmentation and analysis, and image understanding. The most common optical sensors include photometric cameras using CCD arrays. However, due to the volume of information they provide, extraction of visual features for positioning is far from straightforward. Many techniques have been suggested for localization using vision information, the main components of which are: representations of the environment, sensing models, localization algorithms.

The environment is perceived in the form of geometric information such as landmarks, object models and maps in two or three dimensions. Localization then depends on the following two inter-related considerations:

- A vision sensor (or multiple vision sensors) should capture image features or regions that match the landmarks or maps.

- Landmarks, object models and maps should provide necessary spatial information that is easy to be sensed.

However, the vision sensors are getting popular but to complete the three stages of image transformation, segmentation and understanding requires extensive time and very difficult to achieve in real time application, especially, when color image data is considered. Moreover, the angular range and resolution is not enough for outdoor application of vision sensor. For the outdoor application, long-range environmental recognition sensor could be helpful.

2.2.5 Environment Ranging Sensors

Environmental ranging sensors are one of the promising means for position in a long range in outdoor application. Most sensors used for map building involve some kind of distance measurement. Below are the three distinct approaches to measuring range:

- Sensors based on measuring the Time of Flight (TOF) of a pulse of emitted energy traveling to a reflecting object, then echoing back to a receiver.

- The phase-shift measurement (or phase-detection) ranging technique involves continuous wave transmission as opposed to the short-pulsed outputs used in TOF systems.

- Sensors based on frequency-modulated (FM) radar. This technique is somewhat related to the (amplitude-modulated) phase-shift measurement technique.

2.2.5.1 Time of Flight Range Sensors

The measured pulses used in TOF systems typically come from an ultrasonic, RF or optical energy source. The parameters required to calculate range are simply the speed of sound in air or the speed of light. The measured time of flight is representative of traveling twice the separation distance and must therefore be halved in order to give the actual target range.

The advantages of TOF systems arise from the direct nature of their straight-line active sensing. The returned signal follows essentially the same path back to a receiver located in close proximity to the transmitter. The absolute range to an observed point is directly

available as output with no complicated analysis requirements. Potential error sources for TOF systems include variation in propagation speed, detection uncertainties, timing considerations, and surface interaction.

(a) Ultrasonic TOF Systems

This is the most common technique employed on indoor mobile robots to date, which is primarily due to the ready availability of low cost systems and their ease of interface. Over the past decade, much research has been conducted investigating applicability in areas such as world modeling, collision avoidance, position estimation and motion detection. More recently, their effectiveness in exterior settings has been assessed.

(b) Phase-Shift Measurement

Here a beam of amplitude-modulated laser, RF or acoustical energy is directed towards the target. A small portion of the wave (potentially up to six orders of magnitude less in amplitude) is reflected by the target's surface back to the detector along a direct path. The returned energy is compared to a simultaneously generated reference that has been split off from the original signal, and the relative phase shift between the tow is measured as illustrated in Fig. 2.6. The relative phase-shift expressed as a function of distance to the reflecting target surface:

$$\phi_{ps} = \frac{4\pi d_t}{\lambda} \tag{2-8}$$

where, ϕ_{ps} is the phase shift, d_t is the distance to the target, and λ is the modulation wavelength. The desired distance to target d_t as a function of the measured phase shift ϕ_{ps} is therefore given by:

$$d_t = \frac{\phi_{ps}\lambda}{4\pi} = \frac{\phi_{ps}c_{sl}}{4\pi f_{mf}} \tag{2-9}$$

where c_{sl} is the speed of the light and f_{mf} is the modulation frequency.

22
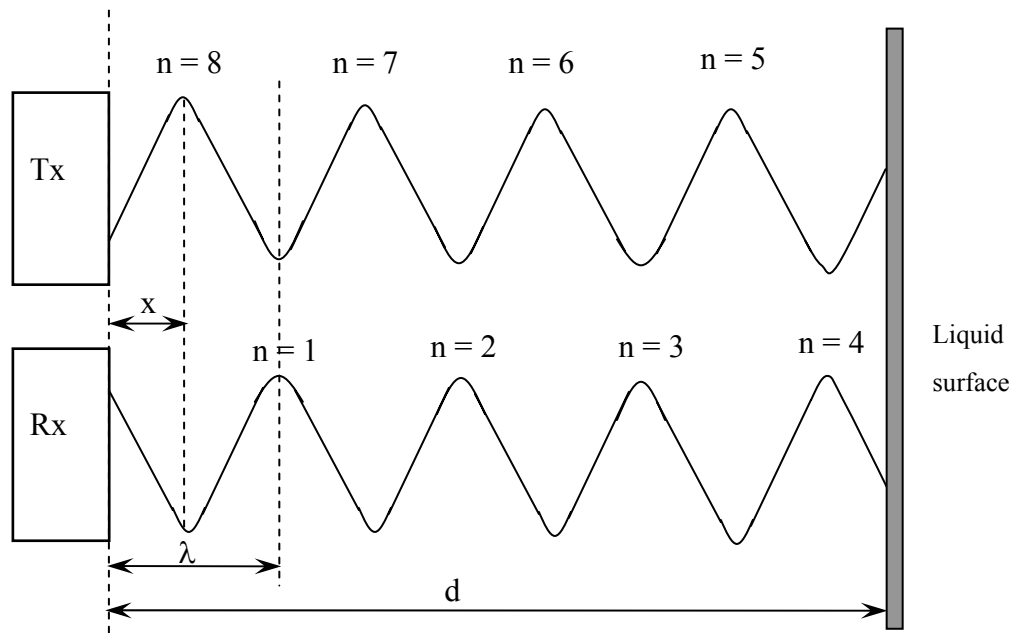
Fig. 2.6 Relation ship between outgoing and reflected waveforms, where x_{dp} is the distance

corresponding to the differential phase ϕ (Woodburry et al., 1993).

Advantages of continuous-wave systems over pulsed time of flight methods include the ability to measure the direction and velocity of a moving target in addition to its range (using the Doppler effect). Range accuracies of laser-based continuous-wave systems approach those of pulsed laser TOF methods. Only a slight advantage is gained over pulsed TOF range finding however, since the time-measurement problem is replaced by the need for sophisticated phase-measurement electronics.

2.3 Algorithms and Methods for Navigation

This section reviews the algorithm and methods for navigation, and the positioning for navigation is addressed briefly. The detail methods and algorithms are reported by Dixon and Henlich, 1997.

2.3.1 Global Positioning System

The basis of GPS is "triangulation" from satellites. To "triangulate," a GPS receiver measures distance using the travel time of radio signals. To measure travel time, GPS

needs very accurate timing, which it achieves with some tricks. Along with distance, need to know exactly where the satellites are in space. High orbits and careful monitoring are the secret. Finally, we must correct for any delays the signal experiences as it travels through the atmosphere. The GPS positioning data from geodetic coordinates to earth center earth fixed (ECEF) coordinates (Farrel and Barth, 1999) using the following equations:

$$x_e = (n_s + h)\cos(\chi)\cos(\varepsilon) \tag{2-10}$$

$$y_e = (n_s + h)\cos(\chi)\sin(\varepsilon) \tag{2-11}$$

$$z_e = \left[n_s(1 - e_e^2) + h\right]\sin(\chi) \tag{2-12}$$

where, (x_e, y_e, z_e) is the position of the ECEF coordinates;(χ,ε,h) is latitude, longitude, and altitude; e_e is the eccentricity of the earth ellipsoid with a value of 0.0818; n_s is the distance from the surface of the earth ellipsoid to the normal intersection with Z axis in the ECEF coordinates is given by

$$n_s(\chi) = \frac{a_e}{\sqrt{1 - e_e^2 \sin^2(\chi)}} \tag{2-13}$$

where a_e is the semi-major axis length of the earth with a value of 6378137.0 m.

The vehicle location is obtained in the coordinate frame of reference used by satellites. For the GPS the earth centers coordinate system using the WGS-84 datum (World Geodetic System 1984). The datum defines the ellipsoid that approximates the curvature of the earth.

2.3.2 Dead Reckoning Sensors

In the dead reckoning sensors, odometry provides good short-term accuracy, which is inexpensive and allows very high sampling rates. A common means of odometric measurement involves optical encoders that directly coupled to wheel axles. Heading information can be indirectly derived from an onboard steering angle sensors, 2) supplied

by a magnetic compass or gyro, 3) calculated from the differential odometry, incremental displacement along the path is broken upto X, Y components, either as a function of elapsed time or distance traveled. For straight-line motion periodic updates to vehicle position coordinate are given by:

$$x_{n+1} = x_n + D \sin \psi \qquad (2\text{-}14)$$

$$y_{n+1} = y_n + D \cos \psi \qquad (2\text{-}15)$$

Where, D is the vehicle displacement along the path, and ψ is the vehicle heading or yaw angle.

The fundamental idea of odometry is the integration of incremental motion information over time, which leads inevitably to the accumulation of errors. Particularly the accumulation of orientation errors will cause large position errors, which increase proportionally with the distance traveled by the robot. Nevertheless, it is widely accepted that odometry is a very important part of a robot navigation system and that navigation tasks will be simplified if odometric accuracy can be improved. Below are some of the reasons why odometry is used for mobile robots:

- Odometry data can be fused with absolute position measurements (using other techniques) to provide better and more reliable position estimation.

- Odometry can be used in between absolute position updates with landmarks. Given a required positioning accuracy, increased accuracy in odometry allows for less frequent absolute position updates. As a result, fewer landmarks are needed for a given travel distance.

- In some cases, odometry is the only navigation information available. For example, when there are insufficient landmarks in the environment or when another sensor subsystem fails to provide useable data.

Another general observation is that errors associated to wheel slippage can be reduced by limiting the vehicle's speed during turning, and by limiting accelerations.

2.3.3 Inertial Navigation

This is an alternative method for enhancing dead reckoning. The principle of operation involves continuous sensing of minute accelerations in each of the three directional axes and integrating over time to derive velocity and position. A gyroscopically stabilized sensor platform is used to maintain consistent orientation of the three accelerometers throughout this process.

Although this method is simple in concept, the specifics of implementation are rather demanding. This is mainly caused by error sources that affect the stability of the gyros used to ensure correct attitude. The resulting high manufacturing and maintenance costs of this method have usually made it impractical for mobile robot applications. One advantage of inertial navigation is its ability to provide fast, low-latency dynamic measurements. Also, INS sensors are self-contained, non-radiating and non-jammable. The main disadvantages are the angular rate data and the linear velocity rate data must be integrated once and twice (respectively), to provide orientation and linear position, respectively.

2.3.4 Landmark-based Navigation

2.3.4.1 Natural Landmarks

The main problem in natural landmark navigation is to detect and match characteristic features from sensory inputs. The sensor of choice for this task is computer vision. Most computer vision-based natural landmarks are long vertical edges, such as doors and wall junctions. When range sensors are used for natural landmark navigation, distinct signatures, such as those of a corner or an edge, or of long straight walls, are good feature candidates. Proper selection of features will also reduce the chances for ambiguity and increase positioning accuracy.

26

2.3.4.2 Artificial Landmarks

Detection is much easier with artificial landmarks, which are designed for optimal contrast. In addition, the exact size and shape of artificial landmarks are known in advance. Many artificial landmark positioning systems are based on computer vision and some examples of typical landmarks are black rectangles with white dots in the corners, a sphere with horizontal and vertical calibration circles to achieve three-dimensional localization from a single image. The accuracy achieved by the above methods depends on the accuracy with which the geometric parameters of the landmark images are extracted from the image plane, which in turn depends on the relative position and angle between the robot and the landmark. There are also varieties of landmarks used in conjunction with non-vision sensors. Most often used are bar-coded reflectors for laser scanners.

2.3.5 Line Navigation

This is another type of landmark navigation that has been widely used in industry. Line navigation can be thought of as a continuous landmark, although in most cases the sensor used in this system needs to be very close to the line, so that the range of the vehicle is limited to the immediate vicinity of the line. These techniques have been used for many years in industrial automation tasks and vehicles using them are generally called Automatic Guided Vehicles (AGVs). However, the techniques are not discussed in detail here since they do not allow the vehicle to move freely - the main feature that sets mobile robots apart from AGVs. The main implementations for line navigation are: electromagnetic guidance, reflecting tape guidance or optical tape guidance, ferrite painted guidance, which uses ferrite magnet powder, thermal marker guidance.

2.3.6 Map-Based Navigation

Map-based positioning (also known as "map matching"), is a technique in which the robot uses its sensors to create a map of its local environment. This local map is then compared

to the global map previously stored in memory. If a match is found then the robot can compute its actual position and orientation in the environment. The pre-stored map can be a CAD model of the environment, or it can be constructed from prior sensor data. In map-based positioning, there are two common representations, namely geometric and topological maps. A geometric map represents objects according to their absolute geometric relationships. It can be a grid map, or a more abstract map such as a line or polygon map. The topological approach on the other hand, is based on recording the geometric relationships between the observed features rather than their absolute position with respect to an arbitrary co-ordinate frame of reference. It uses naturally occurring structure of typical indoor environments to derive position information without modifying the environment. The main advantages of map based positioning: It uses naturally occurring structure of typical indoor environments to derive position information without modifying the environment, and can be used to generate the updated map of the environment. The disadvantages of map based positioning are accurate map and significant amount of sensing and processing power is required.

2.3.6.1 Map Building

As map building problem is very closely related to its sensing abilities, it could be defined as, "Given the robot's position and a set of measurements, what are the sensors seeing?" Error and uncertainty analyses play an important role in accurate estimation and map building. It is vital to take explicit account of the uncertainties, for example, modeling the errors by probability distributions. The representation used for the map should provide a way to incorporate newly sensed information into the map. It should also provide the necessary information for path planning and obstacle avoidance. The three main steps of sensor data processing for map building are feature extraction from raw sensor data, fusion

of data from various sensor types, and automatic generation of an abstract environment model.

2.3.6.2 Map Matching

This is one of the most challenging aspects of map-based navigation. In general, matching is achieved by first extracting features, followed by determination of the correct correspondence between image and model features. Work on map matching in the computer vision arena is often focused on the general problem of matching an image of arbitrary position and orientation relative to a model. Matching algorithms can be classified as either icon-based or feature-based. The icon-based algorithm differs from the feature-based one in that it matches very range data point to the map rather than corresponding the range data into a small set of features to be matched to the map. The feature-based estimator, in general, is faster than the iconic-based estimator and does not require a good initial heading estimate. The iconic-based estimator can use fewer points than the feature-based estimator, can handle less-than-ideal environments and is more accurate. One of the advantages in the landmark-based navigation for map matching is to use an approximate position estimation based on odometry to generate an estimated visual scene. The visual scene is then compared to the one actually seen. One problem with the feature based positioning systems is that the uncertainty about the robots position grows if there are no suitable features that can be used to update the robot`s position.

2.4 Vehicle Motion Planning

Motion planning of Robots belongs to an active research area in robotics. Motion planning can be classified under two major categories: holonomic and nonholonomic motion planning.

2.4.1 Holonomic Motion Planning

When six degree-of-freedom of a robot system can be manipulated independently, this motion planning is called a holonomic one. A person walking is an example of a holonomic system- we can instantly step to the right or left, as well as going forwards or backwards. In other words, our velocity in the plane is not restricted. An Omni-wheel is a holonomic system- it can roll forwards and sideways.

The existence of the collision free path is characterized by a connected component, which is being in the free configuration space. In this context, the steps of the motion planning are build the free configuration space, and then find a path in its connected components. If the start and goal locations of the robot lie in the same connected components of the free configuration space, motion planning problems becomes, solvable. Holonomic systems are characterized by constraint equations, which can be integrated, or integrabale. To be more problem specific an example of holonomic motion planning can be described as follows. The following form described the linear velocity constraints in the mechanical systems,

$$\varpi_i(x)x = 0 \qquad\qquad i = 1, \ldots\ldots, k \qquad\qquad (2\text{-}16)$$

Here $x \in R^n$ is configuration of the system being controlled and $\omega_i(x)$ is a row vector of R^n. These are constraints on velocities on the system. In some cases, the constraints may be explicitly integrable, giving constraints of the following form for some constant c_i.

$$h_i(x) = c_i \qquad\qquad (2\text{-}17)$$

If it is possible, motion of the system is restricted to a level of surface of h_i. Such a constraint is said to be holonomic. By choosing the coordinates for the surface, configuration space methods can be applied.

2.4.2 Non-holonomic Motion Planning

When the degrees-of-freedom of robot system are not independent like a car that cannot rotate around its axis without also changes in its position, this state is called a nonholonomic motion planning. In this case, any path in the free configuration space does

not necessarily correspond to a feasible one. Motion planning like car like robots can   be extremely computationally extensive because of the nonholonomic constraint. A nonholonomic constraint is a limitation on the allowable velocities of an object. Our robot can move in some directions (forwards and backwards), but not others (side to side). This is most easily seen in wheeled robots. Figure 2.7 shows the wheel robot movement and differential drive vehicle model is depicted in Fig. 2.8.

The robot can instantly move forward and back, but cannot move to the right or left without the wheels slipping.

To go to the right, the robot must first turn, and then drive forward
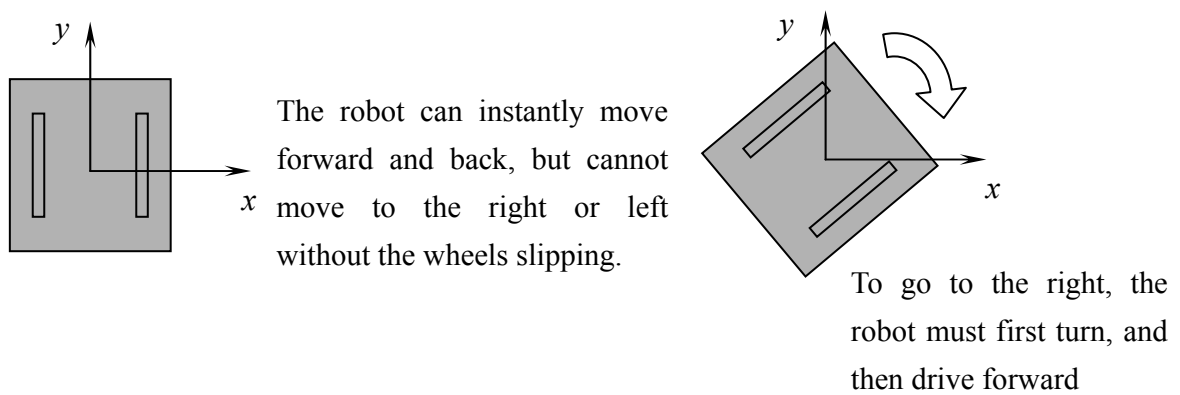
Fig. 2.7 Wheel robot movement
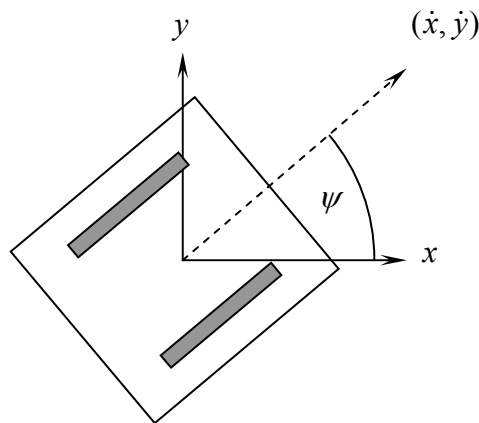
Fig. 2.8 Differential drive vehicle model

For the differential drive, the constraint equation can be expressed as follows:

$$\dot{y}\cos\theta - \dot{x}\sin\theta = 0 \tag{2-18}$$

So if $\psi = 0$, then the velocity in $y = 0$; if $\psi = 90°$, then the velocity in $x = 0$. We can also write the constraint in matrix form, with q the position vector and q dot the velocity, we can write a constraint vector $w_1(q)$ as:

$$q = \begin{bmatrix} x \\ y \\ \psi \end{bmatrix}, \quad \dot{q} = \begin{bmatrix} \dot{x} \\ \dot{y} \\ \dot{\psi} \end{bmatrix} \quad w_1(q) = [-\sin\psi \quad \cos\psi \quad 0] \quad\quad (2\text{-}19)$$

$$w1(q) \cdot \dot{q} = 0 = [-\sin\psi \quad \cos\psi \quad 0] \begin{bmatrix} \dot{x} \\ \dot{y} \\ \dot{\psi} \end{bmatrix} <=> \quad -\dot{x}\sin\psi + \dot{y}\cos\psi = 0 \quad\quad (2\text{-}20)$$

2.4.2.1 Nonholonomic Control Systems

In this section, the models of nonholonomic control systems that have been widely studied in the literature. According to the Kolmanovsky and McClamroch (1995) the model has been classified into kinematic models and dynamic models.

(a) Kinematic Models

A general form of a nonholonomic control system, expressed in kinematic form is given by the drift free non-linear control system

$$\dot{x}_{sv} = g_1(x_{sv})u_1 + \ldots\ldots\ldots\ldots\ldots\ldots + g_m(x_{sv})u_m \quad\quad (2\text{-}21)$$

where $2 \leq m < n$, $x_{sv} = (x_{sv1}, \ldots\ldots, x_{svn})$ is the state vector, defined in an open subset of $\Re^n$, u_i, $i = 1, \ldots\ldots, m$, are control variables, and g_i $i = 1$ to m, are specified vector fields. The vector fields $g_1, \ldots\ldots, g_m$ can be taught of as a basis, at each x_{sv}, for the null space of linear velocity constraints of the form $J^T(x)x = 0$, where $J(x_{sv})$ is a full rank $nx(n-m)$ matrix. A technical but essential assumption is that the rank of the controllability, Lie algebra generated by iterated Lie brackets of $g_1, \ldots g_m$ is n, where the Lie bracket of the vector fields g_1 and g_2 is a new vector field $[g_1, g_2]$, defined by $[g_1, g_2](x) = \left(\dfrac{\delta g_2}{\delta x} g_1 - \dfrac{\delta g_1}{\delta x} g_2 \right)(x)$. This assumption about the Lie algebra guarantees that there is nontrivial functions which integrate the

constraints represented by equation (2-21). In this case, (2-21) is said to be completely nonholonomic, which is equivalent to complete controllability applications from classical mechanics the controls are typically velocity variables and equation (2-16) is an expressions of kinematic constraints on the motion. In many applications holonomic control system have a special form or can be transformed into a special form, that should be recognized and exploited . A special case of non-holonomic control systems is given by:

$$\dot{z} = \sum_{i=1}^{m} \widetilde{g}_i(z,y)\dot{y}_i$$

$$\dot{y}_{bv_i} = u_i, \qquad i = 1,\dots\dots\dots,m \qquad (2\text{-}22)$$

where $m \geq 2$ and $y_{bv} = (y_{bv1}\dots\dots\dots y_{bvm})$ refereed to as base vector, $z_{fv} = (z_{fv},\dots\dots\dots z_{fv(n-m)})$ is refereed as fiber vector $u_i, i = 1$ to m are the controls and, $\widetilde{g}_i(z_{fb}, y_{sv})$, $i=1,\dots\dots,m$ are specified vector fields. We assume that equations (2-22) are completely nonholonomic in the sense of equation (2-21).

Several special classes of systems described by equation (2-22) where the vector fields have special form have been widely studied in the literature. Equation (2-22) are said to Chaplygin(kinematic) form if the fields $\widetilde{g}_1,\dots\dots,\widetilde{g}_m$ depend only on the base vector y_{bv} but not on the fiber vector z. For the case of two controls, $m=2$, several special classes of nonholonomic control systems have been studied; for example system in chained form are given by

$$\dot{z}_{fb_1} = y_{bv1}\dot{y}_{bv2},$$

$$\dot{z}_{fb2} = z_{fb_1}\dot{y}_{bv2}$$

$$\dot{z}_{fb_3} = z_{fb\,2}\dot{y}_{bv2}$$

$$\dot{z}_{fb_{n-m}} = z_{fb\,n-m-1}\dot{y}_{bv2}$$

$$\dot{y}_{bv1} = u_1$$

$$\dot{y}_{bv2} = u_2 \qquad (2\text{-}23)$$

and systems in power form, a special class of Chaplygin form, are given by

$$\dot{z}_{fb_1} = y_{bv1}\dot{y}_{bv2}$$

$$\dot{z}_{fb_2} = \frac{1}{2}(y_{bv1})^2\dot{y}_{bv2}$$

$$\dot{z}_{fvn-m} = \frac{1}{(n-m)!}(y_{bv1})^{n-m}\dot{y}_{bv2}$$

$$\dot{y}_{bv1} = u_1$$

$$\dot{y}_{bv2} = u_2 \qquad (2\text{-}24)$$

Both the chained form and power form satisfy the completely nonholonomic assumption mentioned previously.

(b) Dynamic Models

Although models that include kinematic relationships may be suitable for certain control objectives., models that include dynamic effects (generalized forces) are required for other purposes. Dynamic models of nonholonomic systems can be obtained by a natural extension of the kinematic model as:

$$\dot{x}_{sv} = g_1(x_{sv})\varsigma_1 + \dots \dots \dots + g_m(x_{sv})\varsigma_m \qquad (2\text{-}25a)$$

$$\varsigma_i^{r_i} = u_i, \qquad i = 1,\dots,m \qquad (2\text{-}25b)$$

where $2 \leq m \leq n$, $x = (x_1,\dots,x_m)$ is an n-vector and $\zeta = (\zeta_1,\dots,\zeta_m)$ is an m-vector. The subscripts $r_1,\dots,r_m$ on ζ_i denote the order of time differentiation. As previously, we assume that equation output is completely nonholonomic (Bloch et al., 1992; Campion et al., 1991). Note that ζ is the output of the linear system consisting of chains of integrators. This model is referred to as a dynamic model since in applications from classical machines, where $r_i = 1$, $i = 1$ to m, the controls are typically generalized force variables and the

governing equations include both the constraints on the motion (2-25a) and the dynamic equation of motion (2-25b).

2.4.2.2 Basic Motion Task

The motion planning tasks for nonholonomic systems as pertaining to robots are achieved through the use of the feedback controllers. The tasks are assumed here such that the systems work in an obstacle free environment and are shown in Fig. 2.9. The basic motion tasks considers for a robot as follows:

Point-to-point motion: the robot must reach a desired goal configuration starting from a given initial configuration.

Path following: the robot has to reach a desired final goal configuration starting from a given initial configuration while at the same time, robot have to follow a given geometric path in the Cartesian space. The initial configuration can be considered to be either on or off the path.

Trajectory following: the robot must reach a final configuration while following a trajectory in the Cartesian space with an associated real-time law staring from a given initial configuration either on or off the trajectory.

The tasks can be obtained using either the feed forward (open loop) or feedback (closed loop) control or a combination of the both. Since the feedback control is generally robust well in presence of disturbances, we will make use of feedback control.

Thinking of terms of controls, point-to-point task can be taught of as a regulation control problem or a posture stabilization problem for an equilibrium point in the state space. Trajectory following is the tracking problem such that the error between the reference and the desired trajectories asymptotically goes to zero.

Goal

Start

(a) Point-to-point

Start

Approach

Follow

Path

(b) Path following

Start

Approach

Follow

Trajectory

(c) Trajectory following
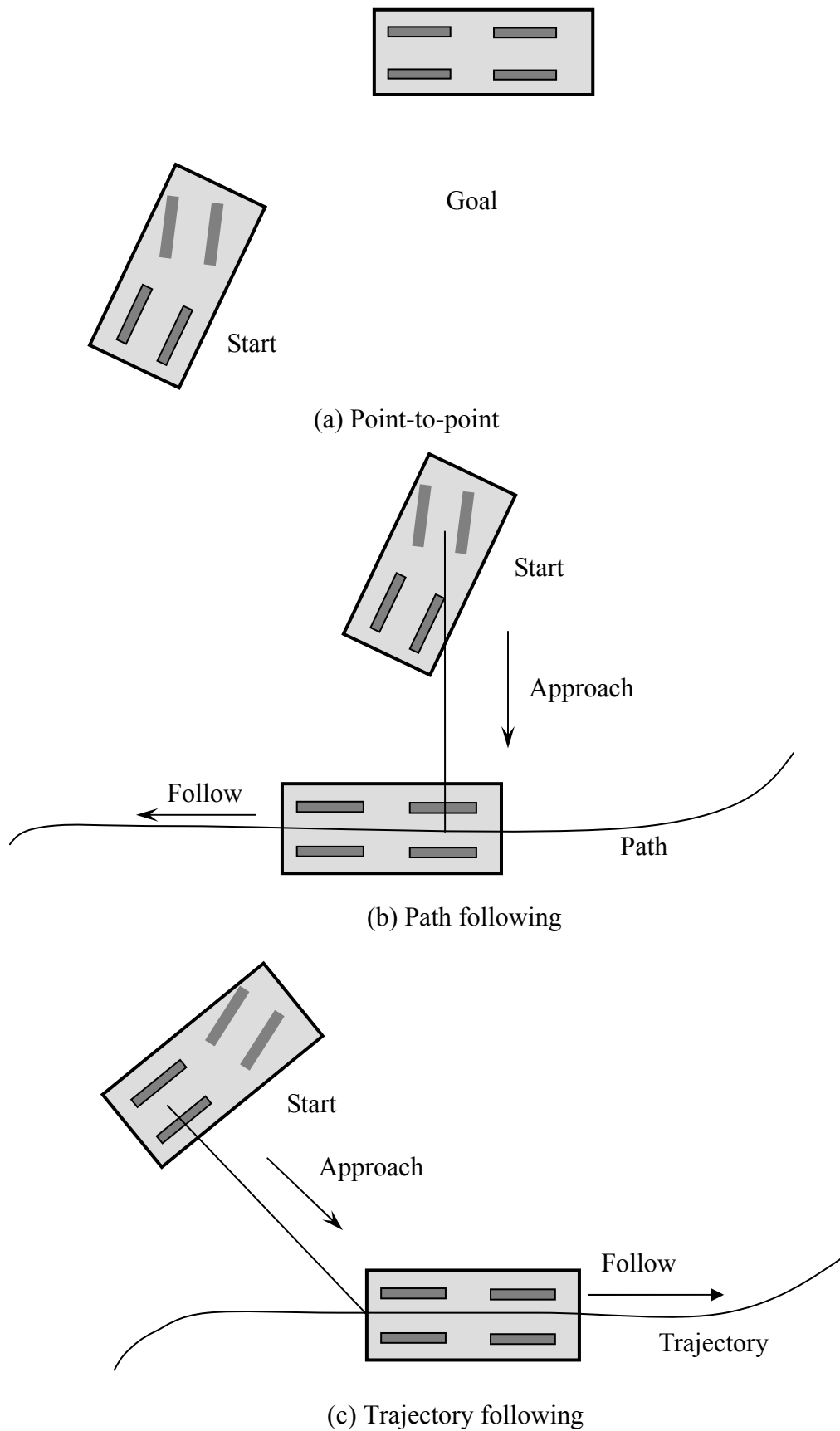
Fig. 2.9 Motion planning task for car like robot

For nonholonomic systems, tracking or path following or both is easier than stabilization, whereas usually reverse is true. This difference can be explained by drawing a comparison between the numbers of inputs and output to be controlled. In case of regulation problem *m* inputs (two in case of car like robot) are required to regulate or control "*n*" independent control variables or states (four incase of a car like robot) with *m* less than *n*. Thus, point-to-point stabilization is the most difficult of all the three. In case of path following and trajectory tracking the output to be controlled has the dimension (p) equal to that of the input (m). Thus these control problems are square and their difficulty level is similar and less than the stabilization one.

For a car like robot, in case of path following *m* is one and *p* is one while for trajectory tracking *m* is two and *p* is two, i.e we have to stabilize to zero the two dimensional error vector associated with the trajectory (Luca de et al., 1998).

2.4.3 Examples of Nonholonomic Systems

The simple example of a nonholonomic system can be a wheel that rolls on the plane surface, such as a unicycle. The constraints here arise due to the roll without slip condition. The configuration or the generalized coordinate vector is $q=(x, y, \psi)$. The coordinates x and y are the position coordinates of the wheel and ψ is the angle which the wheel makes with the x-axis. The unicycle model is shown in Fig. 2.10. The constraint in the model is the wheel cannot slip to the lateral direction. The generalized velocities are subject to the following kinematic constraint.

$$\dot{x}\sin\psi - \dot{y}\cos\psi = 0 \qquad\qquad (2\text{-}26)$$

In other words, the velocity along the plane perpendicular to the point of contact between the wheel and the ground is zero. The above equation is of the form $C(q)\dot{q} = 0$ with the constraint matrix *C(q)= [sinψ -cosψ 0]*.
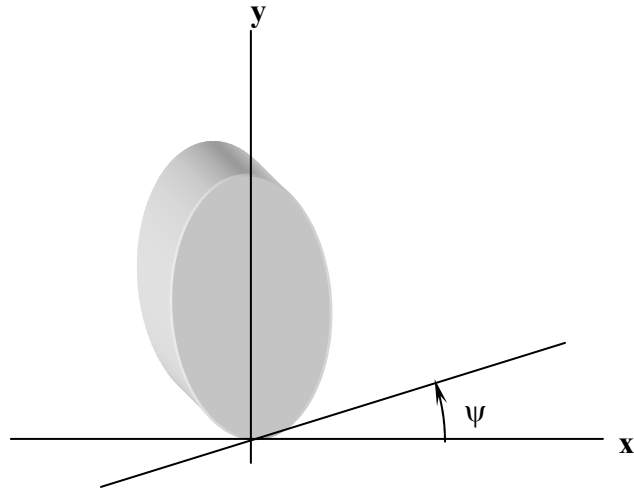
Fig. 2.10 The nonholonomic constraints on a unicycle

Expressing the feasible velocities as a linear combination of vector fields spanning the null space of the matrix $C(q)$, we get the following kinematic model.

$$\dot{q} = g_1(q)v_1 + g_2(q)v_2 \quad \text{or} \quad \begin{bmatrix} \dot{x} \\ \dot{y} \\ \dot{\psi} \end{bmatrix} = \begin{bmatrix} \cos\psi \\ \sin\psi \\ 0 \end{bmatrix} v_{w1} + \begin{bmatrix} 0 \\ 0 \\ 1 \end{bmatrix} v_{w2} \qquad (2\text{-}27)$$

where v_{w1} is the linear velocity of the wheel and v_{w2} is the angular velocity around the vertical axis. Here it was observed that the number of states $n=3$, number of control inputs $m=2$ and number of nonholnomic constraints $k=1$.

Another example is that of car like robot shown in Fig. 2.11. The robot has two wheels and each wheel is subject to one nonholonomic constraint. The constraint is the same as in the case of the unicycle.
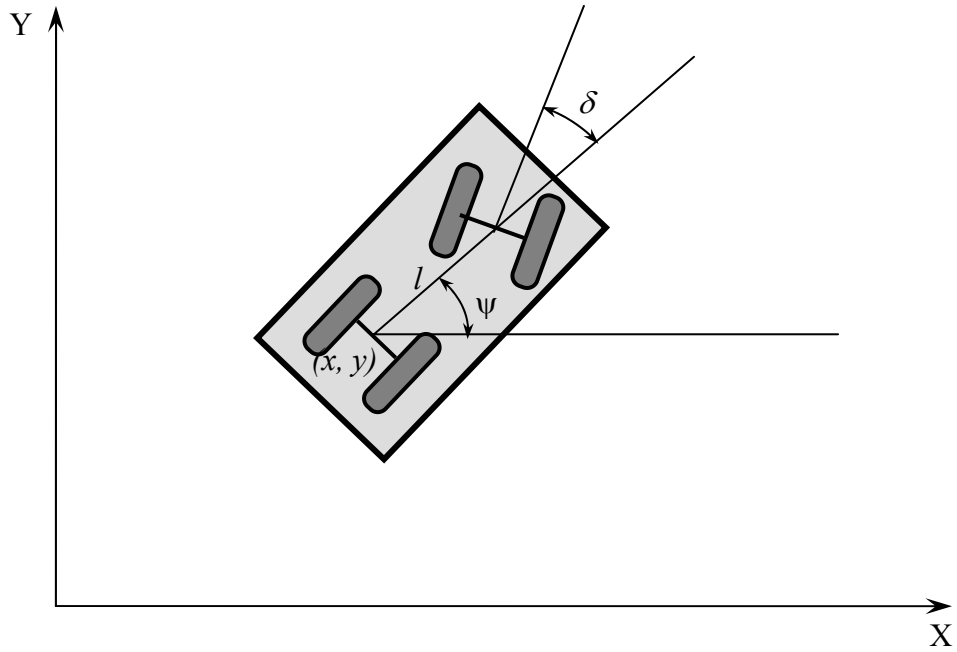
Fig. 2.11 The nonholonomic constraints on a car like robot

The generalized coordinate vector is $q = (x, y, \psi, \delta)$, with x, y and ψ same as before. The angle δ is the steering angle. The two nonholonomic constraints on the front and rear wheels respectively.

$$\dot{x}\sin(\psi + \delta) - \dot{y}\cos(\psi + \delta) - \dot{\psi}\, l\cos\delta = 0 \qquad (2\text{-}28)$$

$$\dot{x}\sin\psi - \dot{y}\cos\psi = 0 \qquad (2\text{-}29)$$

Here l is the distance between the wheels. Again, this is of the form $C(q)\dot{q} = 0$ with

$$C(q) = \begin{bmatrix} \sin(\psi + \delta) & -\cos(\psi + \delta) & -l\cos\delta & 0 \\ \sin\psi & -\cos\psi & 0 & 0 \end{bmatrix}$$

Choosing the rear wheel drive the kinematic model is obtained as:

$$\dot{q} = g_1(q)v_1 + g_2(q)v_2$$

$$\begin{bmatrix} \dot{x} \\ \dot{y} \\ \dot{\psi} \\ \dot{\delta} \end{bmatrix} = \begin{bmatrix} \cos\psi \\ \sin\psi \\ \tan\delta / l \\ 0 \end{bmatrix} v_{c1} + \begin{bmatrix} 0 \\ 0 \\ 0 \\ 1 \end{bmatrix} v_{c2} \qquad (2\text{-}30)$$

here v_{c1} is the car driving velocity input and v_{c2} is the steering velocity input. The above model is not defined at $\delta=\pi/2$, where g_1 is discontinues. Physically this corresponds to car becoming jammed because of its front wheel being normal to axis of the body. The feedback control design, controllability analysis and the motion planning is given details for all the three tasks by Luca de et al. (1998).

Chapter 3
Review of Literature

Research activities concerning automatic guidance of agricultural vehicles have led to various solutions. Indeed, the development of autonomous agricultural machines is challenging when in compared with the adoption of robotics in the industrial sectors. For example, an industrial robot is automatically controlled manipulator with three or more axes, which may be fixed or mobile in the indoor environment. Even the car like robot, the control navigation is convenient due to structured environments. However, incase of agricultural autonomous robots, many factors are needed to consider for navigation: wheel slippage on the soil, undulation of lands, semi-structured and natural environments where many uncertain factors are involved. Thus, the design of sensors for the guidance of the agricultural vehicle depends on field status. Researchers and manufacturers emphasize the selection of sensors for appropriate guidance of agricultural vehicles.

In this chapter, the following sections discuss the contributions regarding guidance system of agricultural vehicles using, GPS, dead reckoning and inertial sensors, machine vision, laser triangulation, multiple sensors data fusion. At the concluding remarks, the distinction between our unified approach and other contributions related with multiple sensor guidance of agricultural vehicle will be addressed.

A brief overview of navigation sensors, vehicle motion models, navigation planner, and steering controller is illustrated in Fig. 3.1.

3.1 GPS

Researchers at Stanford University (O′corner et al., 1995; Bell 1999, 2000) have successfully developed a four-antenna carrier phase GPS system for guiding a John Deere 7800 tractor on prescribed straight row courses with headland turns. Four single channel GPS sensors were mounted on the cab and the receiver produced attitude measurements at 10 Hz. The closed loop heading response was better than 1° and the line tracking standard deviation was better than 2.5 cm. Researchers at the University of Illinois (Stombaugh et al., 1998) utilized a 5 Hz real-time kinematic GPS for guidance of a 2WD Case 7720 tractor. In order to eliminate the lag in the system responses in tracking a 3-m step change in position showed that the lateral position error at 4.5 m/s was within 16 cm (95% confidence). At the institute of Agricultural and Environmental Engineering (IMAG-DLO)
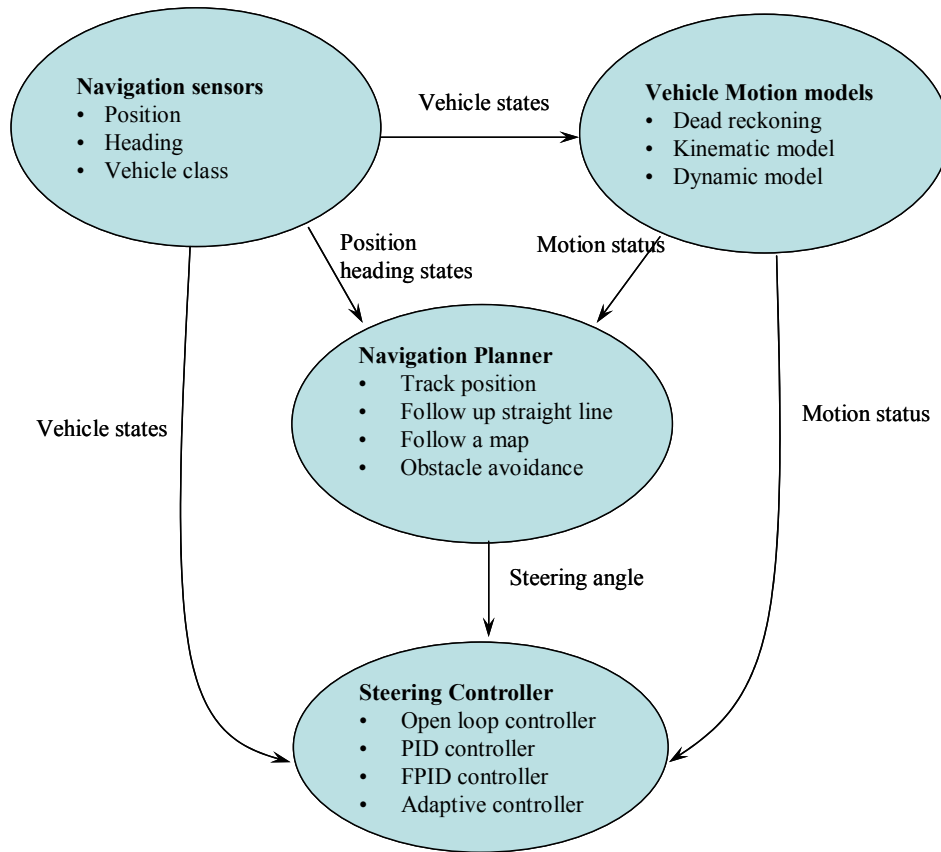
Fig. 3.1 Basic elements of agricultural vehicle autonomous system (Reid et al., 2000)

Wageningen, the Netherlands, a guidance system for agricultural machinery was developed. It used a digital map that contained all the coordinates needed to describe the intended path of the implement in the field. A sensor to measure the actual position of the implement, a comparator to calculate the position error, a controller to generate a correction signal and an actuator, mounted between the tractor and the implement of side-shift the implement into the intended path. On a curved test track, a tractor was driven with a repeatable lateral error movement of ±10 cm. The implement, mounted on the rear of the actuator with the sensor on it, was shifted to match a straight path programmed into the digital map (van Zuydam, 1999). To measure the position of the implement Real-time Kinematics DGPS (RTK-DGPS) was chosen. A set of two Trimble 7400 MSI was used. The differential position information was transmitted by the base to the rover once a second.

In the National Agricultural Research Center (NARC) an autonomous tractor guidance system was developed using DGPS and optical fiber gyroscope (Inoue et al., 1997). A Kalman filter was used in the estimation of the instantaneous position. The accuracy of DGPS was 0.15 m and the optical fiber gyroscope 0.3°. A rotary tillage performed in the

field (100 m x 160 m) at a speed of 1 m/s. The offset error was within 0.1 m, and that of the U-turn was 0.12 m. A RTK GPS and an optical fiber gyroscope were used to guide an autonomous rice transplanter by Nagasaka et al. (1998). The GPS data has a delay time of 2.8 s in communication; compensation for this delay was incorporated in real time position estimation. The GPS antenna was mounted on the top of the vehicle, resulting in an error of 0.1 m at a roll angle of 3°. The inclination error was also corrected. The steering angle was determined according in attitude angle error. The measured and estimated deviation when the rice planter traveled 100 m at 0.7 m/s. The oddest error was less than 0.06 m. This error may decrease when the steering angle is determined by the attitude angle and offset errors.

In the above contribution related with GPS sensors suffered the limitation of signal availability due to interference like trees and buildings. In addition, in the indoor localization, the GPS sensor does not work. In such situations, substitution of sensor, which is reliable for short traveling, could support the GPS for its short failure due to interferences.

3.2 Dead Reckoning and Inertial Sensors

The dead reckoning sensors are usually reliable for the short traveling where a benchmark is not available. These are the internal state sensors and mainly used to measure and monitor the internal state of the vehicle, e.g. velocity, acceleration, attitude, current, voltage, temperature, pressure, balance etc., so that static and dynamic state stability can be maintained, and potential robot failure can be avoided. The dead-reckoning using odometry is not very robust localization technique for robots (Barshan and Durrant-Whyte 1995; Goel et al. 1999) that cover long distances, and are in continuous operation over extended periods. This occurred due to errors in odometry accumulate over time, in accuracies in the kinematic model, precision limitations of encoders, unobservable factors like wheel slippages that are accounted in the kinematic model. This sensors are mostly contact state sensors. The task like perceptions, e.g weeding and spraying requires non-contact object detection. In such a case, vision-based sensor is appropriate for non-contact operations.

3.3 Machine Vision

Machine vision is a non-contact relative position and heading sensor with the image sensor mounted on the vehicle. Different types of sensor modalities can be selected to measure the guidance information. Rapidly increasing performance and decreasing prices make the

technology also attractive for automatic guidance in agriculture.

For example, most crops are cultivated in rows, so an important step toward the long-term goal of autonomous mobile robots is the development of row recognition system, which allows them to follow a row of plants accurately. Center of computer systems architecture at the Halmstad University, Sweden, developed a robust image processing algorithm to detect the position of a rows (Astrand and Baerveldt, 1999). This method is able to adapt to the size of a row plants and is not disturbed by the presence of many weeds. A grey scale camera with near infrared filter is used to detect plants. A binary image is then extracted through thresholding and some morphological operations. Based on the binary image, the detection of the rows of the plants in the image follows. Assuming a row of plants can be approximated by a line and the weeds as noise, the Hough transformation is used to find the guidelines. In the research center, Bygholm, Denmark, a project was started with the aim of first developing a method to recognize and determine the position of plant rows in a field and thereafter to develop a steering system for implements used in the cropping work (Soggard and Olsen, 1999). The system for row detection and position detection is based in a video camera system that obtains color images of the field surface. The three color channels of the image from video camera are combined in such a way that an intensity image is obtained where the living plant tissue appears bright against a nearly uniform background of soil, stones, and similar. The intensity image is segmented into a binary image and treated with specially designed filter. The process creates an image where the rows are concentrated towards their centerlines forming of long rounded blobs. In order to reduce the computational the blobs are skeletonised.

An image-processing algorithm for crop has been developed at the University of Tokyo. This algorithm has been applied to vision guided navigation of a tractor for use in row crop husbandry, including mechanical weeding and the precise application of chemicals. For accurate vision guidance, image analysis of the crop row field is essential. Discrimination of the crop area was performed using color transformation of HIS (hue, saturation and intensity) transform (Torri et. al., 1996). The least square method was used for boundary detection between crop row and soil area, and a three dimensional perspective view transformation was used for position identification. Results show that the offset error within 0.02 m at a speed of 0.25 m/s. The attitude angle error was within 0.5°; these values are sufficient for guidance in the field.

In the Hokkaido University, a crop row detector equipped with a one-dimensional image sensor was developed for use in crop husbandry machinery (Hata et. al., 1993). The principle was that the crop row image was converted, in the hardware, to a one dimensional gray scale level signal, and the software estimated the offset and the heading errors. A prototype machine was developed based on this method, and tested using field images. The execution time was about 40 ms and the accuracy was sufficient for practical use when the camera upto 0.10 m and the attitude angle not more than 6°. Finally, sensor performance tests were conducted on the following of the crop row.

Gerrish and Surbook, in 1984; Gerish and Stockman in 1985 investigated the potential of vision based tractor guidance by studying the accuracy that could be achieved through automatic guidance, and by evaluating several image processing techniques to determine their adaptability. This research led to the development of a vision guided lawn tractor (Fehr and Gerrish, 1995), and the work was implemented later on a Case 7110 tractor (Gerrish et al., 1997). In the final system, a standard RGB sensor was used to measure crop vegetation from a position to the left of the operators cab over the rear axle at a height of 2.79 m above the ground and tilted downward 15° below the horizon.

Carnegie-Mellon University, USA and NASA researchers developed a guidance system for a new Holland hay windrower using machine vision to sense the edge of the uncut crops (Ollis and Stenz, 1996). A color camera on either side of the vehicle was used to track the edge of cut/uncut vegetation. The guidance signal was based on a vertical weighting of the crop edge and a calibration of the steering valve with the horizontal displacement of the crop edge in the image.

Though vision is a vast growing technology, it has much limitation. In general, the video cameras are of CCD type and can or cannot incorporate stereo vision if we want to recognize 3D or 2D objects, respectively. These systems are very expensive and demand a high software computational burden. Moreover, in the long-range application of machine vision is not suitable due to poor dynamic range and resolutions. Eventually, these systems can be fused with other electronic instrumentation signal such as laser sensors, which have capability to recognize object in the long range.

3.4 Laser-based Sensors

The laser-based sensors have longer range and higher resolution. Many works have been contributed for the mobile robots for indoor and outdoor localization using landmarks for

laser range finder. The Arnex Navigation System (1996) used simple passive reflectors as landmark for a laser sensor. The laser-optic sensor unit was mounted on an elevated support on board the moving vehicle. A rotating narrow disc emitted an eye safe laser light, and the sensor detected the light returned from the reflectors placed along the field boundaries. The laser sensor measured the horizontal as well as the vertical angle to the passive reflector. These angles were determined in a coordinate system fixed to the vehicle. A number of sensor measurements from reflector passage were used for calculating a complete six degrees of freedom position. The output data constitute the X, Y and Z position of the vehicle in a coordinate system fixed to the earth, in addition the vehicle's three attitude angles: heading, pitch and roll were calculated. The reflectors were shaped as cylinders with an effective coverage sector of 180° to recognize the reflectors form the longer distances. The navigation reliability was dependant on the reflectors and the way these were allocated around the field. The accuracy was dependant upon the average distance between the reflectors and the vehicle, and the speed of the vehicle. For a vehicle moving of a speed of 2 m/s, and having an average distance to the reflectors of 50 m. the absolute position error was 5 cm in each of the X, Y, Z directions (Holmqvist, 1993). The drawback of the system was placement of the reflector. Once, the position of reflector changed then the errors occurred in positioning of the vehicle.

In the University of Tsukuba, (Takigawa et al., 2002) developed a trajectory control guidance system to approach a target object. In application of this trajectory control, a laser-based triangulation method with reflector was used to reach to the target object (Sutiarso et. al., 2002). After calibration, the accuracy of distance measurement was around 10 cm. Results of the field experiment showed that the trajectory-tracking algorithm could guide the vehicle with satisfactory accuracy for refilling. The main factor contributing to navigation error was the limitation of the steering angle of front wheels.

BRAIN's foundation reported some of the research related with AP-L1 station with automatic tracking of objects was conducted by Yukumoto et. al. in 1995, and 1997. Performance in automatic tracking, position measurement, and data communication was adequate at a distance of 500 m. The trace of autonomous operation using XNAV at a speed of 0.45 m/s. The tillage work was finished in 2 h and 15 min.

In general, there are two problems in the laser–based system, which affect the accuracy of the position estimation. The first system is that the navigation system cannot work well

when some artificial landmarks change their position. If the natural landmarks are used in the navigation process, updating map is necessary in order to registrar them into map building operation. The second problem is that laser measurements are noisy when the vehicle travels on uneven grounds. Hence, the accuracy of vehicle positions degrades gradually and sometime unacceptable during a continuous operation.

3.5 Multiple Autonomous Mobile Robots

There is continuous operation in a large field, for example, cooperation of small combines, or of a large harvester with a transport vehicle in the forage harvesting as shown in Fig. 3.2. The cooperation of multiple small machines is useful. The operator controls one vehicle and the other vehicles follow the main vehicle using ultrasonic or other sensors. A control system that steers an autonomous vehicle following a human operated tractor was developed by Sutiarso et al. (2002). Experiments regarding the application of the laser sensor confirmed that an experimental autonomous tractor could follow a leading human operated tractor without collision.

Fig. 3.2 Multiple machine cooperation system for agricultural operation

In the Kyoto University, an automatic follow up vehicle using two small head feed combines is under development (Iida et. al., 1998). A human operator in the front vehicle controls it, and a computer automatically controls the follow up vehicle. The relative position between the two vehicles is measured using ultrasonic and infrared sensors. Two ultrasonic transmitters (40 kHz) and an infrared receiver are mounted on the leading vehicle, and two ultrasonic receivers and an infrared transmitter on the following vehicle. In the above contributions regarding different sensors, which provide different kind of

information for vehicle navigation, are not reliable all the time. Whatever, the reliable sensor is, failure occurs. Even one sensor cannot be used for all purposes. Thus, fusing in information from different sensors may ensure a complete picture of the real world. More specifically, multi-sensor data fusion aims to overcome the limitations of the individual sensors and relative estimates of the world state based on multi-sensory information.

3.6 Sensor Data Fusion

The principle of sensor fusion is to combine information form various sensing sources since no individual sensor suffice for all purposes of vehicle automation. The appropriate sensor will depend on the field status at the time of operation. The availability of data of multiple sensors provides opportunities to better integrate the data to provide a result superior to the individual sensor.

Noguchi et al. (1998) developed a guidance system by the sensor fusion integration with machine vision, RTK-GPS and GDS sensors. An Extended Kalman Filter (EKF) and statistical method based on a two-dimensional probability density function were adopted as fusion integration methodology. To achieve the navigation planner based on sensor fusion integration, four types of control strategies were built by changing combination of the three kinds of sensors. The developed navigation planner selected from a priority scheme of the control strategies using knowledge based-approach. The average lateral error of the vehicle guidance based on the fusion of the RTK-GPS and GDS was 8.4 cm. The developed sensor fusion methodology with the EKF performed with satisfactory precision, given that the lateral error was less than the precision of the RTK-GPS.

Benson et al. (1998) used GDS and GPS together for vehicle guidance based on dead reckoning as simple path planner. The system was tested at slow speeds (1.12 m/s) and had an average error of less than 1 cm, which compared favorably to GPS-based guidance. When implementing a 3-m step change in response the sensor fusion system had a maximum overshoot of 12%. Under GPS mode, the system experienced a 50% overshoot.

In case of multi-sensor data fusion, the drawback is the computational burden from each sensor. Sometimes bad data affects the good data in the navigation process. The fusing was done with one major sensor, which gives the absolute positional information on the map. If the major sensor fails then sensor data fusion accumulates errors.

The sensors used for the major agricultural guidance systems in different universities and research institutes are summarized and given in Table 3.1.

3.7 Concluding Remarks

Most of the contributions of autonomous research were based on a major sensor, either GPS or Machine Vision. GDS or FOG was used for heading of the vehicle. These sensors have drift, the data fusion using extended Kalman filter improve the performance. Nevertheless, the major sensor, RTK-GPS lost the signal due to interference, like building or trees; the positioning tends to accumulate errors. Even in the indoor to the outdoor navigation, for example, yard to field or finally field to yard, GPS-based positioning fails due to interference of walls and roof. Again, the placement of the implement may vary time to time. It is difficult to predict in advance the position of the implement. GPS-based position will not give the practical information to localize the implement, and even it does not give the orientation of the farm implement. In such a case, laser-based positioning method could guide the vehicle to approach the implements in real time operation. In addition, LRF could detect the implement on the map and GPS could guide the vehicle to the implement position. After completion of fieldwork, the autonomous tractor need to park inside the yard, while vehicle near the wall of the yard, GPS looses signals. In such a case, dead reckoning sensors could provide the position of the vehicle in shorter distances. Thus, the switching of sensors, like GPS to dead reckoning, dead reckoning to LRF, LRF to GPS, or even vice versa could ensure the reliability of navigation in different operational aspects of agricultural autonomous operation. We believe this unified approach of switching of sensors with field condition differentiates our research from other contributions in the compelling research of autonomous vehicle. Multiple-sensory information could be used for path planning by switching sensors according to the field conditions. The reactive path planning will be done using trajectories to accomplish the assigned tasks.

Table 3.1 Major agricultural guidance reports based on the uses of sensors

Sensors	Institute	Machine	Comments	Contributors
Machine Vision	Michigan State University (1984-1986)	Lawn tractor and Case 7110 tractor	6 cm accuracy at 4.9 km/h, 12 cm accuracy at 12.8 km/h	Fehr and Gerrish, 1995; Gerrish et al., 1997
	Texas A&M (1984-92)	Ford Tractor	Vision guidance crop row detection	Reid, J.F., 1987; Reid and Searcy, 1986
	Carnegie Melon University (1994-1998)	New Holland Speed rower	Autonomously harvested over 40 ha	Ollis and Stenz, 1996 Oillis and Stenz, 1996
	University of Tokyo (1998 to present)	Tractor	Lateral offset error 0.02 m with 0.25 m/s	Torii et al., 1998
	Hokkaido University (1992- present)	Tractor	Lateral offset error 0.04 m with 0.26 m/s	Hata et al., 1993
	University of Illinois (1996- present)	Case 8920 MFCD	Vision guidance at 16 km/h on row crops.	Will et al., 1998; Pinto and Reid, 1998,
	University of Giessen, Germany	Tractor	Losses of plants didn't exceed 1% at 12 km/h	Keicher and Seufert, 2000
Laser Ranging	Arnex NS, AB Sweden	Tractor	Position error is about 5 cm in each of the X,Y,Z with 2.5 m/s	Holmqvist, 1993
	University of Tsukuba (2000 to present)	Tractor	Position measurement error was 10 cm with 0.4 m/s	Takigawa et al., 2000
	Kubota	Rice planter	Offset error was 0.05 m with 0.7 m/s	Yoshida, 1996

Image processor and Laser sensor	BRAIN 1997 to present	Tractor	Offset error 0.05 m with 0.4 m/s	Yokomoto et al., 1997
Ultrasonic sensor	University of Kyoto 1998 to present	Combine	Traveling speed 0.55 m/s	Iida et al., 1998
GPS	Stanford University	John Deere 7800 Tractor	1° accuracy in heading, line tracking accuracy with 2.5 cm deviation	O′ corner et al., 1995, 1996; Bell, 1999
	University of Illinois (1996 to present)	2WD Case 7720 Tractor	Lateral position error at 4.5 m/s was within 16 cm	Stombaugh et al., 1998
DGPS and FOG	MAFF (NARC) 1997 to present	Tractor	Errors 0.1 m with 1.0 m/s	Inoue et al., 1997
RTKGPS and FOG	MAFF(NARC) 1997 to present	Rice planter	Errors 0.1 m with 1.0 m/s	Nagasaka et. al, 1998
Angular velocity, acceleration sensor	Mitsubishi	Rice planter	Errors 0.1 m with 0.7 m/s	Nonami et al., 1993
Sensors data fusion	University of Illinois and Hokkaido University	Tractor	Errors 8.4 cm with 8.2 km/h	Noguchi et al., 1998
	University of Illinois	John Deere 4x2 Gator	Maximum offset from trajectory was 0.2 m with 1.3-3.6 m/s	Guo and Zhang, 2005
	Silsoe Research Institute	Tractor	Vision was used for identification of crop and weeds, and vehicle navigation a sensors fusion was done using EKF	Hague et al., 2000

Chapter 4

Path Planning for Navigation of Autonomous Tractor

Path planning problems generally involve computing a continuous sequence (a path) of configurations (generalized coordinates) between an initial configuration (start) and a final configuration (goal) while respecting certain constraints. In the previous chapter, the positioning related with sensors has been discussed elaborately. In this chapter, the posture model of the front wheel steering vehicle, path planning and feed back control will be addressed. Some of the previous research (Takigawa et al., 2002; Sutiarso et al., 2000) contributed for path planning will be reported along with new developed the extended method for feedback control, which prerequisite for multiple segment paths planning in polar coordinate aspect to attend 90° to 360° turn.

4.1 Posture of Vehicle

Figure 4.1 shows a schematic of the front wheel steering vehicle model. The center of the gravity of the vehicle is located at the center of the rear axle to simplify the model.
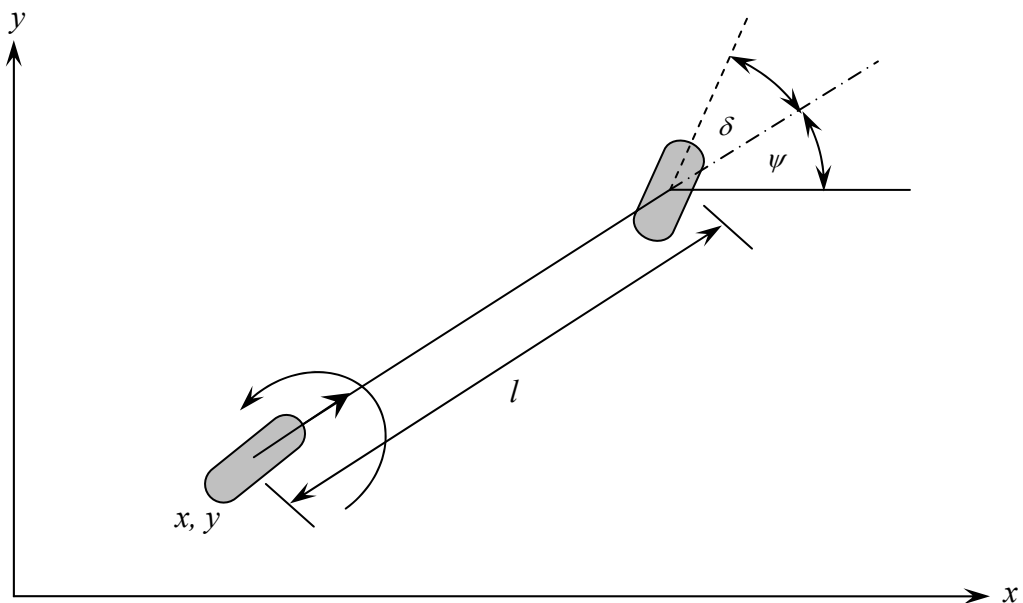
Fig. 4.1 Front wheel steering vehicle model

The two wheels centered model was employed to describe the vehicles movement. In general, the autonomous vehicle control can be described as a relationship matrix between two vehicle control inputs, i.e. velocity (v_{t1}) and steering angle (v_{t2}), and three parameters of vehicle posture (x, y, ψ).

$$\frac{d}{dt}\begin{pmatrix} x \\ y \\ \psi \end{pmatrix} = \begin{pmatrix} \cos\psi \\ \sin\psi \\ 0 \end{pmatrix} v_{t1} + \begin{pmatrix} 0 \\ 0 \\ 1 \end{pmatrix} v_{t2} \qquad (4\text{-}1)$$

$$\dot{\psi} = r_y = \tan\delta/l$$

$$\dot{x}_r = V\cos\psi, \ \dot{y}_r = V\sin\psi$$

where r_y, V, and l denote the yaw angular velocity, the vehicle traveling speed, and the wheel base, respectively.

4.2 Trajectory Control

Two major types of path planning are involved in the trajectory control of wheeled vehicle: Cartesian and Polar paths as illustrated in Fig. 4.2.

(a) Cartesian- based trajectory   (b) polar-based trajectory
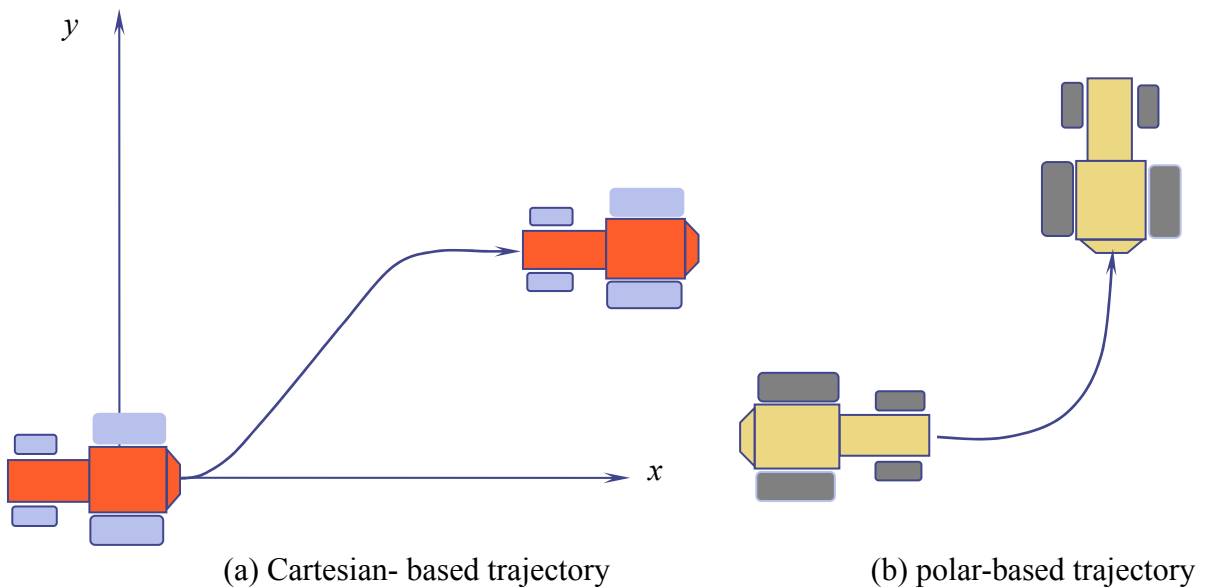
Fig. 4.2 Trajectories for path planning

Cartesian paths are used for x-y coordinates in straight path planning (Fig. 4.2a). In some of the cases, the vehicle need to turn 90° to greater to orient the tractor normal to the yard for parking (Fig. 4.2b). Polar paths (r, θ) are required to attend the turn of 90° or more. The combinations of trajectories are essential for reactive path planning.

The development of trajectory control is given details by Takigawa et al. 2002. The value of y (distance of vehicle in y-coordinate) that was a function of x (distance of vehicle in x-coordinate) can be expressed by the following equations:

$$y = \frac{ax^2}{x_f^2} + \frac{bx^3}{x_f^3} + \frac{cx^4}{x_f^4} + \frac{dx^5}{x_f^5} \tag{4-2}$$

$$y' = \frac{2ax}{x_f^2} + \frac{3bx^2}{x_f^3} + \frac{4cx^3}{x_f^4} + \frac{5dx^4}{x_f^5} \tag{4-3}$$

$$y'' = \frac{2a}{x_f^2} + \frac{6bx}{x_f^3} + \frac{12cx^2}{x_f^4} + \frac{20dx^3}{x_f^5} \tag{4-4}$$

Here, the prime symbol (') denotes differentiation with respect to x, and by differentiating y' with respect to x again, we get y''. When the vehicle is traveling from the start point (initial condition denoted by an index of i) to the target position (final condition denoted by an index of f). Then a, b, c and d can be determined as follows.

$$a = \frac{x_f^2 \tan\delta_i}{2l} - \frac{\pi^2 y_f}{4} \tag{4-5}$$

$$b = \frac{x_f^2}{2l}\left(\frac{\tan\delta_f}{\cos^3\psi_f} - 3\tan\delta_i\right) - 4x_f\tan\psi_f + \pi^2 y_f \tag{4-6}$$

$$c = \frac{x_f^2}{2l}\left(3\tan\delta_i - \frac{2\tan\delta_f}{\cos^3\psi_f}\right) + 7x_f\tan\psi_f - \frac{5\pi^2 y_f}{4} \tag{4-7}$$

54

$$d = \frac{x_f^2}{2l}\left(\frac{\tan\delta_f}{\cos^3\psi_f} - \tan\delta_i\right) - 3x_f\tan\psi_f + \frac{\pi^2 y_f}{2} \tag{4-8}$$

Finally, to control the steering angle of the experimented tractor for following the predetermined trajectory path and by referring to the previous equations, we derive:

$$\tan\delta = l\cos^3\psi\left(\frac{2a}{x_f^2} + \frac{6bx}{x_f^3} + \frac{12cx^2}{x_f^4} + \frac{20dx^3}{x_f^5}\right) \tag{4-9}$$

Furthermore, for minimizing experimental error due to external disturbances, Equation (4-9) should always be corrected by the value of the theoretical vehicle direction (yaw angular feedback control).

4.3 Feedback Control

The above algorithm can steer a vehicle from the start point to the target point with tracing the given trajectory, in practical environment, various surrounding disturbances will cause displacement from the final condition. Thus, feedback terms are to be introduced. For this purpose, as the first step, kinematic equations of displacement from nominal trajectory have to leanearize around nominal trajectory locally. Change of vehicle's position in y coordinate with respect to x can be expressed as:

$$y' = \tan\psi \tag{4-10}$$

thereby the kinematic equation for the displacement in y direction can be given as

$$\frac{d(\Delta y)}{dx} = \Delta y' = \frac{\partial(\tan\psi)}{\partial\psi}\Delta\psi = \frac{1}{\cos^2\psi}\Delta\psi \tag{4-11}$$

In the same manner,

$$\Delta\psi' = \frac{\partial}{\partial\psi}\left(\frac{\tan\delta}{l\cos^3\psi}\right)\Delta\psi + \frac{\partial}{\partial\psi}\left(\frac{\tan\delta}{l\cos^3\psi}\right)\Delta\delta = \frac{3\tan\gamma\sin\psi}{l\cos^4\psi}\Delta\psi + \frac{1}{l\cos^3\psi\cos^2\delta}\Delta\delta$$

We can describe these equations in linear forms by rewriting

$$\Delta y = z_1, \Delta\psi = z_2, \Delta\delta = u$$

$$\begin{bmatrix} \dot{z}_1 \\ \dot{z}_2 \end{bmatrix} = \begin{bmatrix} 0 & A \\ 0 & B \end{bmatrix} \begin{bmatrix} z_1 \\ z_2 \end{bmatrix} + \begin{bmatrix} 0 \\ C \end{bmatrix} u \qquad (4\text{-}12)$$

In order to calculate feedback control gains, a pole placement method was selected. For example when poles were assigned as $p_1 = -1$ and $p_2 = -3$, then feedback gains are given

$$k_1 = \frac{3}{AC}, \quad k_2 = \frac{4+B}{C}$$

Finally, the equation for steering with feedback terms can be described as follows,

$$\delta_{feedback} = \delta_{no\min al} + k_1 \Delta \psi + k_2 \Delta y \qquad (4\text{-}13)$$

4.3.1   Cartesian and Polar Coordinate System

This section is the further development of feedback control system in the polar-based trajectory. Switching of navigation mode from polar to Cartesian and Cartesian to polar is required for operational aspect. Figure 4.3 shows the kinematics model of polar coordinate guidance system. The geometrical relationship for polar coordinate system is given details by Takigawa et al., 2002. Fundamental relations can be described as:

$$V \cos \psi = r \dot{\theta} \qquad (4\text{-}14)$$

$$V \sin \psi = \dot{r} \qquad (4\text{-}15)$$

Where (r, θ) denotes the polar coordinates of the centre of the rear axle of the wheel and ϕ is the angle between a tangent line and the running direction of the vehicle.

$$\tan \psi = \frac{\dot{r}}{r\dot{\theta}} = \frac{r'}{r} \qquad (4\text{-}16)$$

Where the prime symbol means the differentiation with respect to θ. Differentiation of the above equation with respect to θ yields:

$$\psi' = \frac{r''r - r'^2}{r^2 + r'^2} \qquad (4\text{-}17)$$
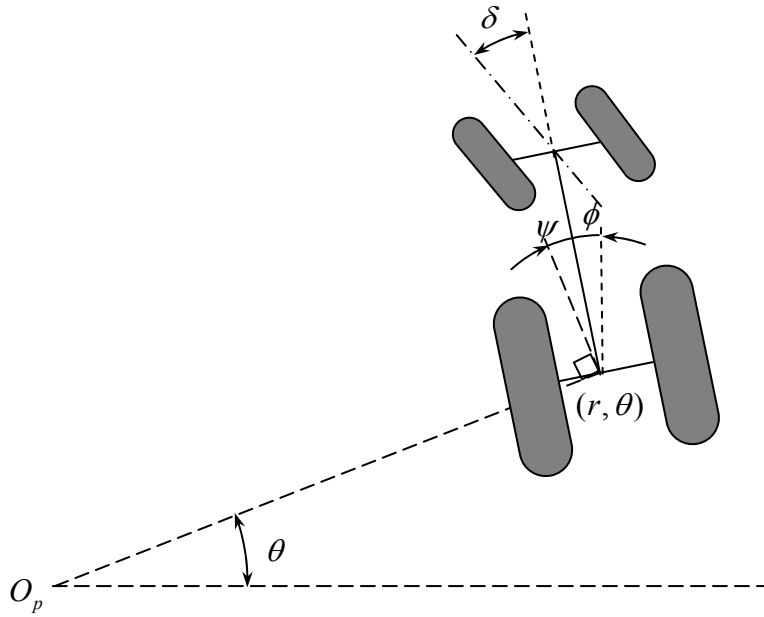
Fig. 4.3 Kinematics model for guiding the vehicle using polar coordinates

Since $\theta=\phi+\psi$, differentiating with respect to θ gives us $1=\phi'+\psi'$. By substituting this equation in (4-17)

$$\phi' = \frac{r^2 - r''r + 2r'^2}{r^2 + r'^2} \qquad (4\text{-}18)$$

Because ϕ' is the yaw angular velocity of the vehicle, it can be expressed as a function of the steering angle (δ) as follows:

$$\phi' = \frac{r \tan \delta}{l \cos \psi} \qquad (4\text{-}19)$$

By substituting equation (4-17) and (4-18) and rearranging we can calculate the steering angle as a function of r and its derivative as follow:

$$\frac{\tan \delta}{l} = \frac{\cos \psi \, (r^2 - r''r + 2r'^2)}{r \, (r^2 + r'^2)} = \frac{(r^2 - r''r + 2r'^2)}{(r^2 + r'^2)^{3/2}} = \frac{1}{\rho} \qquad (4\text{-}20)$$

Where ρ is the instantaneous turning radius of the centre of the rear axle

$$\cos \psi = \frac{1}{\sqrt{1 + \tan^2 \psi}} = \frac{r}{(r + r'^2)^{1/2}}$$

57

This equation shows that the yaw angle rate coincides with the curvature of the trajectory.
Now the procedure employed in Cartesian coordinates can be applied. This means r is expressed by a polynomial function of θ:

$$r = a + b\xi + c\xi^2 + d\xi^3 + e\xi^4 + f\xi^5 \tag{4-21}$$

Where
$$\xi = \frac{\theta - \theta_i}{\theta_f - \theta_i}$$

In addition, the initial and final conditions are given as follows:

when $\theta=\theta_i$
$$r_i . r_i' = r_i \tan \phi_i . r_i'' = r_i + \frac{2 r_i'^2}{r_i} - \frac{(r_i^2 + r_i'^2) \tan \delta_i}{l \cos \psi_i} \tag{4-22}$$

when $\theta=\theta_f$
$$r_f . r_f' = r_f \tan \phi_f . r_f'' = r_f + \frac{2 r_f'^2}{r_f} - \frac{(r_f^2 + r_f'^2) \tan \delta_f}{l \cos \psi_f} \tag{4-23}$$

Thus the parameters are given as:

$$a = r_i, b = \theta_f r_i', c = \theta_f^2 r_i''$$

$$d = 10(r_f - r_i) - 6\theta_f r_i' - 4\theta_f r_f' - 3\theta_f^2 r_i''/2 + \theta_f^2 r_f''/2$$

$$e = -15(r_f - r_i) + 8\theta_f r_i' - 4\theta_f r_f' + 7\theta_f r_f' + 3\theta_f^2 r_i''/2 - \theta_f^2 r_f''$$

$$f = 6(r_f - r_i) - 3\theta_f r_i - 3\theta_f r_f' - \theta_f^2 r_i''/2 - \theta_f^2 r_f''/2$$

4.3.2 Feedback Control in Polar Coordinate

In actual experiments sensory and modeling have positional error at the destination point (Sutiarso et al., 2000). Therefore, feedback terms were added to the control algorithm to minimize the influences of such disturbances. The feedback algorithm was developed for radial distance and vehicle directional angle. From equation (4-16), we find:

$$r' = r \tan \psi \tag{4-24}$$

$$\frac{dr}{d\theta} = r \tan \psi = h$$

Therefore,
$$\frac{d(\Delta r)}{d\theta} = \frac{\delta h}{\delta r}\Delta r + \frac{\delta h}{\delta \psi}\Delta \psi$$

$$\frac{d(\Delta r)}{d\theta} = \frac{\delta}{\delta r} r \tan \psi \Delta r + \frac{\delta}{\delta \psi} r \tan \psi \Delta \psi$$

$$\frac{d(\Delta r)}{d\theta} = \tan \psi \Delta r + \frac{r}{\cos^2 \psi}\Delta \psi \tag{4-25}$$

Since $\theta = \phi + \psi$, differentiating with respect to θ gives us, $1 = \phi' + \psi'$, by substituting (4-19), into $\psi = 1 - \phi'$, we have,

$$\frac{d\psi}{d\theta} = 1 - \frac{r \tan \delta}{l \cos \psi} = g$$

$$\frac{d(\Delta\psi)}{d\theta} = \frac{\delta g}{\delta r}\Delta r + \frac{\delta g}{\delta \psi}\Delta \psi + \frac{\delta g}{\delta \delta}\Delta \delta$$

$$\frac{d(\Delta\psi)}{d\theta} = \frac{\delta}{\delta r}\left(1 - \frac{r \tan \delta}{l \cos \psi}\right)\Delta r + \frac{\delta}{\delta \psi}\left(1 - \frac{r \tan \delta}{l \cos \psi}\right)\Delta \psi + \frac{\delta}{\delta \delta}\left(1 - \frac{r \tan \delta}{l \cos \psi}\right)\Delta \delta$$

$$\frac{d(\Delta\psi)}{d\theta} = -\frac{\tan \delta}{l \cos \psi}\Delta r + \frac{r \tan \delta \sin \psi}{l \cos^2 \psi}\Delta \psi - \frac{r}{l \cos \psi \cos^2 \delta}\Delta \delta$$

The approximate linearization gives,

$$\frac{d}{d\theta}\begin{bmatrix} \Delta r \\ \Delta \psi \end{bmatrix} = \begin{bmatrix} a_{11} & a_{12} \\ a_{21} & a_{22} \end{bmatrix}\begin{bmatrix} \Delta r \\ \Delta \psi \end{bmatrix} + \begin{bmatrix} 0 \\ b \end{bmatrix}\Delta \delta \tag{4-26}$$

$a_{11} = \tan\psi$, $a_{12} = r/\cos^2\psi$, $a_{21} = -\tan\delta/l\cos\psi$, $a_{22} = r\tan\delta\sin\psi/l\cos^2\psi$, and $b = -r/l\cos\psi\cos^2\delta$

Using the relation $|SI-A|=0$ and obtaining the characteristics equation, we have,

$$\det\begin{bmatrix} S - a_{11} & -a_{12} \\ -(a_{21}+f_1 b) & S - (a_{22} + f_2 b) \end{bmatrix} = (S - a_{11})(S - (a_{22} + f_2 b)) - a_{12}(a_{21} + f_1 b)$$

$$= (S^2 + S(-a_{11} - a_{22} - f_2 b)) +$$
$$(a_{11}a_{22} + a_{11}f_2 b - a_{12}a_{21} - a_{12}f_1 b)$$

In order to calculate the feedback control gains, a pole placement method was sleeted. After trial and error, we have assigned the poles as $p_1 = -8$ and $p_2 = -6$, then feedback gains are given as:

$$f_2 = \frac{-a_{11} - a_{22} - 8}{b} \qquad (4\text{-}27)$$

$$f_1 = \frac{-6 + a_{11}a_{22} + a_{11}f_2 b - a_{12}a_{21}}{a_{12}b} \qquad (4\text{-}28)$$

Therefore, the feedback in steering angle,

$$\delta_{feedback} = \delta_{no\,min\,al} + f_1 \Delta r + f_2 \Delta \psi \qquad (4\text{-}29)$$

4.4 Conclusions

In the path planning of the vehicle, trajectory control with feedback support is essential to guide the vehicle from start point to the target point accurately. In the multiple segmented paths, the polar-based feedback control is extended with the previously developed methods for trajectory control. The posture information of the vehicle is required to generate the trajectories from start point to the goal point. Hence, the accurate installation of sensors is needed for positions, velocity, and heading of experimental tractor with digital I/O systems.

Chapter 5

Installation of Sensors in the Experimental Tractor

5.1 Basic Instrumentation

A computer-controlled four-wheel drive 15.4 kW tractor was used in this study (Fig. 5.1).

The experimental tractor was modified for autonomous control using a Keyence KZ-A500

Programmable Logic Controller (PLC) and relay switches as its executive control

regulating hydraulic actuators based on data measured by sensors. The sensory data and

control status were transmitted to an upper level controller through parallel communication.

The basic instrumentation system for the autonomous tractor is depicted in Fig. 5.2.

Fig. 5.1 The experimental autonomous tractor

5.1.1 Steering Configuration

The steering controller configuration is shown in Fig. 5.3. In the configuration, the tractor

was equipped with a hydraulic motor as steering actuator. The steering valve was an

electrohydrualic proportional flow and direction control valve (Nachi ESD-G01

-C**10/20-12), which controls direction by supplying an input current into one of the two

proportional solenoids and controls flow by changing the input current. When autonomous mode of the tractor was activated, the steering controller overrode manual steering inputs, but did not interfere with the manual steering when the autonomous mode was not activated.
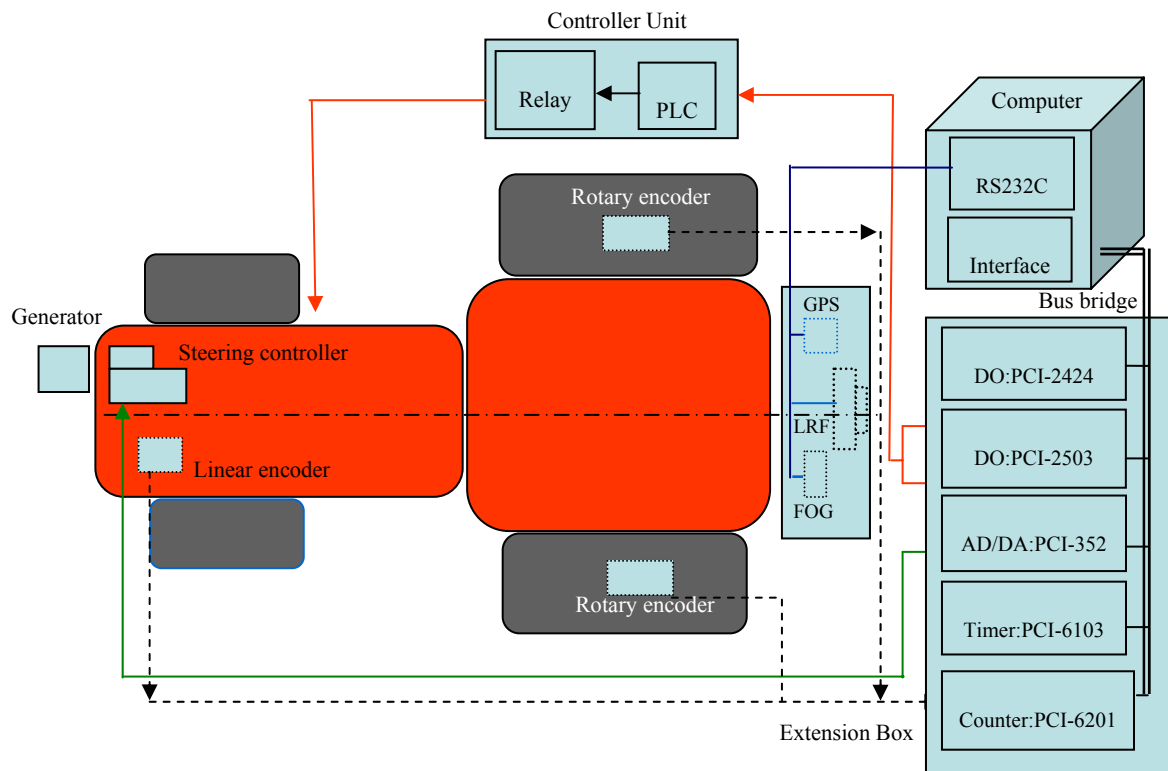
Fig. 5.2 Schematic diagram of basic instrumentation system

5.1.2 Steering Angle

A linear encoder (Mutoh D540), which had a resolution of 2.5 pulse/mm, was installed on the tractor for measuring the steering angle. The linear encoder was interfaced to the computer by the counter board equipped with two times decoding mode. The maximum steering angle of the tractor was about 40°.
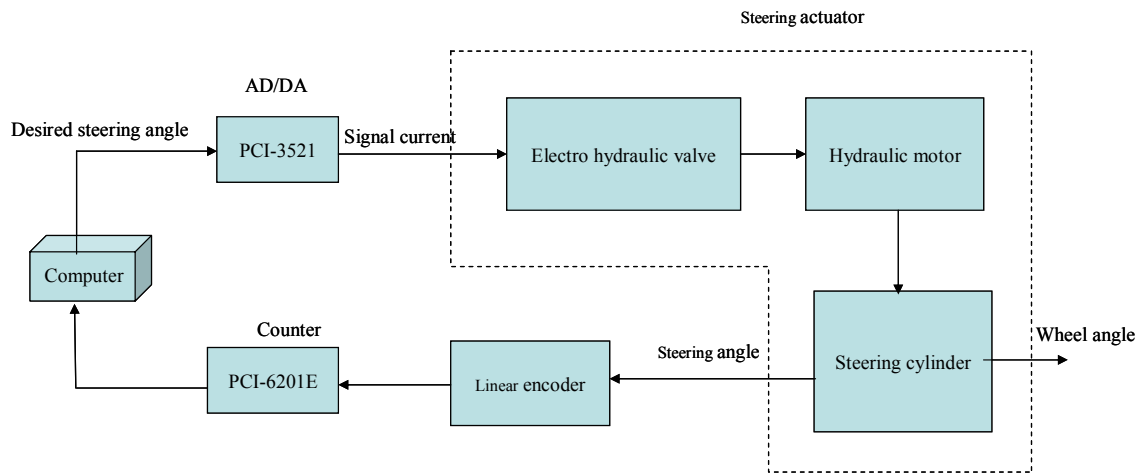
Fig. 5.3 Steering controller configuration

The technical specification of the tractor is summarized in Table 5.1.

Table 5.1 The technical specification of the tractor

Item	Technical specification
Tractor Model	Kubota KL21
Drive System	4WD
Steering system	Power steering
Length(mm)	2965
Width(mm)	1220
Height (mm)	1955
Wheel base(mm)	1550
Ground clearance(mm)	335
Length of drawbar(mm)	500
Power output(kW)	15.4

5.2 Posture Sensors

5.2.1 Fiber Optic Gyroscope

Fiber optic gyro sensors can be configured as either closed loop or open loop, but the complexity of the former restricts it to avionics and inertial navigation grade applications. A JCS-7401 fiber optic gyroscope was used for measuring the vehicle direction. The FOG could measure the angular velocity within the range of 100°/s. It also could measure roll

and pitch angles within the range of ±45°, and yaw angle of ±180°. The drift rate of this gyro was specified as 6.35°/h, and had the capability of outputting both analog and digital signals with the resolutions of 0.2° and 0.1°, respectively. The digital output signal was transmitted to computer at a frequency of 25 Hz through RS232C serial interface. Figure 5.4 shows the gyro sensor, which was used in the autonomous tractor.

Fig. 5.4 Fiber optic gyroscope used in the autonomous tractor

5.2.2 Rotary Encoder

A rotary encoder is a device used to convert an angular position of a shaft to a digital signal. An incremental type rotary encoder was used in the autonomous tractor. It is consists of LED source, grating disk, grating board and optical detector and outputs square wave signals. The output signal usually consists of A-phase, B-phase and Z-phase. Difference between A phase and B phase is 90°, and Z phase is the reference output.

A pair of Omron E6D-CWZ1E incremental rotary encoder (2000 and 1000 pulse/rev) was used for measuring the running distance (Fig. 5.5). Each encoder was attached with rubber wheel on their shafts and was installed at rear wheel of the autonomous tractor so that the rubber wheel met the inner carcass surface in order to prevent slipping. Traveling distance of each wheel was calculated by multiplying the rotation counts with a proper constant

Fig. 5.5 The incremental rotary encoder used in the autonomous tractor

value. Total traveling distance of the experimental vehicle was determined by averaging traveling distances.

5.2.3 Laser Range Finder

A SICK LMS-211 laser range finder was used in the autonomous tractor for the relative positioning of the vehicle in respect to the implement as shown in Fig. 5.6. The LMS 211 operates according to the time of flight principle. A light pulse emitted for a defined length of time is reflected off a target object and is received via the same path along which it was sent. The laser scanner in the LMS 211 range is optimized for distance measurements. The basic operating principle of the system is the initial pulse evaluation, which means that the first return pulse received by the laser scanner triggers the distance measurement. The LMS 211 can function in three different measuring modes:

● Measurements of the distance value

● Measurements of the energy value (also known as reflectivity value)

● A combination of both options for a restricted scanning area

LMS 211 outdoor laser range finder's technical specification is given in Table 5.2.

Fig. 5.6 The SICK LMS 211 laser range finder used in the autonomous tractor

Table 5.2 The technical specification of the Laser Range Finder

Item	Technical Specification
Field view	100°
Angular resolution	1…0.25°
Response Time	13…..52 ms
Resolution	10 mm
Systematic error	+/- 15 mm
Statistical error (1 sigma)	5 mm
Laser Class	1
Enclosure Rating	IP 67
Ambient operating temperature	-30° C…..+50°C
Scanning range	80 m
Data interface	RS-232C, RS 422
Data transmission rate	9.6/19.2/38.4/500 Kbaud
Switching outputs	3xPNP
Supply voltage	24 V DC +/-15%
Power consumption	20 W
Storage temperature	-30°C …..+70°C
Weight	9 kg
Heater current rating	6A
Dimensions	194 x 352 x 266 mm

The detail characterization of the laser range finder will be discussed in the following chapter.

5.2.3.1 LMS Telegram Structure

Some telegrams are sent by the host computer to the LMS 211, while other s sent to the host by LMS 211. Because the commands are control commands sent to the LMS 211 or responses received from the LMS 211, they are referred as "send telegrams" and "response telegrams". A send telegrams always contains only ONE control command for the LMS 211. A response telegram contains ONE response from the LMS 211. Commands and responses are always ONE Byte long. The LMS 211 normally responds to send telegram with a response telegram. The entire telegram has an LMS 211 specific frame around the commands and data.

To send the data to the LMS 211, the telegram must be structured as follows. The LMS 211 responds using the same structure. The telegram itself is binary.

	Frame				Commands and Data		
Description	STX	ADR	LEN		Command/Response	Data	Checksum
Byte position	1	2	3	4	5	6 to n	n+1 n+2

The following Table 5.3 provides more information of the structure of telegrams.

Table 5.3 Description of telegram structure for the LMS 211 LRF

Designation		Data width [bits]	
STX		8/1 BYTE	Start Byte
ADR		8/1 BYTE	Address to the subscriber contacted. The LMS add the value 80h to the address when responding to the HOST Computer
Len		16/2/WORD	Number of subsequent data bytes excluding the checksum
CMD		8/1/BYTE	Command byte from the HOST computer to LMS
Data	Data for send telegrams	Nx8(nx1)	Refers to the previous command
	Status (response telegram only)	8/1/BYTE	LMS 211 transmits it status message only when it transfers data to the HOST computer.
Checksum		16/2/WORD	CRC checksum of the entire data package, starting with STX and up to and including the status byte

5.2.4 GPS

A Trimble GPS receiver as shown in Fig. 5.7 was installed in the autonomous system using differential correction services to calculate sub-meter positions in real-time.

Fig. 5.7   Single receiver differential GPS used in the autonomous system

Integrated 12-channel receiver/dual-channel, MF differential beacon receiver/satellite differential receiver, built-in virtual reference station (VRS) ensures satellite differential correction uniformity. It had RTCM SC-104 and NMEA-0183 differential correction input.

5.3 Programming Modules

The programming modules were constructed using object oriented classes using C++ Builder 6.0. The modules were divided into four major classes: hardware class, sensory class, control class and navigator class; the schematic diagram of class concept for the vehicle control system is illustrated in Fig. 5.8. The class listing of header files is also listed in the Appendix.
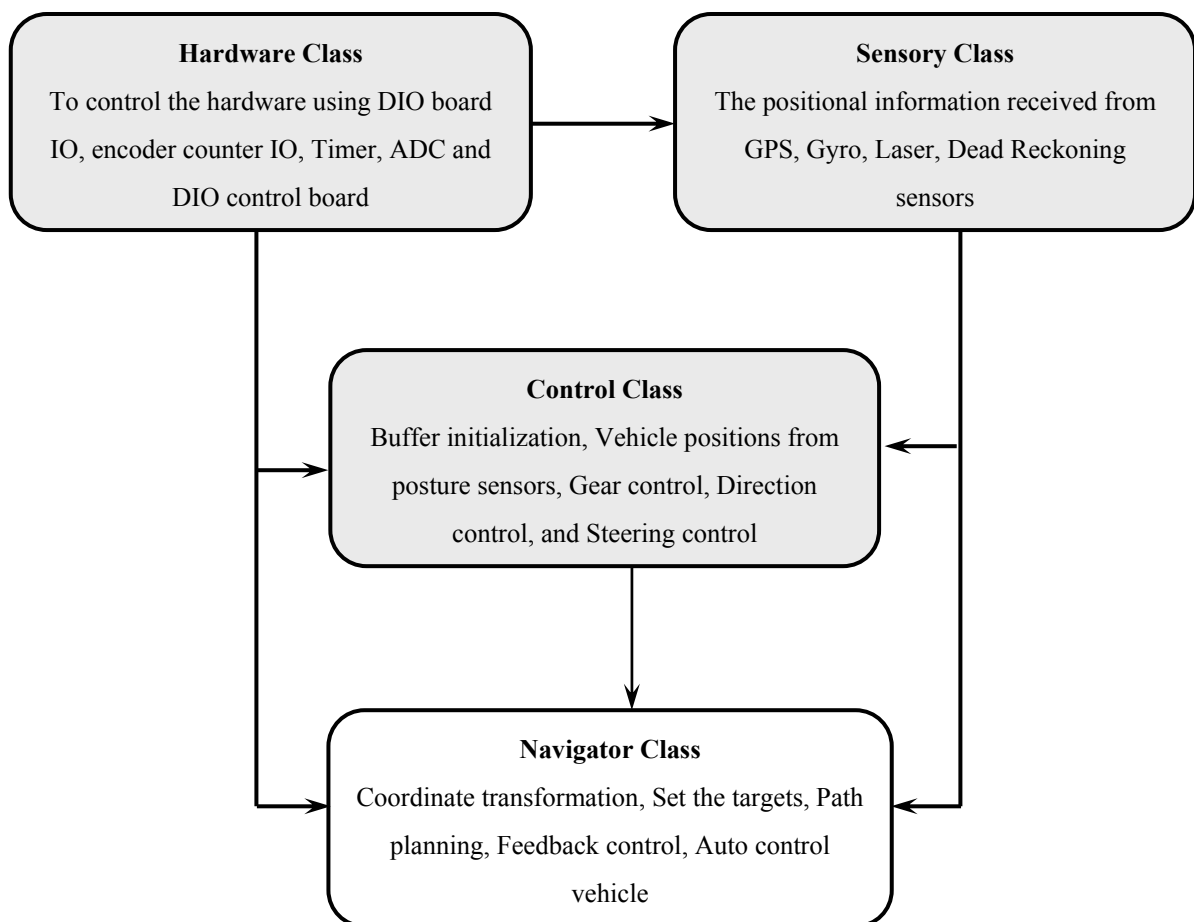
Fig. 5.8 Basic class structure of autonomous tractor control

5.4 Conclusions

The experimental tractor was modified for the autonomous tractor and the platform is ready for experiments. The sensors performance and drift were calibrated. The single receiver GPS had not enough accuracy to conduct the navigation experiments. At this situation, need to substitute GPS with the dead reckoning sensors for short traveling. In the multi-sensor platform, it is still required for the SICK LRF to discriminate the landmark from the environment. Once the discrimination and localization can be done using SICK LRF, then approach navigation toward the object can be performed in a robust way.

Chapter 6

Discrimination and Localization of Landmark for Approach Navigation

In the approach navigation, the discrimination and localization of the implement is prerequisite. Once the position of the implement is known, it is easy to approach the implement. To recognize the implement, landmark could help to localize the implement's position. To discriminate the landmark from the environment requires robust method to recognize the landmark. Once the landmark is discriminated and localized on the *x-y* coordinates then approach can be performed. In absolute positioning the location of an object is expressed as *x*, *y* coordinates on a map, and object position should be known in advance on the map. In case of agricultural operation, it is practically impossible to know in advance the position of the implements, containers, or object. The position of the implement or container may place time to time at different location in the course of field operation. Thus, the absolute positional sensor does not work in approach navigation; consequently, the relative sensor is required to approach the implement. To identify the landmark, range sensors are appropriate. Range sensors are commonly used to measure relative position and orientations of the object for approaching. They include the triangulation, interferometry, time of flight, swept focus, radar, phase shift, return signal intensity, and frequency modulation. Electronic distance meters that use the measurement of time of flight or phase shift are frequently used for positioning in agricultural vehicles. Stereoscopic ranging with cameras is used for locating objects, such as fruits. Ultrasonic sensors are used to measure relatively close objects. The laser range finder (LRF) has been the most popular device in outdoor applications to measure the relative distance of objects. As a variety of a laser-based

positioning system, a simple configuration using three or more detectors positioned around workspace can be considered. Laser distance meter can cover distances of over 100 meters with an accuracy of less than 1 mm (Everett, 1995). Shemulevich et al. (1989) used laser beams for positioning a multi-joined truss system, and reported an accuracy of 150 mm over a 400 m x 400 m area. Søgaard (1999) reported that the standard deviation of the cross truck position error obtained with an autonomous traveling system employing laser optic position determination in actual field operations was less then 5 cm. Inahata et al. (1999) developed a positioning method for agricultural robots with a simple laser sensor to measure the direction angles of light reflectors around the field.

In this chapter, discrimination and localization of landmark is discussed. Basic experiments are reported to discriminate the landmark and template fitting of the landmark using Laser Range Finder (LRF) is characterized.

6.1 Reflector as Landmark

In the relative positioning, landmark is essential. Reflectors function as reliable artificial landmarks for robust relative positioning systems in LRFs. The navigation concept by reflector using reflector bit is relatively new in agricultural application. Availability of reflector bit in the laser sensor is important for navigation. For computational efficiency, activation of reflector bit to distinguish reflectors from other objects is significant for robust positioning of landmarks. In time-based time-of-flight measurements with light, the reflected light energy depends on how far away the measured object is from the scanner and on the surface characteristics of the object. The LRF uses the received energy to evaluate the distance and compare this with an internal reference. The received energy value is known as reflectivity. The output of the reflectivity values can help to discriminate the reflector from its surroundings.

The inherent problem of laser beam in distance metering is the increase of spot diameter with increase of distance. The measured points decrease with increase of distance. The template fitting is much accurate for many measured points of landmark.

6.2 Laser Ranging: Operating Principle

The laser scanner, LMS 211 range operates according to the time of flight principle (TOF). Figure 6.1 shows the operating principle of laser range finder. A light pulse emitted for a defined length of the time is reflected off a target object and is received via the same path along which it was sent. A counter status as soon as the light pulse is transmitted and steps when the signal is received. The counter value correlates with the appropriate path. The emitted pulse is diverted by a rotating mirror in the scanner. Since the time of flight runs at the speed of the light, the rotation of the mirror for an individual pulse measurement is not relevant. In a TOF of system a short laser pulse is sent out and the time until it return is measured Δt, l_s is the speed of the light($3x10^8$ m/s). In the standard measuring configuration data bits 0 to 12 are used to represent the distance. The reflectivity information with distance depends on the transmission strength of the scanner. Reflector bit which are greater than 0 indicates the reflectors from other objects in the environment, and these reflector bits are in 8 levels. Bits 0 to 12 are used for measurement and bits 13 to 15 are used for reflectivity information. A light pulse emitted for a defined length of the time is reflected off a target object and is received via the same path along which it was sent. The systematic error that is caused by any factor such as instrumental effects that systematically affect measurement is +/- 15 mm, statistical error which is the tendency for a measured value to "jump around" from measurement to measurement is 5 mm, and it is expressed with the statistical distribution. A value pair comprises a measured distance value and reflectivity value, with reflectivity ranging from 0% to approximately 13000%.
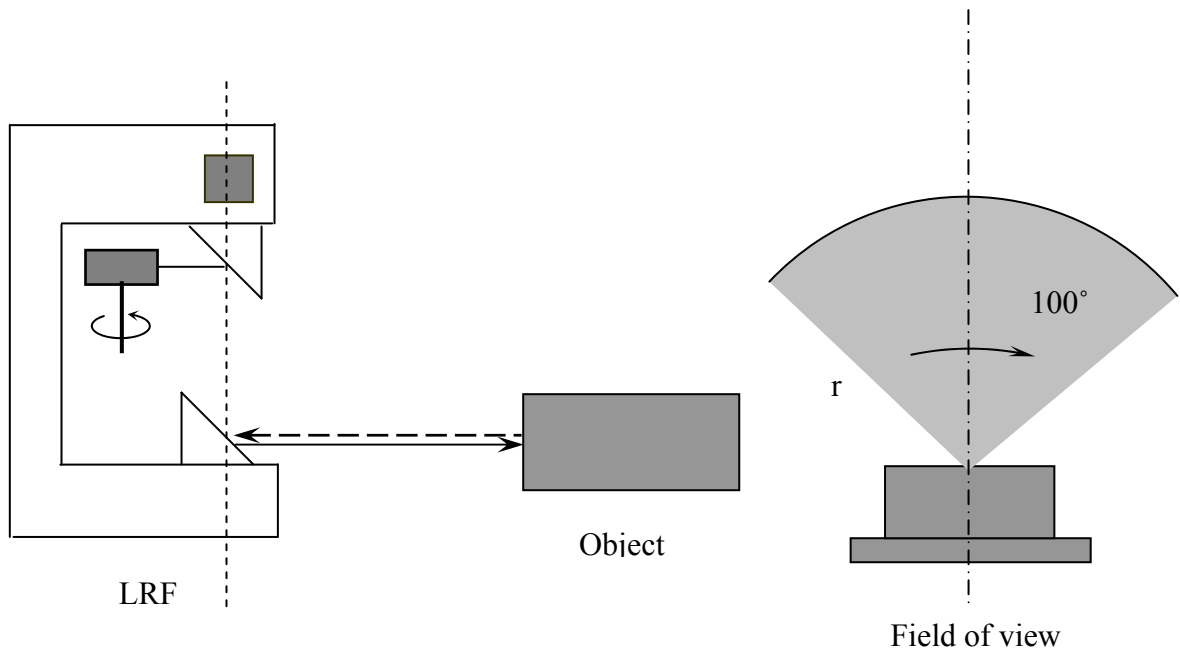
Fig. 6.1 Operating principle using time-of-flight method for LMS 211 LRF

Materials such as cardboard wood, aluminum, steel, and even shiny materials have lower values and their reflectivity varies from 10% to 200%. The reflectors return higher measured values and reflectivity is more than 2000%. In the standard measuring configuration data bits 0 to 12 are used to represent the distance, and bits 13 to 15 are used for reflectivity information. The reflector bits that are used for reflectivity information are calibrated from 0 to 8. Having a non-zero value indicates that the object is a reflector from the environments.

6.3 Design of Reflectors

Three different shapes of reflectors were used in experiments. One was flat reflector by pasting light reflective sheets on the 28 cm x 30 cm x 2 cm aluminum frame. The cylindrical one was made by plastic pipe that has the diameter of 26.5 cm and height 30 cm. The trapezoidal reflector was fabricated by using three aluminum frames 35x30x0.5, 30x30x0.5, and 35x30x0.5 cm with 30˚ to -30˚ adjustable side frame. The frames were flats and could be adjusted within a mentioned angular range.

6.4 Template Fitting Algorithm for Landmarks

With properly segmented data sets from a laser scan it is not certain which templates in the template library is to be used for the object fitting without human involvement. For computational efficiency, the attempt was made to implement algebraic fitting which does not require any iteration. In this aspect, line was fitted for the flat reflectors, circle for the cylindrical reflectors, and geometrical shape using line for the trapezoidal reflectors.

6.4.1 Line Fitting

A flat rectangular reflector was used as landmark. In each scan by the LRF at a 10 m distance using 0.25° angular resolution, approximately, 12 to 8 Cartesian measured values (x, y) can be obtained from the LRF for a flat reflector. With properly segmented data sets from a laser scan, it is not certain which template in the template library is to be used for the object fitting without human involvement. For computational efficiency, we implemented an algebraic fitting for straight line and circle that does not require any iteration. The two parameters of the straight line $y=mx+c$ can be found using the standard formula for a least square fit for n data points of (x_i, y_i) is shown in Fig. 6.2. Here n is a number of sampled coordinates, and parameters for the straight line can be expressed as:

$$m = \frac{n\sum_{i=1}^{n} x_i y_i - \left(\sum_{i=1}^{n} x_i\right)\left(\sum_{i=1}^{n} y_i\right)}{n\sum_{i=1}^{n} x_i^2 - \left(\sum_{i=1}^{n} x_i\right)^2} \tag{6-1}$$

$$c = \frac{\sum_{i=1}^{n} y_i}{n} - m\frac{\sum_{i=1}^{n} x_i}{n} \tag{6-2}$$
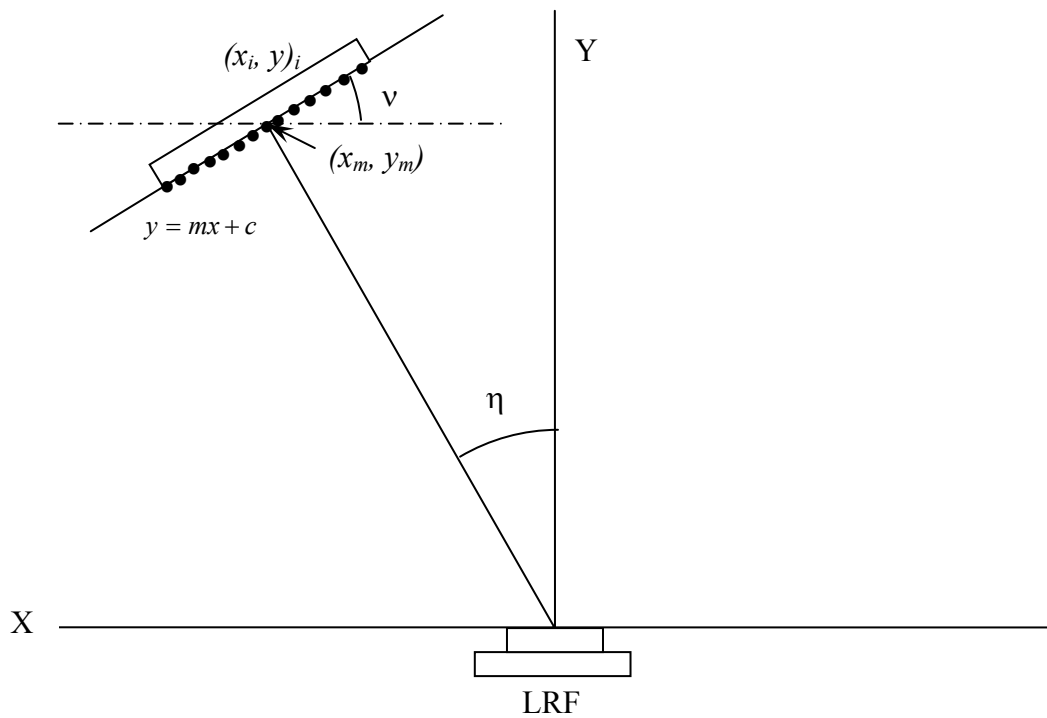
Fig. 6.2 Line fitting model from the LRF data for flat reflector

The inclination angle (v) of the fitted straight line for the single reflector can be calculated from the following expression:

$$v = \tan^{-1}(m) \tag{6-3}$$

where m is the line parameter for the fitted straight line and could be obtained by equation (6-1) using the LRF scanned data points (x_1, y_1), (x_2, y_2)........(x_n, y_n). These values were fitted as a line using least square method. At the closer distance to the reflector maximum number of measured values were obtained. Our prime concern was the middle of the reflector, for this, we calculated the midpoint using x Cartesian measured value for the first and last measured value of the reflector. The midpoint of each fitted line for a flat reflector can be expressed as:

$$x_m = \frac{x_n + x_1}{2} \tag{6-4}$$

$$y_m = mx_m + c \tag{6-5}$$

It is worth stating that since the length of a reflective object can be estimated from raw data, we can utilize it to check whether the object is our landmark or not. In addition, the standard error of estimate S_{est} provides a measure of how well the data points could be fitted and is given by

$$S_{est} = \sqrt{\frac{\sum\limits_{i=1}^{n}[y_i - (mx_i + c)]^2}{n - 2}}$$

(6-6)

The inclination of the fitted straight line can be calculated from the tangent of each reflector using the data points (x_1, y_1), $(x_2, y_2)\ldots\ldots(x_n, y_n)$. The midpoint of each reflector was set on the bar. The tangents and midpoint of each fitted line can be expressed as:

6.4.2 Circle Fitting

There are various methods of fitting circle is described by Umbach and Jones (2000). Our interest was limited on the modified least square method which is robust in a reasonable measure of the fit of the circle $(x-a)^2+(y-b)^2=r^2$ to the points (x_1, y_1), $(x_2, y_2)\ldots\ldots\ldots(x_n, y_n)$ is given by the summing the squares of the distance from the points to the circle (Fig. 6.3). This measure is given by.

$$SS(a,b,r) = \sum_{i=1}^{n}\left(r - \sqrt{(x - a)^2 + (y - b)^2}\right)^2$$

(6-7)

It was found that equating the partial derivatives to zero produces a pair of linear equations whose solution can be expressed as:

$$a_M = \frac{DC - BE}{AC - B^2}$$

(6-8)

$$b_M = \frac{AE - BD}{AC - B^2}$$

(6-9)

Where,
$$A = n\sum_{i=1}^{n}x_i^2 - \left(\sum_{i=1}^{n}x_i\right)^2 = n(n-1)S_x^2$$

$$B = n\sum_{i=1}^{n}x_iy_i - \left(\sum_{i=1}^{n}x_i\right)\left(\sum_{i=1}^{n}y_i\right) = n(n-1)S_{xy}$$
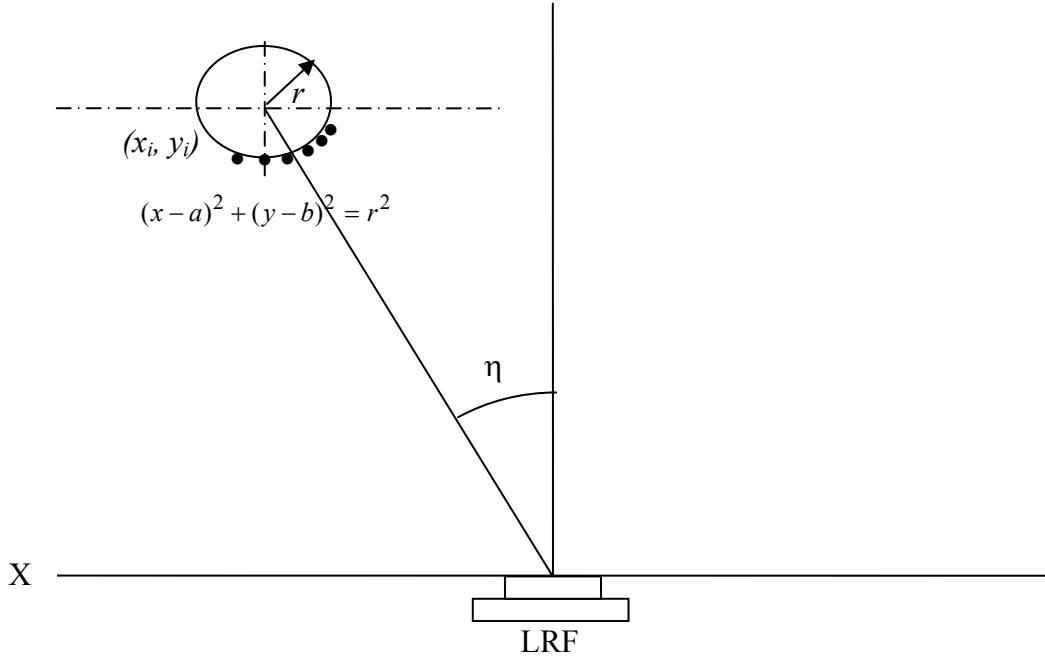
Fig. 6.3 Circle fitting model from the LRF data for cylindrical reflector

$$C = n\sum_{i=1}^{n} y_i^2 - \left(\sum_{i=1}^{n} y_i\right)^2 = n(n-1)S_y^2$$

$$D = \left\{ n\sum_{i=1}^{n} x_i y_i^2 - \left(\sum_{i=1}^{n} x_i\right)\left(\sum_{i=1}^{n} y_i^2\right) + n\sum_{i=1}^{n} x_i^3 - \left(\sum_{i=1}^{n} x_i\right)\left(\sum_{i=1}^{n} x_i^2\right) \right\} = 0.5n(n-1)(S_{xy^2} + S_{xx^2})$$

$$E = \left\{ n\sum_{i=1}^{n} y_i x_i^2 - \left(\sum_{i=1}^{n} y_i\right)\left(\sum_{i=1}^{n} x_i^2\right) + n\sum_{i=1}^{n} y_i^3 - \left(\sum_{i=1}^{n} y_i\right)\left(\sum_{i=1}^{n} y_i^2\right) \right\} = 0.5n(n-1)(S_{yx^2} + S_{yy^2})$$

The minimizing value for radius r_M can be expressed as:

$$r_M = \sqrt{\sum_{i=1}^{n} ((x - a_M)^2 + (y_i - b_M)^2)/n} \tag{6-10}$$

6.4.3 Geometrical Shape Fitting

The trapezoidal shape reflector consisted of three plates where two side plates could rotate -30° to 30°. At the end of the grid face was moved to measure maximum data. The

laser range data measured in the instant k is represented by the set of LMS_k, of N data points P_i with angle α_i and distance value r_i.

$$LMS_k = \left\{ P_i = \binom{\alpha_i}{r_i}, i \in [0, N] \right\} \tag{6-11}$$

The segmentation represent scan points clusters that belong together. It was based in the computation of the distance between two consecutive scan points, calculated by

$$d(P_i, P_{i+1}) = \|P_i - P_{i+1}\| = \sqrt{r_i^2 + r_{i+1}^2 - 2 r_i r_{i+1} \cos \Delta \alpha} \tag{6-12}$$

The threshold for segmentation of data had chosen according to the length of each plate. The segmented clusters were calculated, using the following expressions:

$$S_1 = \sum_{i=1}^{n_1} d(P_i, P_{i+1}) \le l' + a_0 \tag{6-13}$$

$$S_2 = \sum_{i=n_1+1}^{n_2} d(P_i, P_{i+1}) \le l'' + a_0 \tag{6-14}$$

$$S_3 = \sum_{i=n_2+1}^{n_3} d(P_i, P_{i+1}) \le l''' + a_0 \tag{6-15}$$

In which $S_1, l'; S_2, l''; S_3, l'''$ are segmented clusters and lengths of reflector's plate respectively. The constant a_0 allows an adjustment of noise and overlapping of scan points. The orthogonal regression fitted straight lines for each cluster and expressed as:

$$y = m_1 x + c_1 \qquad y = m_2 x + c_2 \qquad y = m_3 x + c_3 \tag{6-16}$$

The intersecting points of three lines can be expressed as:

$$x', y' = \left[\frac{c_2 - c_1}{m_1 - m_2}, \frac{m_1 c_2 - m_2 c_1}{m_1 - m_2} \right] \tag{6-17}$$

$$x'', y'' = \left[\frac{c_3 - c_2}{m_2 - m_3}, \frac{m_2 c_3 - m_3 c_2}{m_2 - m_3} \right] \tag{6-18}$$

The midpoint of reflector can be calculated by using intersecting points, and β_m is the position angle of reflector.

79

$$x_m, y_m = \left[\frac{x' + x''}{2}, \frac{y' + y''}{2} \right]$$

(6-19)

$$\beta_m = \tan^{-1}\left(\frac{y_m}{x_m} \right)$$

(6-20)

6.5 Preliminary Experiments for Positioning

The positioning algorithm using LRF for the navigation of autonomous tractor was developed into four phases: switching the operating mode, changing the data transmission rate, configuration for activation of reflector bit, changing of variants with increasing distance. The novelty of this algorithm was point clustering and scan fusing was done for recognizing the reflectors from all other objects in real time approach, as each scan is received by LMS laser range finder. The algorithm was coded in C++ Builder environment.

6.5.1 Field Set up

Our preliminary positioning experiment was conducted in a 20mx20m square field as shown in Fig. 6.4. The Topcon DT-120 and Leica DISTO^{TM} Classic[5] laser distance meter was used to survey and determine the locations of light reflectors. The laser range finder was installed on the surveying tripod for accuracy and to eliminate the effect of inclination on the position of the grid. A computer was equipped with the laser sensor using RS 232C serial communication. The resolution for the laser range finder was set on 0.25˚. The reflectors were set on the 120 cm length bar at 60 cm interval, which was placed over the theodolite (DT-120, Topcon) for measuring orientation angle accurately. The experiments were repeated at the distance of 5 to 20 m in the y co-ordinate and 0 to ±10 m in the x co-ordinate, and the orientation angle was setted -30˚, 0˚ and 30˚. For each position and orientation angle of reflectors in the grid after 5 m interval 40 measurements were taken with the laser sensor.
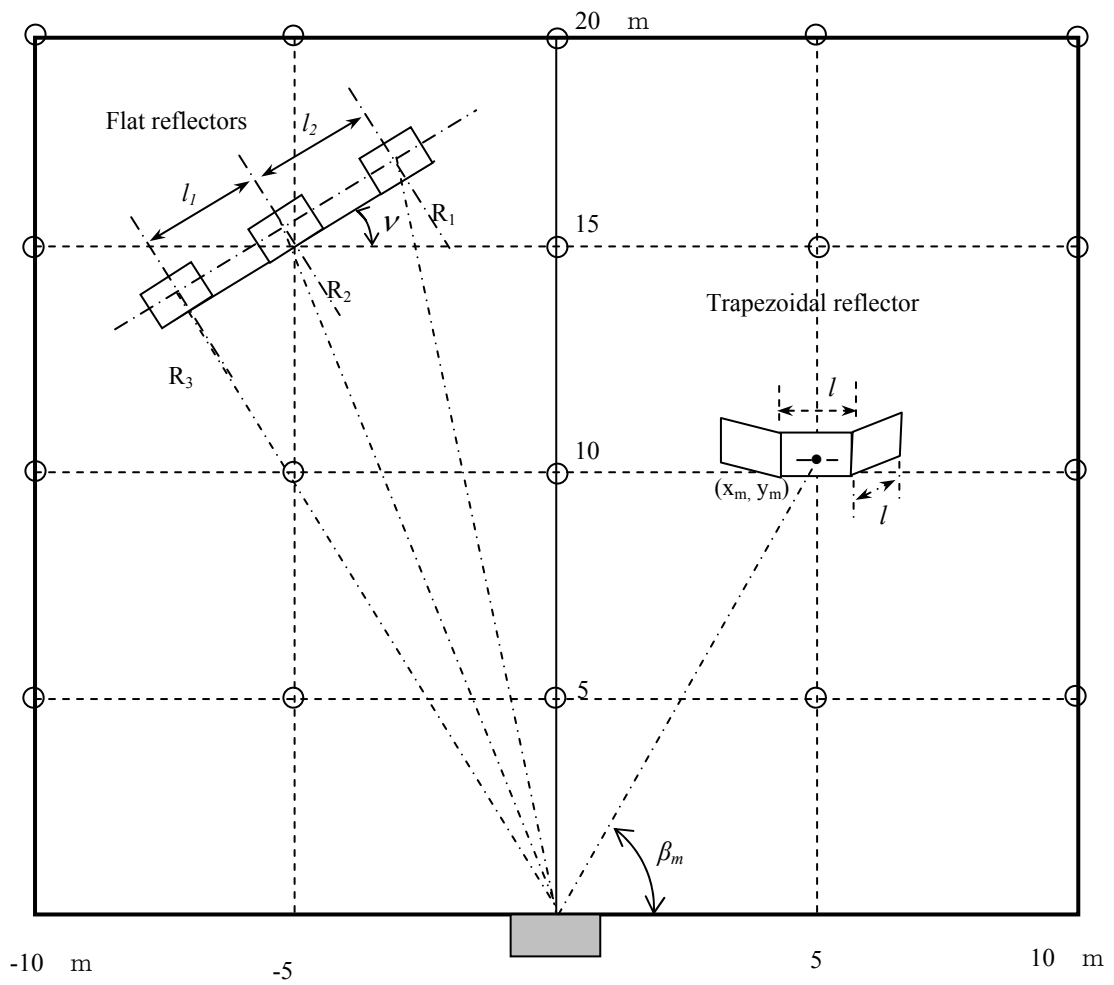
Fig. 6.4 Field layout and position of reflector(s) relative to the position of laser sensor

(circle indicates the position of reflectors in the field)

6.5.2 Preliminary Experimental Results

6.5.2.1 Positioning Error for Reflectors

The scanning profiles for the different reflectors are shown in Fig. 6.5(a, b, c, d, e, f). The positioning errors for the reflectors were the minimum at 5 m distance from the laser sensor, and increased gradually with increasing of distance. Moreover, the spot diameter also increased with increasing of distance. We found that error occurred largely at the end of the grid due to few numbers of measured data of reflectors can detect at the $\pm 30^{\circ}$ orientation. The flat reflectors formed line, it had better accuracy, and line could fit at the end of the grid though the numbers of data were few. The cylindrical reflector formed circular shape from the measured data. The modified least square regression method was applied to estimate the circle parameter (x_c, y_c, r). The trapezoidal reflector had shape fitting problem at the end of the grid. The positioning of reflectors using reflector bit for laser sensor successfully recognized the reflectors from other objects. The clusters of scanned data formed line and circular shape. The least square template matching algorithms were applied to estimate the position of reflectors. Line parameter estimation is difficult while the number of measured data is the minimum in the flat rectangular reflectors. The cylindrical reflectors did not satisfy the positioning at the longer distance due to measured data formed flatter surface instead of circular shape. In the cylindrical reflector, circle parameter estimation using modified least square regression method was not suitable at the longer distances and accuracy was worse while number of measured data were few. Flat rectangular and cylindrical reflector could detect few numbers of measured data at -30˚ and 30˚ orientation. At the end of 20 m x 20 m grid, 2 reflectors at 120 cm interval were better then three reflectors at 60 cm interval.
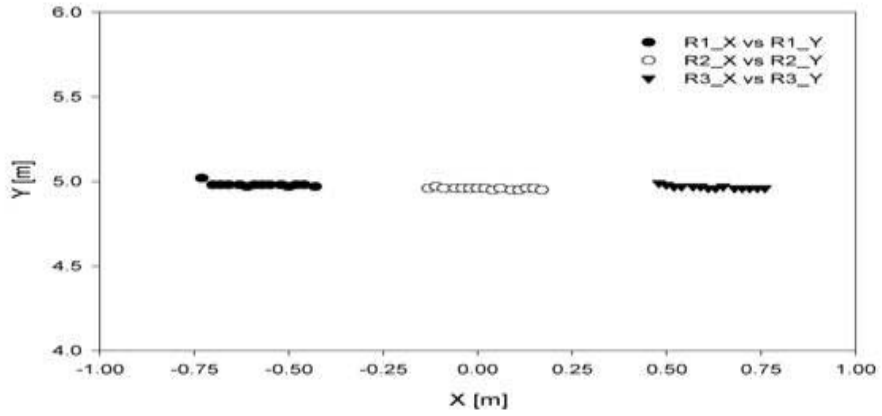
(a) Location of flat reflectors at the 5 m distance from the laser sensor in the grid with $x=0$ and $v=0°$
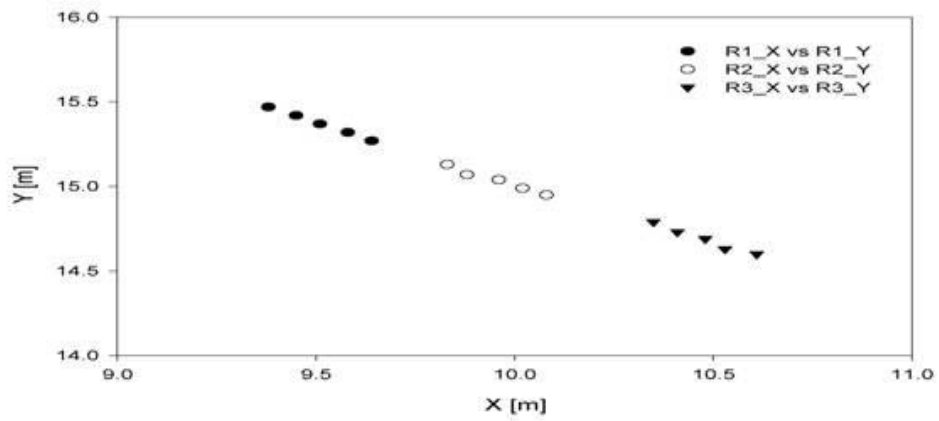
(b) Location of flat reflectors at the 10 m distance from the laser sensor in the grid with $x=5$, and $v=30°$
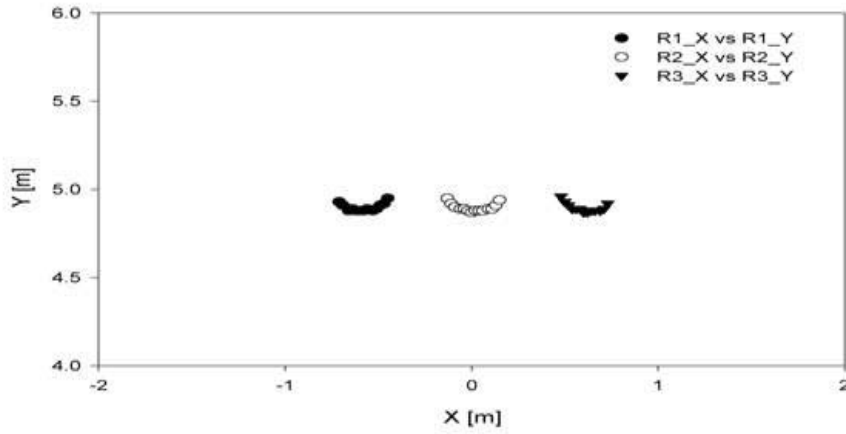
(c) Location of cylindrical reflectors at the 5 m distance from the laser sensor in the grid with *x=0 and v =0˚*

(d) Location of cylindrical reflectors at the 15 m distance from the laser sensor in the grid with *x=10 and v =30˚*
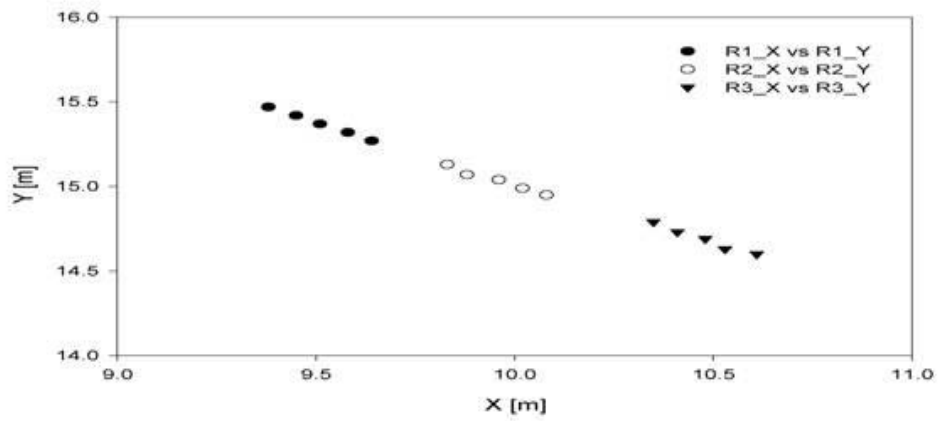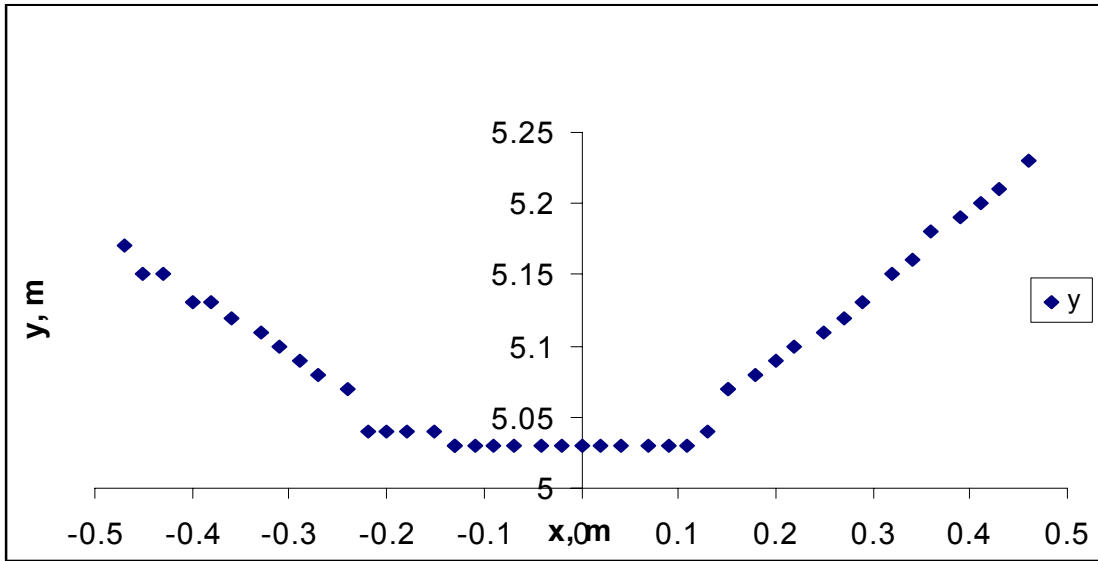
(e) Location of trapezoidal reflector at the 5 m distance from the laser sensor in the grid with *x = 0 and v = 0˚*
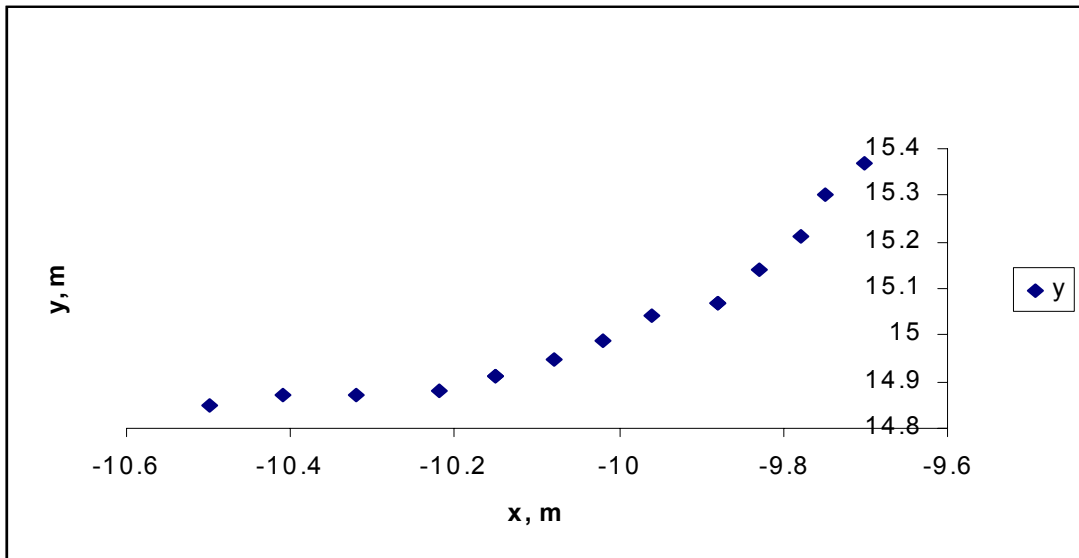
(f) Location of flat reflectors at the 15 m distance from the laser sensor in the grid with *x=-10 and v=30˚*

Fig. 6.5(a-f) Scanning profiles of different reflectors at 20 m x 20 m grid with different inclination angle *v*

6.6 Discussion

In the localization of landmark for approach navigation, the positioning accuracy was the maximum for trapezoidal reflector, but it had a problem of shape-fitting at the end of the grid and at the longer distance from the LRF. The intersection points could be detected easily using least square regression for the clusters of near distances. The position, and pose angle estimation was acceptable for the longer distances. The template matching of the flat rectangular reflector was better than cylindrical and trapezoidal reflector at the longer distances and at the end of the grid. The systematic error for line and circle parameters included systematic range error types: constant bias, bias increased linearly with distance, bias changing with the incidence angle of target surface, and laser beam. The error contribution also came from setting of light reflectors and laser plane misalignment on the surveyor tripod.

6.7 Conclusions

The basic experiment was conducted to characterize the LRF for outdoor navigation using reflectors. The shape of the reflectors and orientation angle were considered for the high accuracy positioning and calibration was performed for the inclination of object in real time operation. The precise positioning experiment is needed to confirm the approach accuracy using reflectors attached with the implement. From our preliminary experiment, it can be concluded that:

- The LMS 211 LRF can be implemented in the outdoor navigation using reflectors as artificial landmark.

- Out of three designs of reflectors, trapezoidal reflector had better accuracy then flat and cylindrical reflectors. The cylindrical reflector had the drawback of fitting data in the regular shape of circle from a longer distance.

- The flat reflectors were easy to attach with the implement, and the accuracy was satisfactory at the longer distances. It had the advantages in the appropriate template fitting than the cylindrical or trapezoidal shape. The precise experiment of the positioning accuracy with the flat reflector will be conducted to approach the implement on the field.

- The discriminated and localized landmark using reflectors could be used to navigate the tractor to the implement's position. Thus, the relative positioning method between the implement and the tractor is needed to develop for approaching.

Chapter 7

Navigation to Approach the Implement using Single Path

Approach to the implement to perform the hitching is one of the major aspects in agricultural safety context, and this approach to the object needs a robust positioning method. For this approach, relative positioning is essential. This is the geometrical disposition between a vehicle and objects. Typically, it relies on external references, such as beacons, reflectors or other environmental landmarks. If the position of these external references is known, then the position of the mobile element can be computed, usually with good accuracy. Suppose a tractor is deployed to pick up a loaded container in the field with a front loader. Since a farmer may vary the placement of the container, its position is not necessarily known in advance. Similarly, in many cases the relative position of an object is also requisite for approach. Absolute positioning has less practical value in these conditions. Dead reckoning is a simple method for determining the present position from the previous position and the traveling distance or speed and direction measured with internal sensors over a given length of time. Ishida (1998) developed a system equipped with ultrasonic Doppler speedometer and a fiber-optic Gyro. Though they reported that dead reckoning is accurate for short distances, it tends to accumulate observation errors; thus, for longer distances error correction with an external reference is needed.

7.1 Scopes and Objectives

In the last few years, researchers and manufacturers have placed emphasis on autonomous operations, including straight runs and turns at a row's end. Our vision is to concentrate on some other frequently essential agricultural operations. One of these is approaching an implement's position. In this aspect, robust positioning of the implement is prerequisite in the outdoor environment. The LRF is one of the promising means for robust positioning in outdoor applications with landmarks. Once an approach has been made with satisfactory accuracy using an LRF to determine the implement's position, hitching maneuvers can be performed with minimum human involvement and thus ensures safety during the coupling. Therefore, the specific objectives of this chapter can be summarized as follows:

- To develop a robust positioning method using LRF for an autonomous agricultural vehicle.

- To approach an implement by autonomous tractor using reflectors as artificial landmarks.

7.2 Development of Positioning Method for the Landmark-based Navigation

7.2.1 Positioning with a Single Reflector

The measurement model with a single reflector is shown in Fig 7.1. The position of the reflector was calculated on x-y coordinates while the vehicle was stationary; the LRF measured the reflector's position x_o, y_o and fixed it on the x-y coordinates. The reflector's position can be expressed as:

$$x_o = l_t \times \cos(\boldsymbol{f}_{lt}) + l_s \times \cos(\boldsymbol{h}_i) \tag{7-1}$$

$$y_o = l_t \times \sin(\boldsymbol{f}_{lt}) + l_s \times \sin(\boldsymbol{h}_i) \tag{7-2}$$

where (x_o, y_o) is the position of the reflector from the rear wheel of vehicle, $\boldsymbol{h}_i$ is the initial orientation angle of the reflector with respect to the LRF, and $\boldsymbol{f}_{lt}$ is the angle between the LRF and the center line of the tractor. For angular directions, the counter clockwise was considered as positive. At the initial condition, the vehicle was along the x coordinate, therefore, the yaw angle ($\boldsymbol{y}$) of the vehicle was considered zero. l_s and l_t are the distances from the reflector to the LRF, and from the LRF to the rear axle of the tractor, respectively. The geometrical relation between the LRF and the rear axle of the tractor can be expressed as follows:

$$\boldsymbol{f}_{lt} = \tan^{-1}\left(\frac{h_y}{h_x}\right), \qquad l_t = \sqrt{h_x^2 + h_y^2} \tag{7-3}$$

where h_x (=0.94 m) is the horizontal distance between the center of the rear axle and the LRF and h_y (=0.13 m) is the vertical distance between the centre of the rear axle and the LRF. The geometrical relationship for the yaw angle ($?$) between the LRF and the reflector can be expressed as:

$$\boldsymbol{q}_{rx} = \boldsymbol{y} + \boldsymbol{p}/2 + \boldsymbol{n} \tag{7-4}$$

where $?_{rx}$ is the geometrical angle between the reflector and the x axis. At the initial condition, $?_{rx} = p/2 + \boldsymbol{n}$, therefore, the yaw angle can be calculated as:

$$\boldsymbol{y} = \boldsymbol{q}_{rx} - \boldsymbol{p}/2 - \boldsymbol{n} \tag{7-5}$$
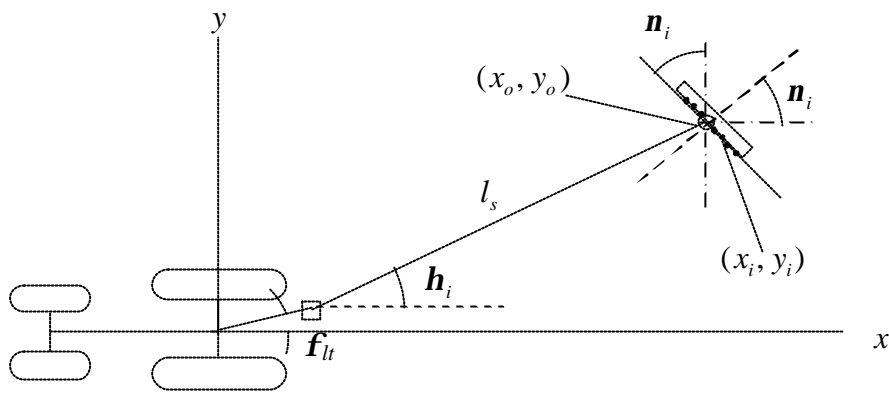
(a) Measurement view from the vehicle
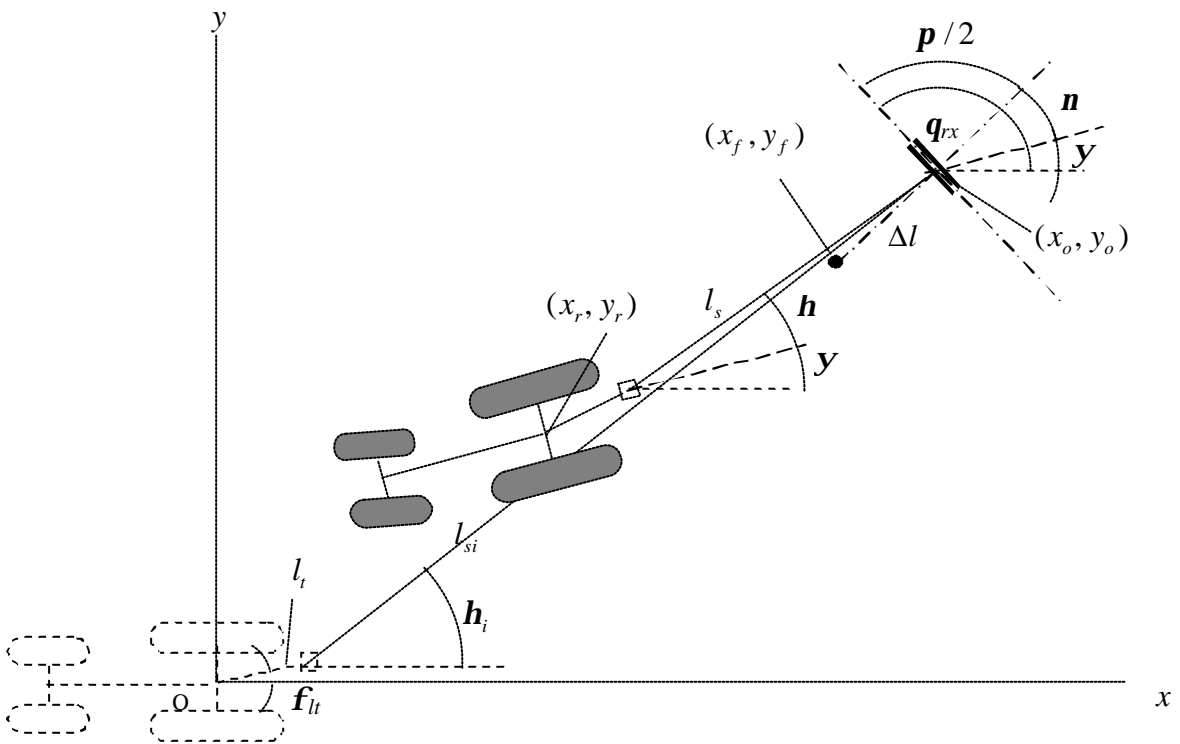
(b) Single reflector positioning model

Fig. 7.1 Laser measurement model for positioning of implement using reflector

The yaw angle can be found from the above relation or from the gyro sensor. We have observed while conducting experiments that the LRF was vibrated due to the inclination of the tractor in traveling. To avoid such noisy situations we preferred the gyro sensor to

provide the yaw angle. The final yaw angle $(\mathbf{y}_f)$ also can be calculated from the following relation:

$$\mathbf{y}_f = \mathbf{n}_i \qquad (7\text{-}6)$$

Since the reflector was attached to the implement, we kept a distance to avoid a collision between the implement and the top link of tractor. The vehicle's final position or the goal point was calculated using the following expressions:

$$x_f = x_o - \Delta l \times \cos(\mathbf{y}_f) \qquad (7\text{-}7)$$

$$y_f = y_o - \Delta l \times \sin(\mathbf{y}_f) \qquad (7\text{-}8)$$

where (x_f, y_f) is the final position of the vehicle. Δl is the distance between the object and the rear wheel center of the tractor at the target position. The trajectory to reach the goal point was estimated using the information of final position (x_f, y_f).

The position of the vehicle was calculated from the geometrical disposition of the implement while traveling towards the implement continuously and while maintaining orientation with respect to the object. The position of the tractor at the rear wheel center can be expressed as:

$$x_r = x_o + l_s \times \cos(\mathbf{h} + \mathbf{y}) + l_t \times \cos(\mathbf{y} + \mathbf{f}_{lt}) \qquad (7\text{-}9)$$

$$y_r = y_o + l_s \times \sin(\mathbf{h} + \mathbf{y}) + l_t \times \sin(\mathbf{y} + \mathbf{f}_{lt}) \qquad (7\text{-}10)$$

where (x_r, y_r) is the position of the centre of the tractor's rear axle.

7.2.2 Positioning with Two Reflectors

In approaching some objects, as when refilling a fertilizer applicator, it is much more convenient to use two reflectors, e.g., at either end of the hopper bar. The positioning system with two reflectors has been shown in Fig 7.2. The geometrical relationship between the LRF and the reflectors can be expressed as follows:

$$l_3 = \sqrt{(x_1 - x_2)^2 + (y_1 - y_2)^2} \qquad (7\text{-}11)$$

$$l_m = \sqrt{l_1^2 + \left(\frac{l_3}{2}\right)^2 - l_1 l_3 \cos(\mathbf{p}/2 - \mathbf{h}_1 + \mathbf{n})} \qquad (7\text{-}12)$$

$$= \sqrt{l_2^2 + \left(\frac{l_3}{2}\right)^2 - l_2 l_3 \cos(\mathbf{p}/2 - \mathbf{h}_2 - \mathbf{n})}$$

l_1, l_2, and l_3 are the distances from the first reflector to the LRF, from the second reflector to the LRF, and between the midpoints of the two reflectors, respectively. l_m is the distance
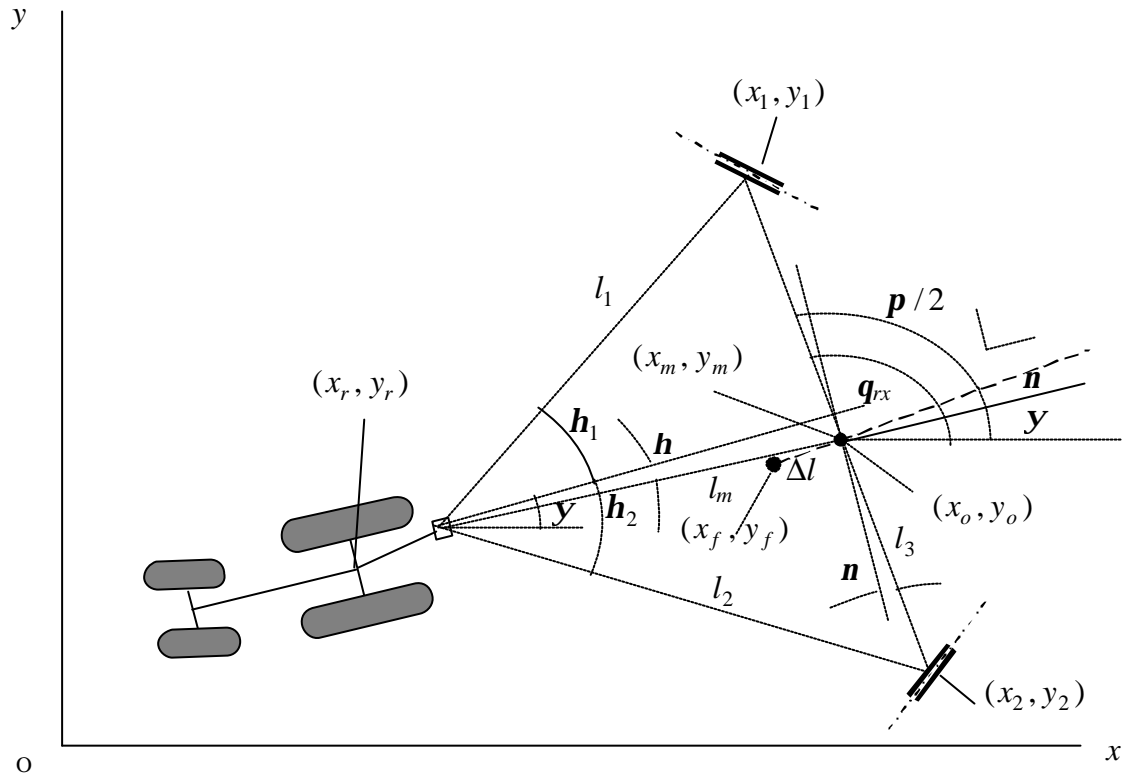
Fig. 7.2 Laser model with two-reflectors positioning method

from the midpoint of two reflectors to the LRF. (x_1, y_1) and (x_2, y_2) are the positions of the

two reflectors from the LRF. $\boldsymbol{h_1}$ and $\boldsymbol{h_2}$ are the orientation angles of the two reflectors with

respect to LRF. The midpoint of the two reflectors from the LRF can be estimated using

the following geometrical relations:

$$(x_m, y_m) = \left(\frac{x_1 + x_2}{2}, \frac{y_1 + y_2}{2} \right) \qquad (7\text{-}13)$$

$$\boldsymbol{n} = \tan^{-1}\left(\frac{y_2 - y_1}{x_2 - x_1} \right) \qquad (7\text{-}14)$$

$$\boldsymbol{h} = \tan^{-1}(y_m / x_m) \qquad (7\text{-}15)$$

where $\boldsymbol{h}$ is the orientation angle of the midpoint of the two reflectors with respect to the

LRF. While the vehicle was stationary, the LRF scanned five times and measured the

positions of the two reflectors and calculated the midpoint of the two reflectors, which was fixed as the goal point (x_o, y_o) on the x-y coordinates. The position of the goal point from the tractor can be expressed as:

$$x_o = l_t \times \cos(\boldsymbol{f}_{lt} + \boldsymbol{y}) + l_m \times \cos(\boldsymbol{h} + \boldsymbol{y}) \tag{7-16}$$

$$y_o = l_t \times \sin(\boldsymbol{f}_{lt} + \boldsymbol{y}) + l_m \times \sin(\boldsymbol{h} + \boldsymbol{y}) \tag{7-17}$$

The final position of the vehicle (x_f, y_f) was calculated by the same principle as the single reflector positioning method.

The position of the vehicle at the rear wheel of the tractor can be expressed using the following relations:

$$x_r = x_o + l_m \times \cos(\boldsymbol{h} + \boldsymbol{y}) + l_t \times \cos(\boldsymbol{y} + \boldsymbol{f}_{lt}) \tag{7-18}$$

$$y_r = y_o + l_m \times \sin(\boldsymbol{h} + \boldsymbol{y}) + l_t \times \sin(\boldsymbol{y} + \boldsymbol{f}_{lt}) \tag{7-19}$$

The trajectory generation algorithm was based on polynomial function to steer the vehicle to a target point, and is given details by Takigawa et al. (2002). The steering angle (d) was also calculated from the second derivatives of the polynomial function and can be expressed as:

$$\tan \boldsymbol{d} = l \cos^3 \boldsymbol{y} \left(\frac{2a}{x_f^2} + \frac{6bx}{x_f^3} + \frac{12cx^2}{x_f^4} + \frac{20dx^3}{x_f^5} \right) \tag{7-20}$$

where a, b, c, and d are the coefficients in the polynomial functions.

7.3 Experiment of Positioning Accuracy by Utilizing Flat Reflectors

We conducted experiments on a concrete surface using a grid of 6 m x 15 m. Two flat reflectors of 30 cm x 40 cm were placed over the two digital theodolites (Topcon DT 20S and DT 120). Reflectors were placed at every 3 m interval on the grid. The positional errors are shown in Fig 7.3(a, b, c, d). The error was increased at the end of grid with a ±30° orientation of the reflectors, since the number of data observed was minimal. The errors were less than 5 cm up to 15 m from the LRF.
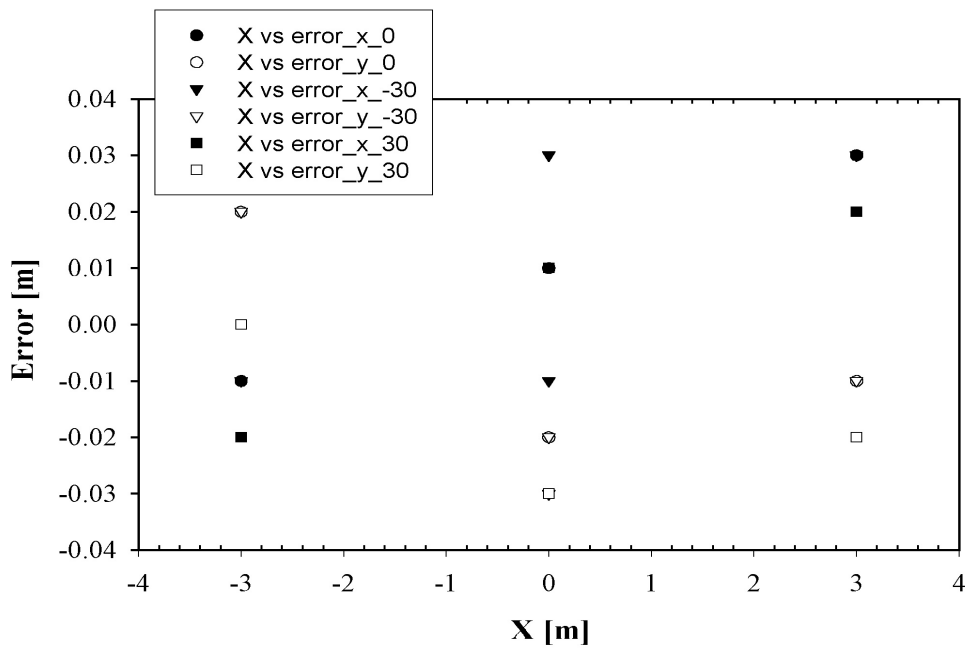
(a) At 6 **m** distance from LRF
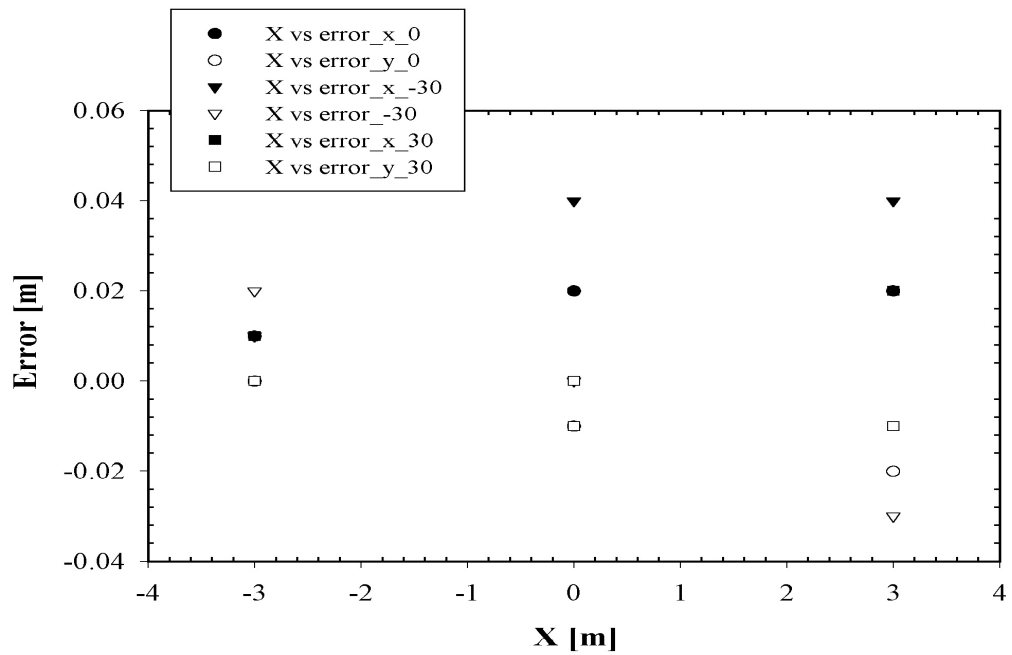
(b) At 9 m distance from LRF

94
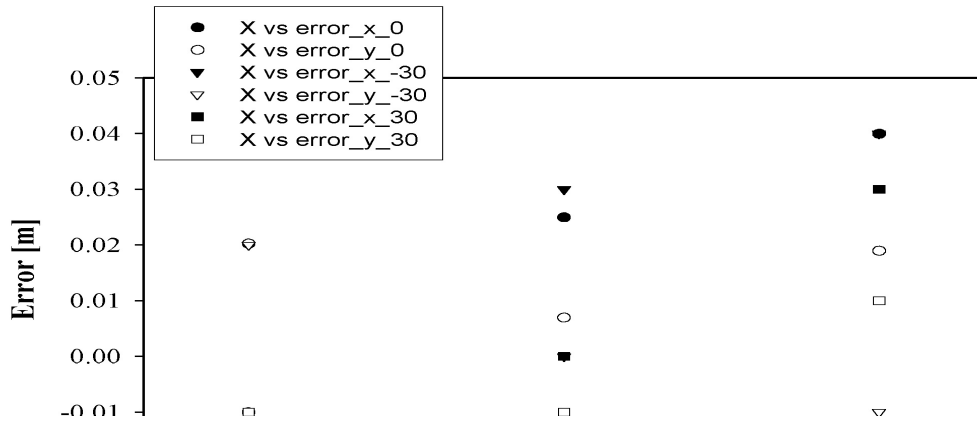
(c) At 12 **m** distance from LRF
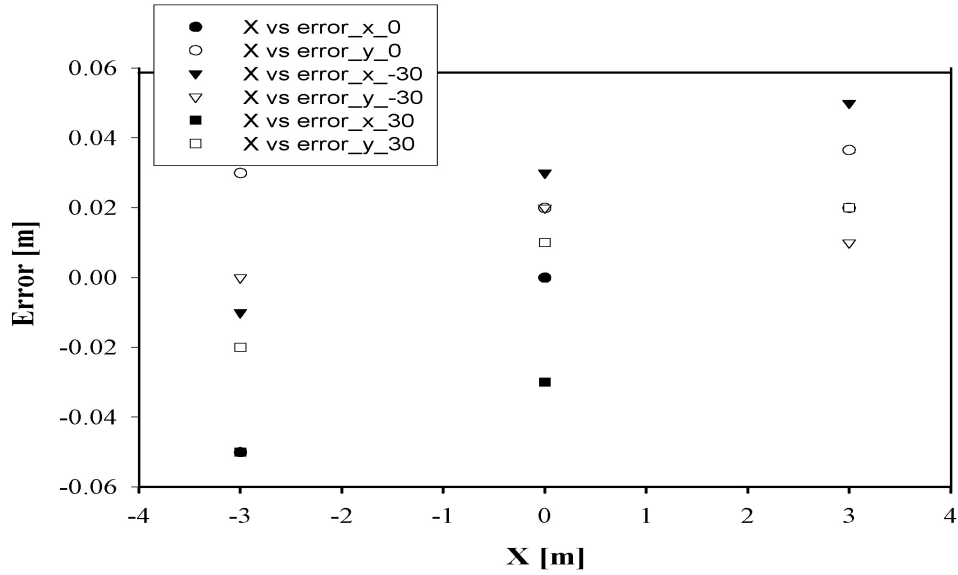
(d) At 15 **m** distance from LRF

Fig. 7.3 (a, b, c, d) Positional error of two flat reflectors at different inclinations on a 6x 15 m

grid

7.4 Approach Experiments to the Object

The principle for measuring the target position (x_f, y_f) was discussed in positioning sections. A concrete surface and a field covered with grasses were considered for the vehicle's approach to the implement. The experiments were conducted with a running speed of 0.10 m/s to verify the trajectory performance of the vehicle in the backward directions to approach the object with high accuracy. The higher speed causes the larger final lateral positional error (Junyusen et al., 2005). The position of the vehicle was calculated using LRF, and the dead reckoning method was employed to compare the navigation performance. The process of approaching the paddy harrow was as follows: first, the vehicle measured the relative distance between the tractor and the paddy harrow using flat reflectors; second, the current position was taken as the origin of the coordinates (x=0 m, y=0 m, $\boldsymbol{y}$=0°, $\boldsymbol{d}$=0°) and the goal point (x_f, y_f) was set just before the implement. A trajectory was generated that permitted the vehicle to run from the start point to its goal point. The stages of the approach are shown in Fig. 7.4. The directions at which photos were taken at different positions of traveling course are shown by arrows in Fig 7.5. A single reflector 30 cm wide and 100 cm height was placed behind the paddy harrow. The reflector was placed at approximately the centerline of the top link point of the paddy harrow, and the stopping distance was considered to be 50 cm from the center of rear axle of the vehicle to the reflector. Therefore, the tractor stopped when it reached the goal point just before the implement. In two-reflector positioning, the reflectors were 22 cm by 85 cm, and were placed at 110 cm apart from each other on the implement. We considered a stopping distance 2.0 m from the midpoint of the two reflectors to the center of rear axle of the vehicle to keep the reflectors within the field view of the LRF. The flow chart of the navigation procedure is depicted in Fig. 7.5

7.5 Results and Discussion

7.5.1 Results

On the concrete surface and the field covered with grasses, several trails were performed to confirm the method's accuracy. Figure 7.6 shows the experimental result from the concrete surface using a single reflector to approach the implement. The actual trajectory obtained with feedback control coincided with the theoretical trajectory. It can be seen that the proposed positioning method was able to generate the proper trajectory and navigated the

Fig. 7.4 Stages of approach toward the implement using experimental autonomous tractor
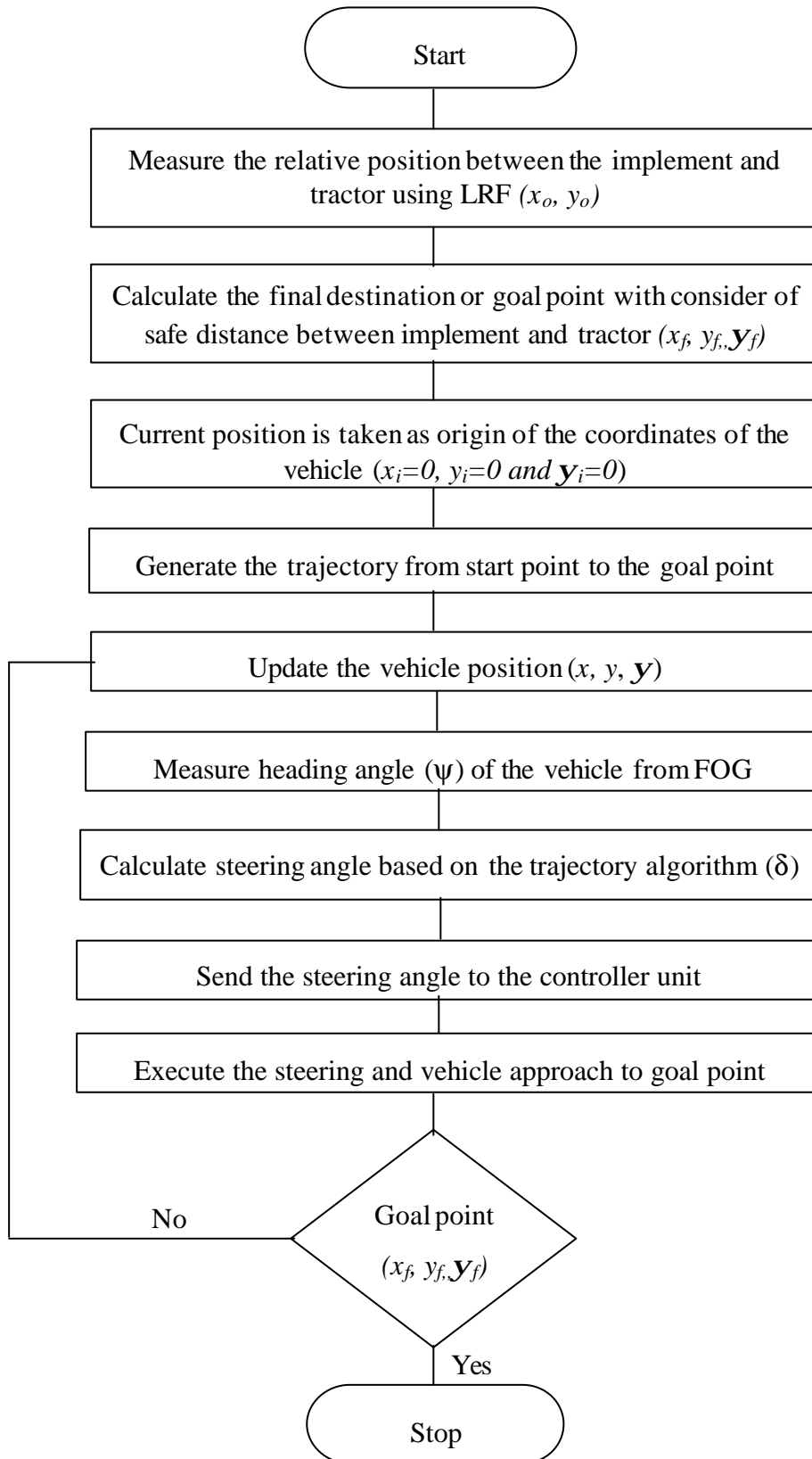
Fig. 7.5 Flow chart of navigation system to approach the implement in the single path
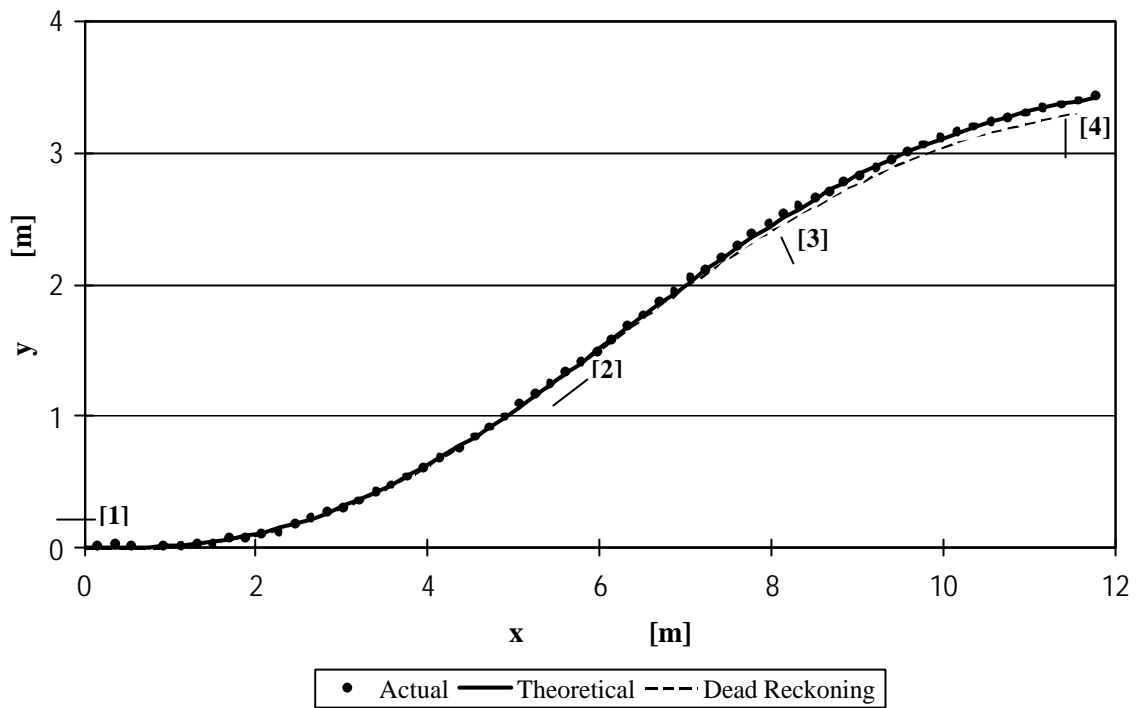
Fig. 7.6 Trajectories during approach to the implement using single-reflector positioning

on the concrete surface

Fig. 7.7 Trajectories during approach to the implement using single-reflector positioning
on the field covered with grasses

autonomous vehicle from the start point to the goal point by tracking the given curves accurately. In all trial runs on the concrete surface, it was observed that the positional accuracy of the approach to the implement at the target position calculated from the LRF data could be executed with a final lateral error within 1 cm and directional error less than 1°. In the middle of the traveling course, the errors were observed higher due to slower response of the controller. The feedback control minimized the error and guided the tractor to the final position within 1 cm accuracy. Figure 7.7 shows the experimental result for the grass surface using a single reflector to approach the implement. The actual trajectory obtained with feedback control coincided with the theoretical trajectory, with less than 1 cm lateral error and 0.7° directional error.

Figure 7.8 shows the theoretical and experimental trajectory for the concrete surface using the two-reflector positioning method. The final positional error at the goal point had a lateral error of 0.5 cm and directional error of 0.56°. The feedback control improved the tracking ability of the tractor according to the theoretical trajectory. Figure 7.9 shows the theoretical and experimental trajectory for the field covered with grasses using the two-reflector positioning method. The final lateral positional error at the target point was 2 cm and directional error was 0.5°. By comparison, the dead reckoning method had an error of 15 cm. This error occurred from wheel slippage; when wheel slippage occurred, the final positional errors were relatively higher and orientational errors increased significantly as well.

An attempt was made to examine the yaw angle or vehicle direction that could be obtained from the geometrical disposition between the LRF and a reflector. We assumed that better performance of the yaw angle from the LRF could eliminate the cost of the fiber-optic gyroscope. Figure 7.10(a, b, c, d) shows the experimental results between the yaw angles received from the gyroscope, the yaw angle estimated from the LRF and the calculated yaw angle. It was observed that the vibration of the LRF affected the yaw angle due to the inclination of the tractor while the tractor was traveling. Figure 7.11(a, b, c, d) shows the steering angle while traveling in the backward direction towards the implement. It was observed that the steering oscillation was higher due to larger feedback gains, which were selected for faster response of the steering controller.
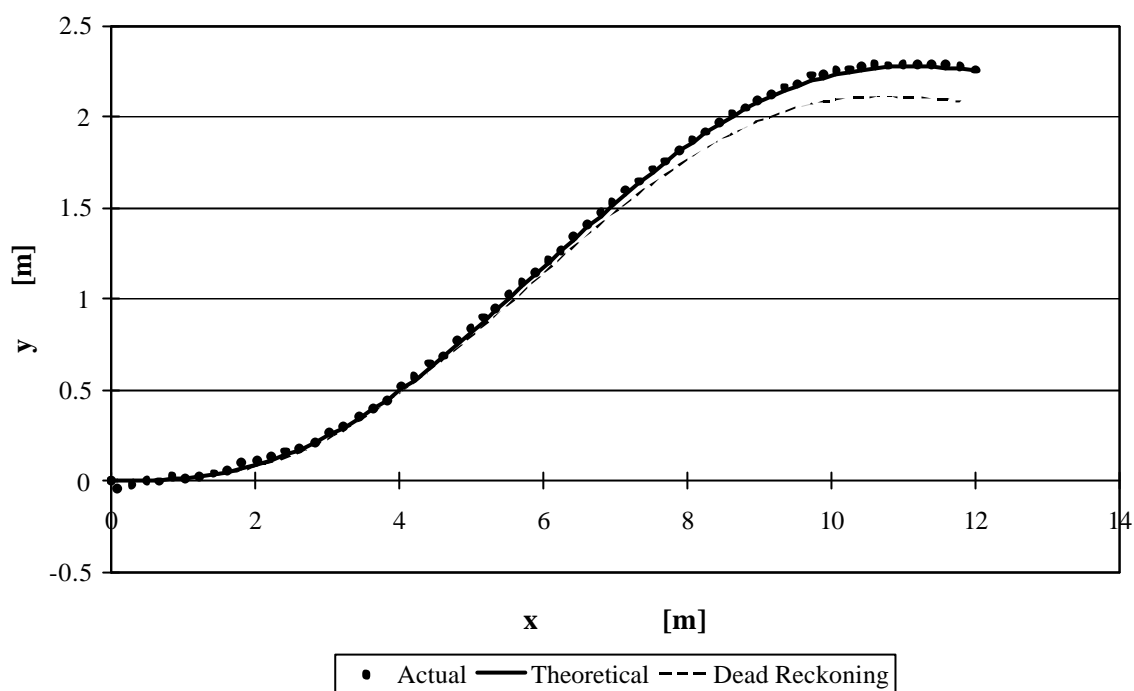
Fig. 7.8 Trajectories during approach to the implement with two-reflector positioning on

the concrete surface
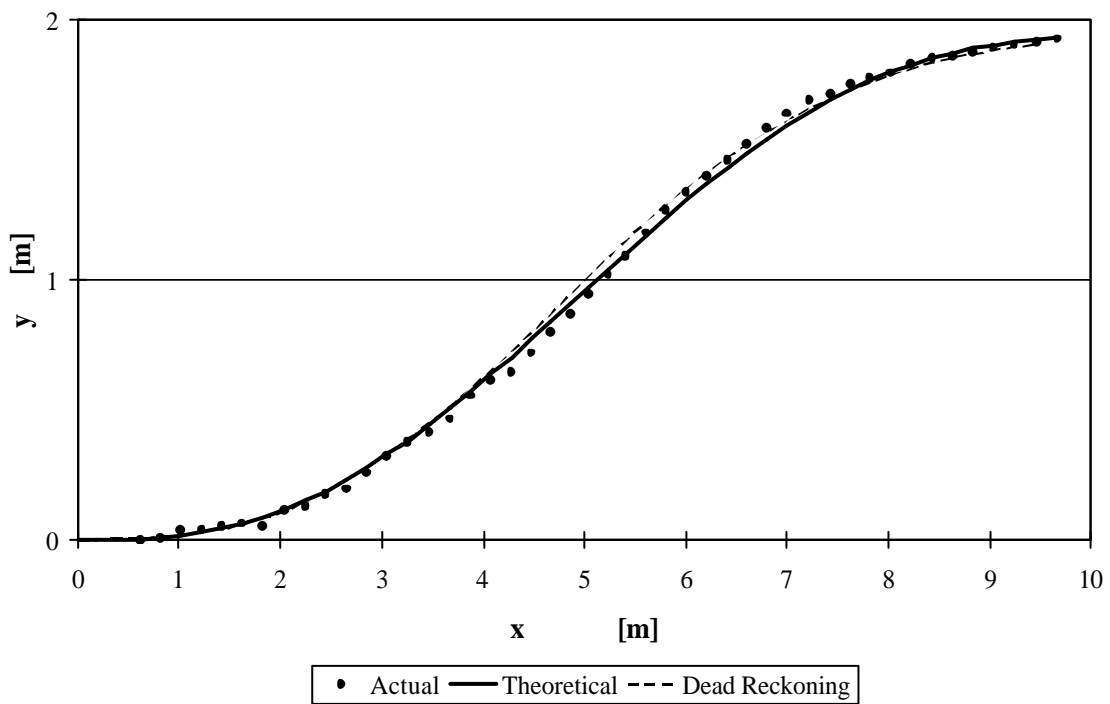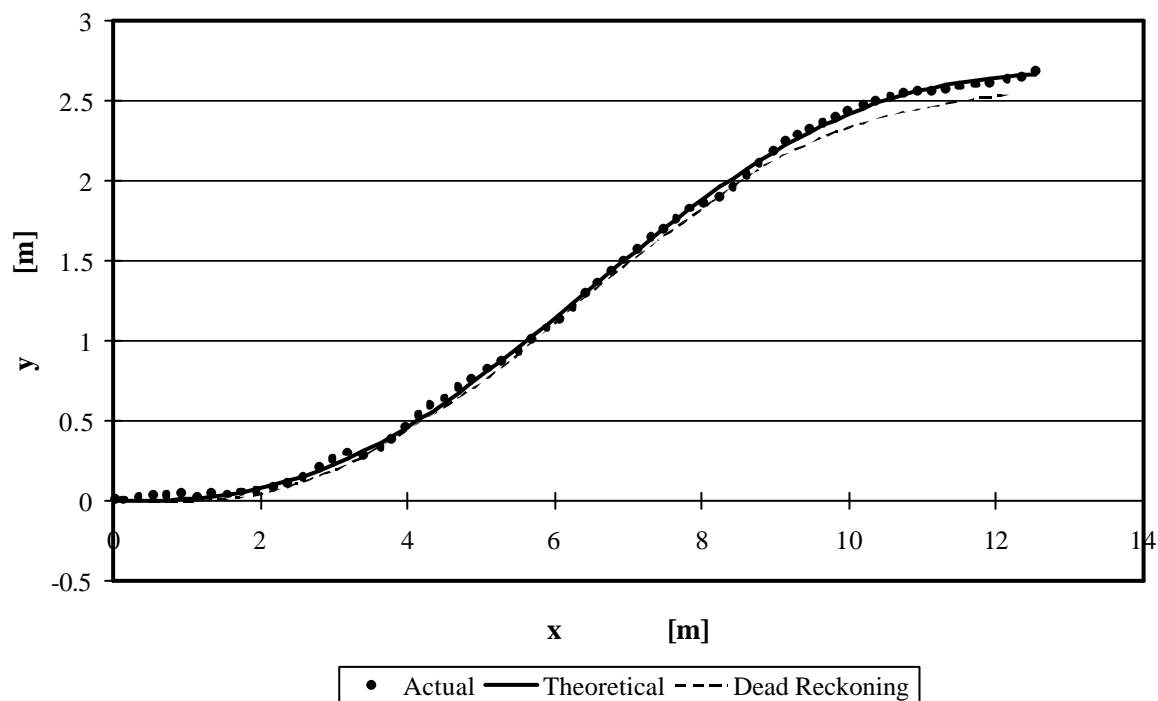

Fig. 7.9 Trajectories during approach to the implement with two-reflector positioning on

the field covered with grasses
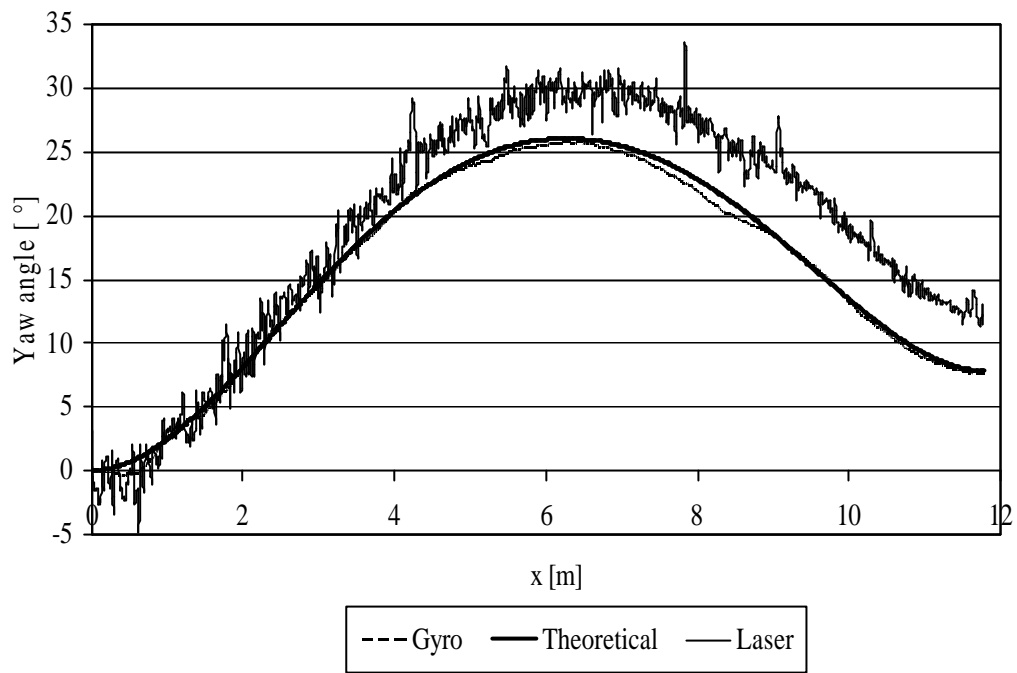
(a) Single reflector on the concrete surface
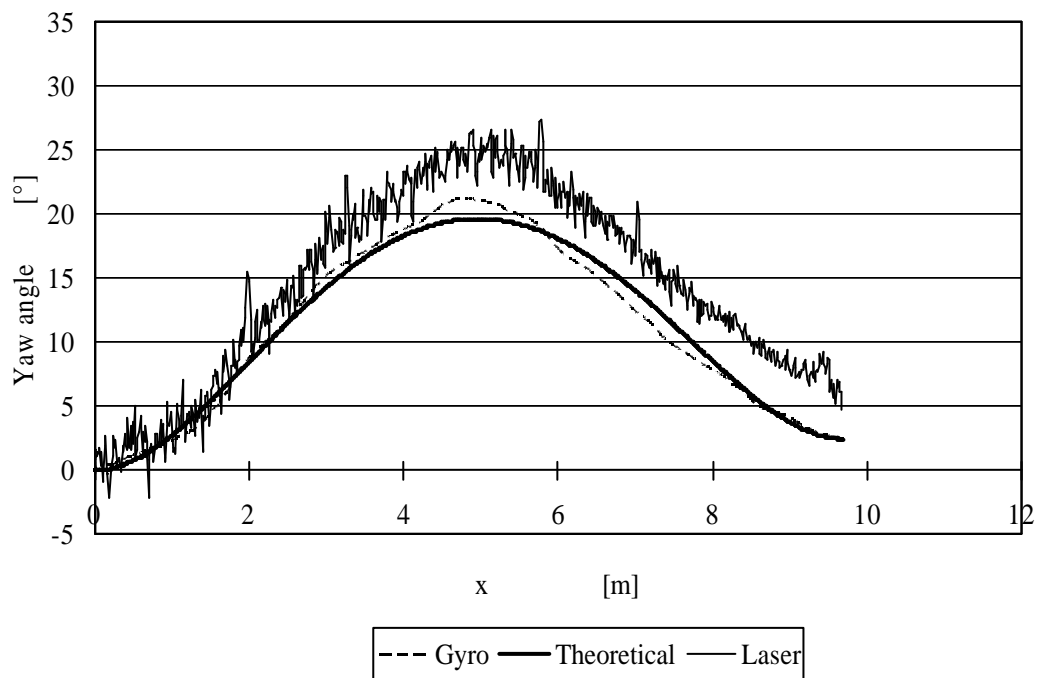
(b) Single reflector on the field covered with grasses
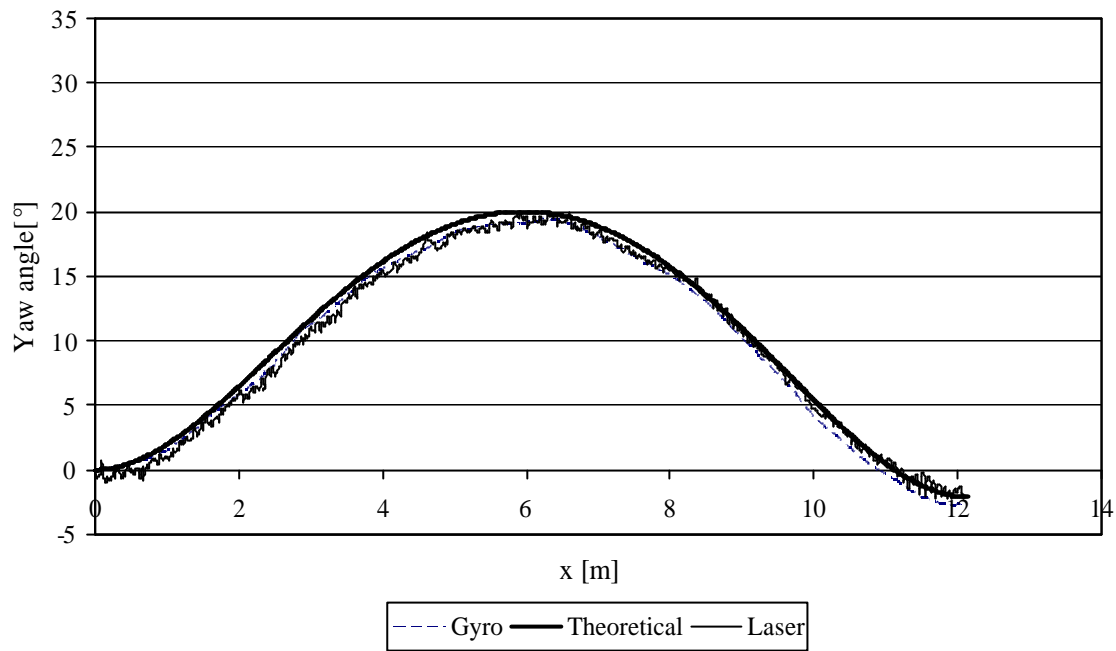
(c) Two reflectors on the concrete surface
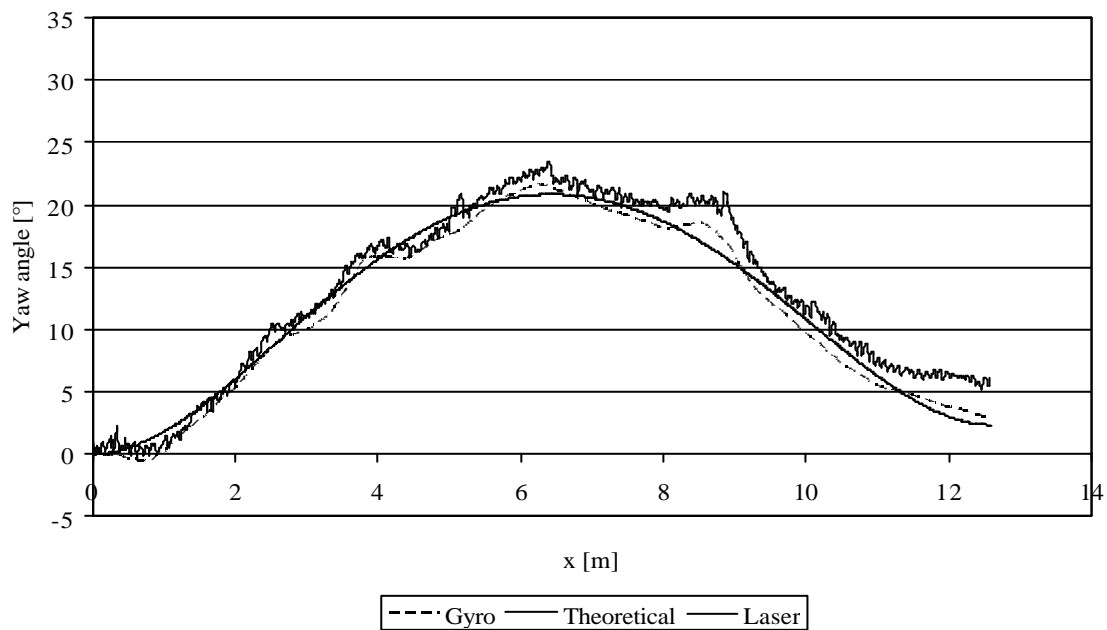
(d) Two reflectors on the field covered with grasses

Fig. 7.10(a-d) Comparison of yaw angle provided by gyro sensor and yaw angle calculated
from the geometrical relation between the LRF and reflectors at different conditions
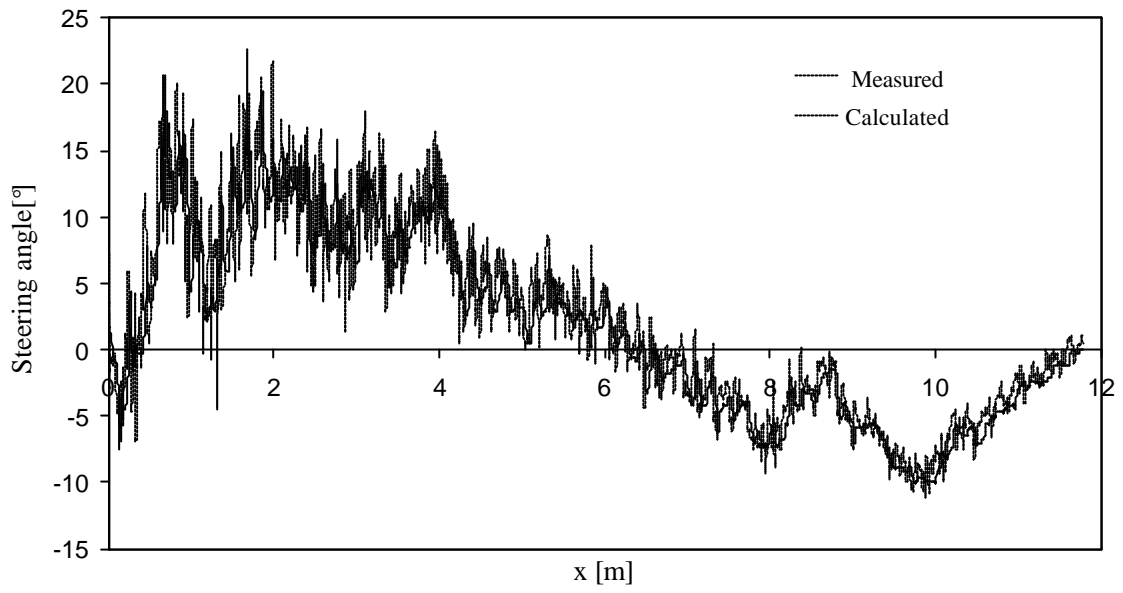
(a) Single reflector on the concrete surface
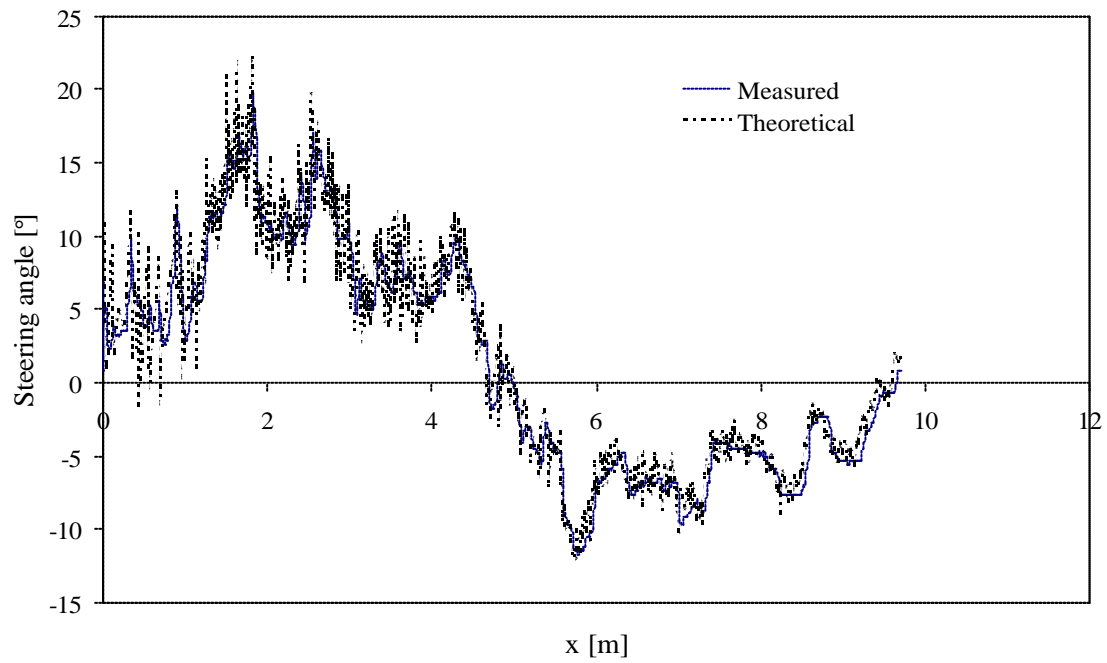
(b) Single reflector in the field covered with grasses
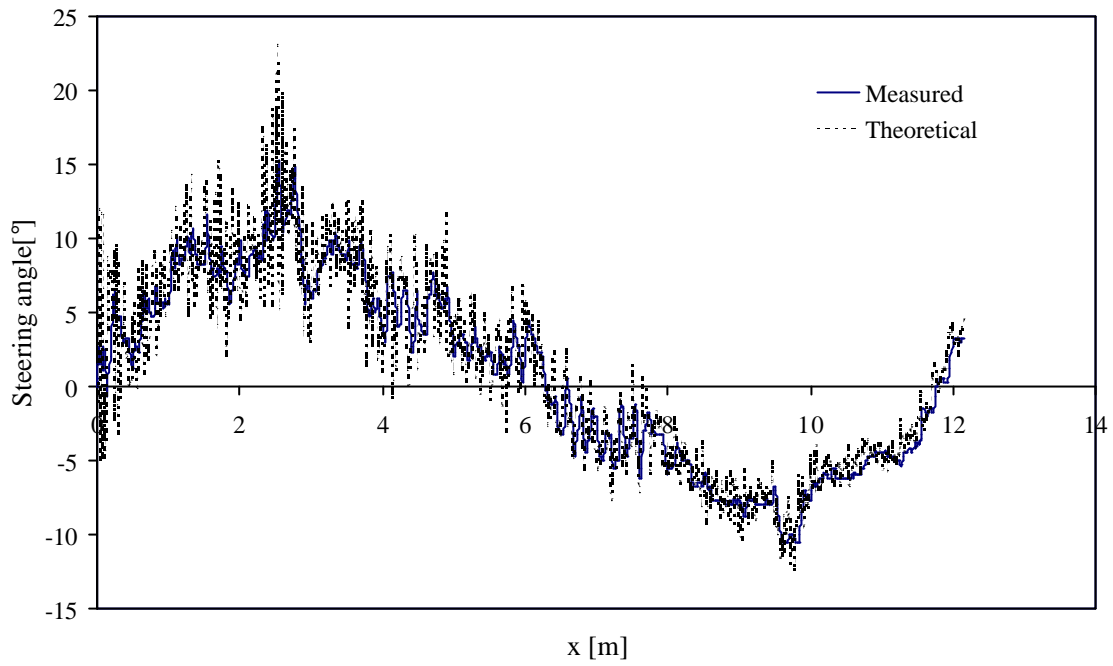
(c) Two reflectors on the concrete surface
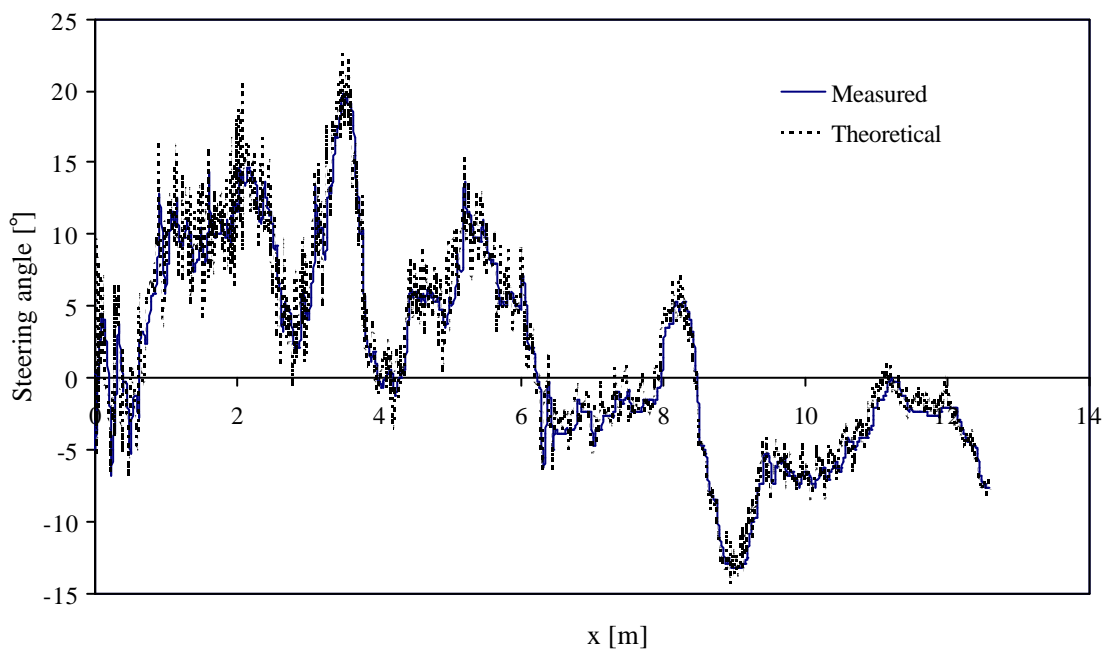
(d) Two reflectors on the field covered with grasses

Fig. 7.11(a-d) Comparisons of steering angles at different conditions for single and two reflectors on the concrete and grass surface

Smaller feedback gains in pole placement method caused the late response in the steering controller. On the concrete surface shown in Fig. 7.11 (a, c), the vehicle inclination was less than the field covered with grasses, which is shown in Fig. 7.11 (b, d). The field was undulating and surface was soft which caused the higher fluctuations of steering angle.

7.5.2 Discussion

The developed positioning method using an LRF and reflectors could be used to approach a farm implement with satisfactory accuracy. There was no significant difference in the results between single and two-reflector positioning in the short distances. In some of the cases, one reflector could not give an accurate position, and if we placed the reflector at the middle then it would become an obstacle to further travel. For example, in the road running, we intend to place two reflectors on the two sides of the road; hence, the LRF could estimate the two reflectors positions, calculate the midpoint, and guide the tractor accordingly.

In case of the single reflector, the autonomous tractor traveled towards the reflector, and the reflector was set on the middle of the implement. Therefore, the tractor could approach the implement without missing the reflector. The stopping distance 50 cm was selected by trail and error to reach in nearest position of the top link of the paddy harrow. Since the LRF has the field view of 100° from -50° to 50°, and single reflector was set on the middle of the implement, thus in the shorter distance it was always observable.

The two-reflector positioning method using LRF was more suitable in the longer distance. However, in case of approaching towards the implement, when the vehicle was

closer to the implement, then the possibility of missing the reflector was higher due to the field view of LRF. With 1 m apart of two reflectors on the implement, it was found by trail, 2.0 m stopping distance was suitable in the field view of LRF to observe the reflectors. The stopping distance may vary on implement's size and length.

The inherent problem of the LRF beam in distance metering is the increase of spot diameter with increase of distance. The measured points decrease with increase of distance, but the template fitting is more accurate the more measured landmark points there are. Another drawback of the LRF is that it has fan-like beam, which misses the reflector sometimes due to the undulation of the land under the vehicle; in such a case, a vertical axis motor could move the LRF. There is another way to solve this problem: when the reflector is missed in traveling course, then a change in the sensor-positioning mode could

help guide the tractor until the reflector becomes visible again. For example, when the reflector is not observable by LRF, then the dead reckoning method could navigate the vehicle until the reflector is observable. We have considered the limitations of the steering angle of the vehicle to be -40° to 40°, in wide offset and shorter distances. In such cases, traveling forward and then performing the approach would make it easier to generate the trajectory and guide the vehicle to the goal point. Therefore, multi-path navigation would be required with a combination of Cartesian and polar path planning.

The results of the field experiment confirmed that the developed positioning method using an LRF could be used for other landmark-based navigation tasks such as parking inside a yard, refilling the hopper with fertilizer, following a vehicle, and picking up loaded containers in the field, as well as other agricultural operations requiring precise approach maneuvers.

7.6 Conclusions

1) The positioning method using the LRF could distinguish the reflectors from other objects in the outdoor environment. The positioning algorithm successfully navigated the vehicle to the implement's position.

2) The positional accuracy of the approach to the implement fell within a lateral error of 1 cm and directional error of less than 1° using a single reflector on both a concrete surface and a field covered with grasses. In the two-reflector positioning method, the approach to the implement was performed within a lateral error of less than 1 cm for a concrete surface and 2 cm for a field covered with grasses; the directional error was less than 1° for both surfaces.

3) The developed positioning method could be implemented in other essential approaching: parking of tractor inside the yard, fertilizer refilling, loading and unloading of the containers, where the path planning is based on multiple segments.

Chapter 8

Navigation for Approach Composed of Multiple Paths

Because of constraints in a vehicle's motion, there is a practical reachable area for a single direction run. Human drivers switch running directions to attain a desired position with minimum effort using forward backward approaches. Similarly, in approaching of implements or objects using autonomous tractor has the limitations for the positioning sensors in the navigation scheme. Navigation that switches running directions frequently requires switching of positioning methods, because the applicable area of positioning sensors is usually limited. The principle can be understood from the fact that when a vehicle is entering a garage, the vehicle should change from GPS-based positioning to a landmark detection-based method. Agricultural operation routinely requires forward and backward approaches. Suppose a tractor needs to approach an implement located beside the tractor. A skilled driver usually moves the tractor forward to a place from which the implement is accessible, and then approaches the implement by backing up. While the approach is being made, the operator observes the current position of the vehicle and makes appropriate steering adjustments. Once an approach has been done properly and the tractor is outfitted with the appropriate implement, it can till, plant, weed, fertilize, spray, haul, mow or harvest. Another example is parking the tractor inside the yard while the tractor is parallel to the yard. As frequently observed in parking, the driver may have to make a 90° turn in the forward direction and then back the vehicle into the parking place. Other, similar maneuvers are required in many agricultural operations. In most cases described above, since the position of the destination is usually not given on a map, the vehicle or its driver must find and locate the place. Thus, an autonomous vehicle should utilize both absolute and relative positioning effectively. As depicted in Fig. 8.1, in the process of hitching an agricultural implement, a vehicle goes straight forward or makes a turn to a position where the implement is observable. This process will be done based on absolute information from a map; then the approach to the implement must be done by using an adequate relative sensor.
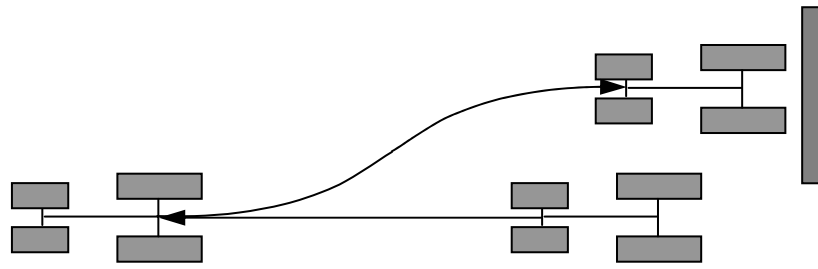
(a) Approach to the implement
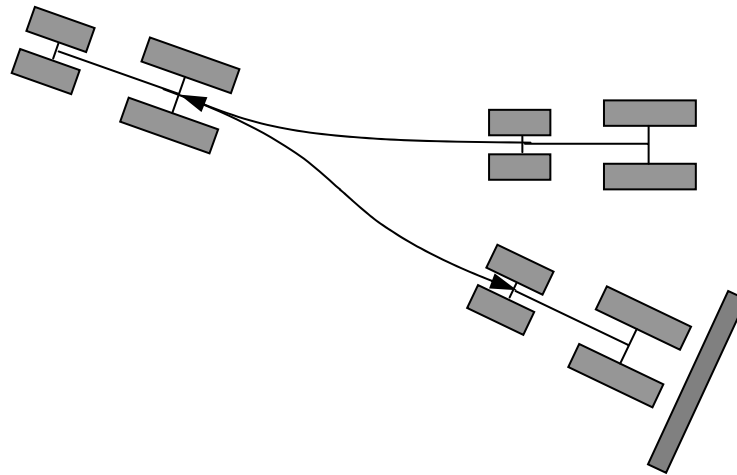
(b) Approach to the implement
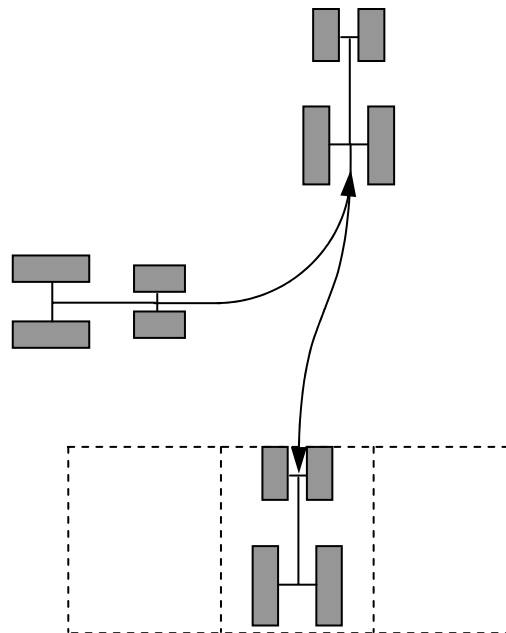
(c) Parking of tractor inside the yard

Fig. 8.1 Different forward and backward approaches in agricultural operations in both Cartesian and polar coordinates

8.1 Scopes and Objectives

In the existing research on agricultural robotic vehicles, few studies have addressed approaches composed of multiple paths. Most of the researches are related to straight runs in the field and turns at a row's end. Although this research covers sensor selection during navigation, path selection and planning, few studies in the robotic field have been conducted for outdoor localization in the context of performing an approach.

Ultrasonic sensors have been widely used in indoor applications (Elfes A., 1987), but they are not adequate for outdoor applications due to range limitations and bearing uncertainties. Stereoscopic (Drocout et al., 1999) omni-directional systems have been used in indoor localization applications. This type of sensor is based on a conical mirror and camera that returns a panoramic image of the environment surrounding the vehicle. Although it is a promising technology, the complexity of its poor dynamic range makes this technique unreliable for outdoor applications. In the land navigation, an appropriate combination of dead reckoning and LRF can be used to obtain a reasonable prediction of the trajectory of the vehicle (Sukkarieh et al., 1999).

Although RTK-GPS is getting popularity due to its centimeter level of accuracy, but it has the limitations for signal interruptions by walls or trees and RTK-GPS cannot use in the indoor navigation. In some of the agricultural operations inside the greenhouse, RTK-GPS does not give any practical information. Ohno et al. (2002) found that RTK GPS was not suitable for moving vehicles, as positioning initializing was often flawed as a result of "cycle slip". Once RTK GPS began initialization, the receiver had to remain stationary to finish the initialization; even though RTK GPS has an OTF (On the Fly) function, it is not always effective in a walkway environment among buildings or trees. Another drawback is that GPS does not measure the orientation of the target. Significant work has been devoted to the use of range sensors for location purpose both in structured environment and in outdoor applications. Jensfelt et al. (1999) addressed localization using position information where updating the position of the vehicle was based on the determination of the transformation between the position of the robot and the laser measurements. Guivant et al. (2000) presented a design for a high-accuracy outdoor navigation system based on standard dead reckoning and outdoor LRF (SICK LMS 200). Beacon design and location of landmarks were also discussed in relation to the desired accuracy and required area information.

Few researchers are investigating what we believe to be the central problems in the autonomous farm vehicle: approaching the implement position during coupling, and parking inside the yard after completion of operation. These approaching needs the maneuverability accompanied with switching of running direction for the autonomous vehicle. The positioning method, which was developed in the previous chapter, could be implemented to solve the above problems. Thus, the specific objectives of this chapter can be summarized as follows:

- To conduct field tests by forward and backward guidance of tractor to approach the implement with enabling the switching of sensor during the navigation course, while one sensor could not suffice for the operation.

- To develop a basic navigating scheme to park an autonomous tractor inside a yard and test its performance.

8.2 Theoretical Consideration

The basic positioning method using LRF and dead reckoning were described in detail in the previous chapter, which reported navigation following a single path and confirmed that LRF positioning could guide the tractor to the implement's position with high accuracy. The present chapter considered multi-path tracking accompanied by forward and backward motion switching, and switching of sensors and coordinate-based reactive path planning.

8.2.1 Transformation of Coordinates for Navigation of Tractor

In autonomous vehicle research, two levels of planning occur. One level of planning called global planning, which is based on global coordinates and examines the whole world; an autonomous vehicle can plan its paths from one point to the next dependent point upon this world. Information is usually given on a map. Another level of planning is local or reactive planning based on local coordinates; it sets out a short path for the vehicle to traverse based only on the environment surrounding the vehicle, and typically uses only a detection sensor. Integrated navigation systems measure the position of the vehicle with respect to a local reference, and then transform the output into global coordinates.

In our navigation scheme, navigation is performed by repeating point-to-point movement; i.e., segmented path tracking. In each segmented movement the vehicle controller generates the local coordinates at the start point by taking the centerline of the vehicle as the X coordinate, and the start point as the origin as shown in Fig. 8.2. The direction of the
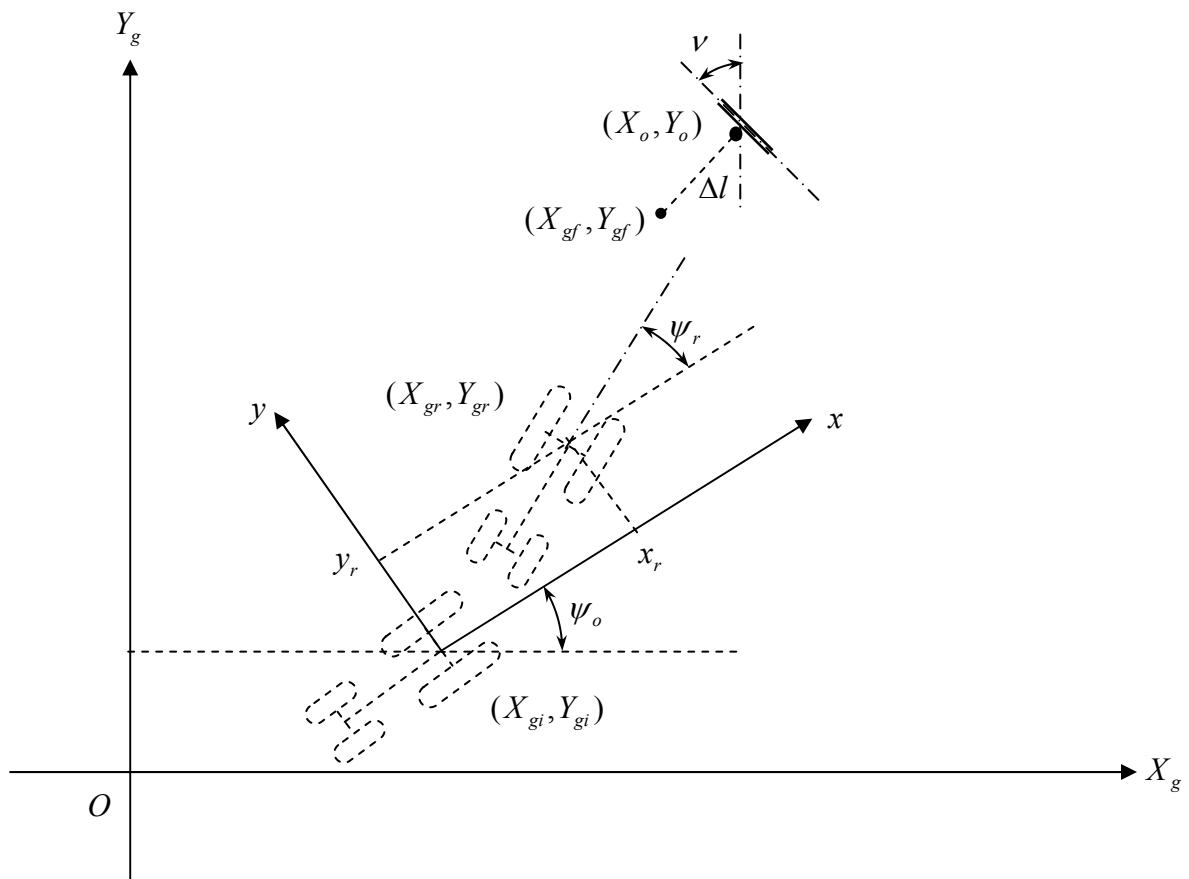
Fig. 8.2 Tractor positioning method on the global coordinates of the map

X coordinate coincides with the direction of movement. When the global coordinates of the destination are known, it is easy to convert the coordinates to those in the local coordinates, hence enabling navigation. The navigation for approaching the implement with local planning to enable the navigation from the start point to the implement's position is performed by using an actual size autonomous tractor. In approaching, position of the implement is unknown. In our navigation process, we emphasized on the reflector position, which is attached with the implement. Since we activated the reflector bit for the LRF, therefore, the LRF could easily recognize the reflector from the environment. When the reflector position is known, consequently, the position of the implement could be known, and the reflector becomes an artificial landmark for the implement (target). Thus, at the starting point, the vehicle should locate reflectors and then set local coordinates as shown in Fig. 8.2. Once the positions of the reflectors are acquired, the vehicle can calculate its

own position and orientation with respect to the local coordinates from continuous observation of reflectors with the LRF. This means that the vehicle locates implement position by a measurement at the start point, and then calculates its position during navigation. To enable the GPS navigation using global planning system, the position of the target, i.e, the implement and the parking positions should be known in advance. In such a case, LRF could recognize the object, using reflector from the environment. While the position of the implement is known, the switching of sensor would be useful to enable the GPS for the global planning system. On the other hand, global to local planning system is required while the GPS receiver could not get the signal from the satellite. In case of approaching, the relative positioning sensor needs to activate. Again, when the vehicle enters and leaves from the parking yard, the GPS receiver may not get the signal from the satellite due to walls and roof inside the yard. Switching of sensors is also required to change the positioning mode in the above situations. For example, dead reckoning method could be used until the GPS receiver get the signal from the satellites, and approaching could be performed by switching GPS or dead reckoning to LRF based positioning method. Therefore, the switching of sensors may need in global planning system for different operational aspects.

In the multi-sensor based navigation system, we made some assumptions to approach the implement using multiple paths for different positions of the implement. If the vehicle runs forward direction using an absolute positioning sensor in a considerable distance more than 5 m, than the reflector could be observable, while the implement is besides the tractor and the reflector is not visible by LRF due to 100° field view of the LRF. In the similar way, for the polar to Cartesian path planning, when the reflector is inside the yard, and locates the parking lot, the tractor could travel the considerable radial distance more than 3 m, then the reflector inside the yard would be visible.

When designing a multi-sensor navigation system, it is necessary to relate information from different sensors to a single set of coordinates for navigation planning. The local coordinates fixed on the tractor are given by the following expressions:

$$x_r = \left(X_{gr} - X_{gi}\right)\cos\psi_o + \left(Y_{gr} - Y_{gi}\right)\sin\psi_o \tag{8-1}$$

$$y_r = \left(Y_{gr} - Y_{gi}\right)\cos\psi_o - \left(X_{gr} - X_{gi}\right)\sin\psi_o \tag{8-2}$$

where (x_r, y_r) is the vehicle position at the current point in local coordinates, (X_{gi}, Y_{gi}) is the initial position on the map, and (X_{gr}, Y_{gr}) represent the current position in global

113

coordinates. ψ_o is the initial yaw angle in global coordinate. The expressions for yaw angle and final target position at the goal point were as follows:

$$\psi_f = \psi_{gf} - \psi_o \qquad (8\text{-}3)$$

$$\psi_{gf} = v_i \qquad (8\text{-}4)$$

$$X_{gf} = X_o - \Delta l \cos \psi_{gf} \qquad (8\text{-}5)$$

$$Y_{gf} = Y_o - \Delta l \cos \psi_{gf} \qquad (8\text{-}6)$$

where ψ_f is the yaw angle at the final position in local coordinates and ψ_{gf} is the yaw angle at the final position of the vehicle in global coordinates. v_i is the inclination angle of the reflector while the vehicle at the static position. (X_{gf}, Y_{gf}) is the final position of the vehicle in global coordinates. (X_o, Y_o) is the position of the reflector from the rear wheel of the vehicle. Δl is the distance that can be set as the safe stopping distance between the implement and the center of the rear axle of the tractor. The global coordinates on the map were estimated by the following expressions:

$$X_{gr} = X_{gi} + x_r \cos \psi_o - y_r \sin \psi_o \qquad (8\text{-}7)$$

$$Y_{gr} = Y_{gi} + x_r \sin \psi_o + y_r \cos \psi_o \qquad (8\text{-}8)$$

$$\psi_g = \psi_r + \psi_o \qquad (8\text{-}9)$$

where ψ_g is the yaw angle in global coordinates and ψ_r is the yaw angle of the vehicle at the current position in local coordinates.

8.2.2 Trajectory Tracking Control on Cartesian and Polar Coordinates Systems

In the path-following task, the controller gives a geometric description of the assigned path, with either Cartesian or polar coordinates. Cartesian paths are used for x-y coordinates in straight path planning and trajectory generation using polynomial functions. In some of the operations in which vehicles need to execute a greater than 90° turn, Cartesian path planning is impossible to implement; hence, polar path planning (r, θ) is required (Fig. 4.3). Here r denotes radius or the distance between the center and the center of the rear axle of the tractor, and θ is the turning angle with respect to the center. Switching the navigation mode from polar to Cartesian and Cartesian to polar is also required for operational aspects. Since four-wheel vehicles have constraints, known as non-holonomic constraints, a nonlinear control theory was developed by Takigawa et al. (2002) to generate a trajectory

that would permit a vehicle to run from a start point to its goal within these constraints by using both Cartesian and polar coordinates.

8.3 Field Experiment

The computer-controlled 15.4 kW actual-size autonomous tractor described in the chapter 4, was used in the experiments. Experiments were conducted on a concrete surface at a traveling speed of 0.10 m/s to verify the trajectory performance during forward-backward movements.

8.3.1 Forward and Backward Approaches to an Agricultural Implement

In the experiment, two sectional trajectories were designed in Cartesian coordinates. The first trajectory for forwarding was designed for travel from the origin (0 m, 0 m) to the given point on global coordinates. The positioning method was dead reckoning. When the tractor had traveled 6 m it stopped autonomously. The positioning was then switched from dead reckoning to LRF-based positioning. The LRF scanned the range -50° to 50° in real time to measure the position of the implement, which was marked with a reflector. After locating the implement, the tractor approached the implement by tracking the designed trajectory together with real-time feedback to minimize the tracking error. Figure 8.1(a) and (b) show two different situations for approaching the implement using forward and backward movements.

8.3.2 Parking inside the Yard

For parking inside the yard, two trajectories were designed using polar and Cartesian coordinates. The first trajectory on polar coordinates to execute a 90° turn forward was performed by the dead reckoning method. Then, LRF was used for backing into the parking space by referring to one reflector planted in the yard. Figure 8.1(c) shows the parking process of the tractor inside the yard.

8.4 Experimental Results and Discussion

Figure 8.3 shows the positions of the autonomous tractor during the approach to the implement. In the Fig. 8.4, the flow chart of approaching while the reflector was not observable and tractor moved forward to view the reflectors. Figure 8.5 shows the directions at which the photos were taken at different positions in the traveling course are shown by arrows, and the trajectories obtained in forward-backward approach to the implement. The start point (SP), midpoint (MP), and goal point (GP) of the moving of
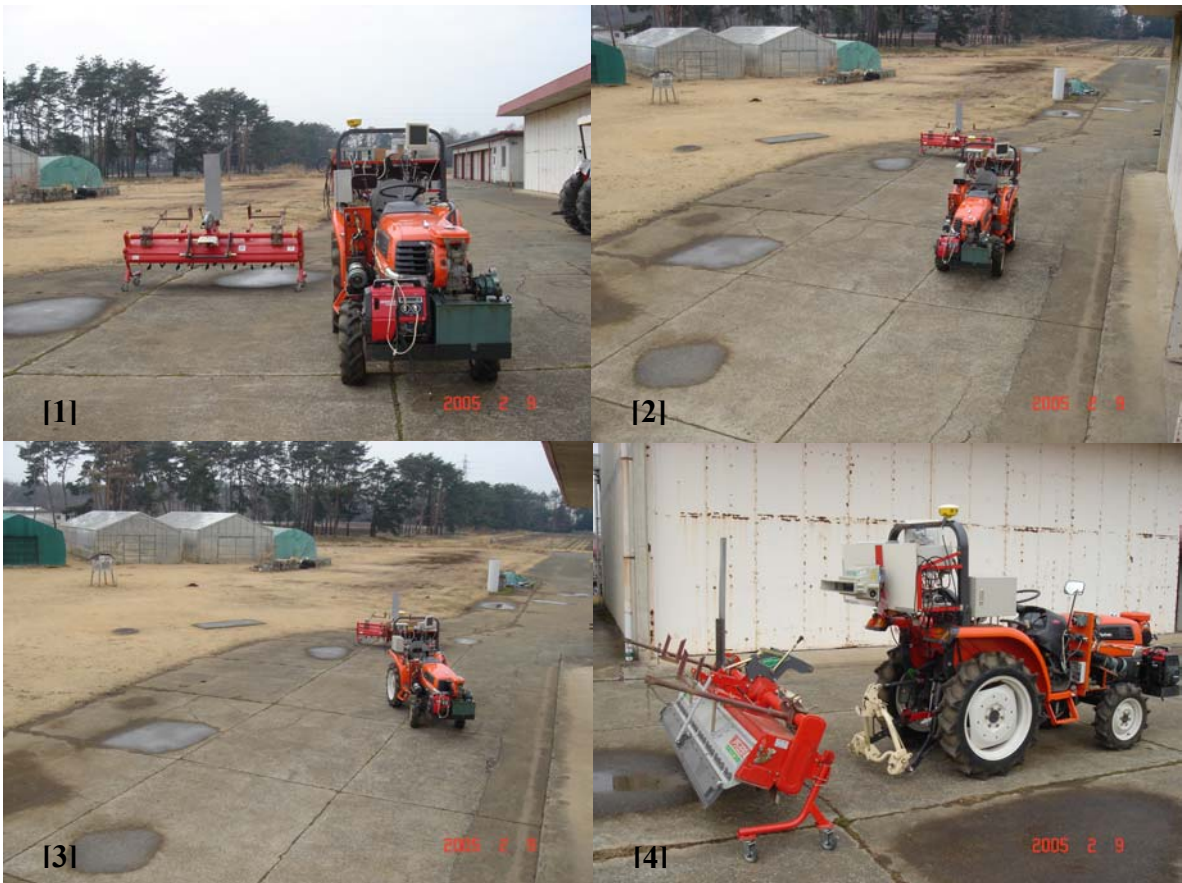
Fig. 8.3 The forward-backward approach to the implement on the concrete surface

Start

Reflector is observable in 100° of LRF.

Yes → Activate the LRF to approach the implement in the backward movement.

No

Current position is taken as origin of the coordinates of the vehicle ($x_i=0$, $y_i=0$ and $\psi_i=0$, target $=0$)

Execute the dead reckoning position method in the forward movement of 6 m in the y direction to view reflectors. *($x_f=0$, $y_f=6$)*

Measure the relative positions between the implement and tractor using LRF *(x_o, y_o)*

Calculate the final destination or goal point with consider of safe distance between implement and tractor *(x_f, y_f, ψ_f)*

Generate the trajectory from start point to the goal point

Update the vehicle position (x, y, ψ)

Measure heading angle (ψ) of the vehicle from FOG

Calculate steering angle based on the trajectory algorithm (δ)

Send the steering angle to the controller unit

Execute the steering and vehicle approach to goal point

Target =1
(x_f, y_f, ψ_f)

No   Yes

Target=2
(x_f, y_f, ψ_f)

No   Yes

Stop

Fig. 8.4 Flow chart for approaching the implement with the combination of dead reckoning and the LRF

117

vehicle are indicated in Fig 8.5. The distance of forward movement was set at 6 m to bring the position of the implement into the LRF's range. First, the vehicle traveled 6 m in a straight line. The lateral error of forward movement at the stopping position was about 1 cm and the directional error was 0.5˚. After the backward approach to the implement, the positional error at the goal point was about 2 cm and the directional error was 2˚. Figure 8.6 shows a comparison of the measured orientation angle and the theoretical angle in forward and backward motion. Figure 8.7 shows the steering angle during the forward-backward approach. Figure 8.8 shows the turning of the tractor with small lateral distance (x =6 m, y =1 m) traveled in the forward motion using the dead reckoning method. The lateral error was less than 1 cm and the directional error was less than 0.5˚. In the backward motion when LRF was used to locate the implement and the measured trajectory followed the theoretical trajectory. At the goal point, the lateral error was less than 8 cm and directional error was less than 4˚. The lateral error and directional error were higher due to the implement position in the y direction, placed at 3.58 m. In such a case, the controller could not smoothly follow the theoretical trajectory due to feedback limitations, and the magnitude of the feedback output for the backing-up motion was higher than for the forward motion. A comparison of yaw angles in wide offset turning is shown in Fig. 8.9.
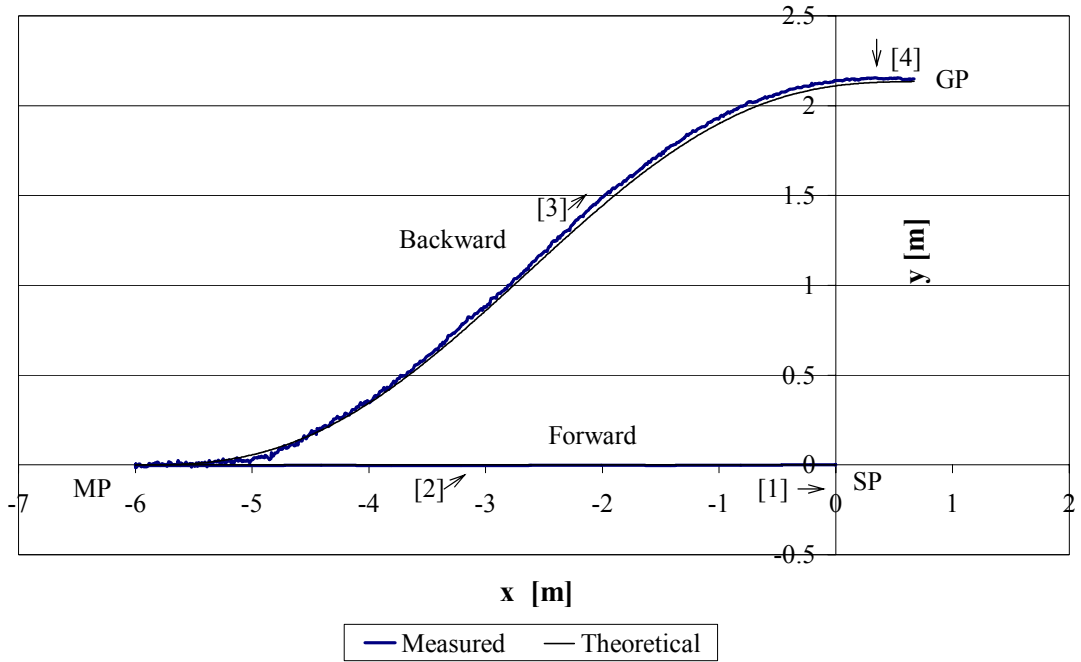
Fig. 8.5 Trajectories during forward-backward approach, SP (Start Point), MP (Midpoint),GP (Goal Point)
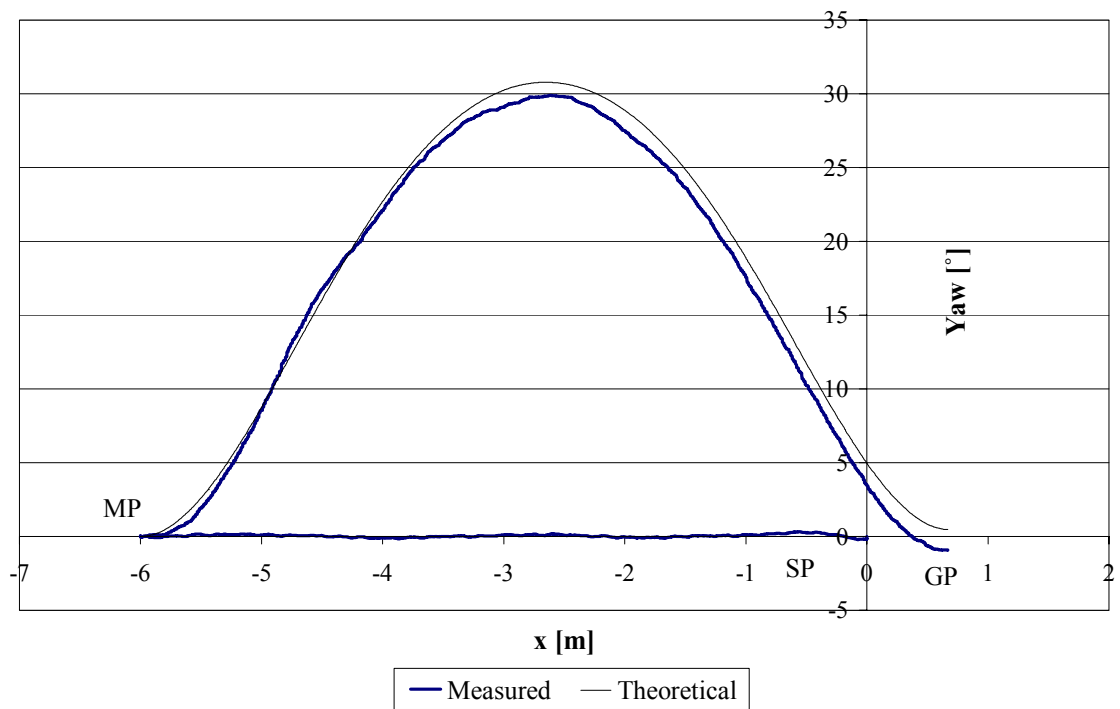
Fig. 8.6 Comparison of theoretical and measured yaw in forward-backward approach of tractor
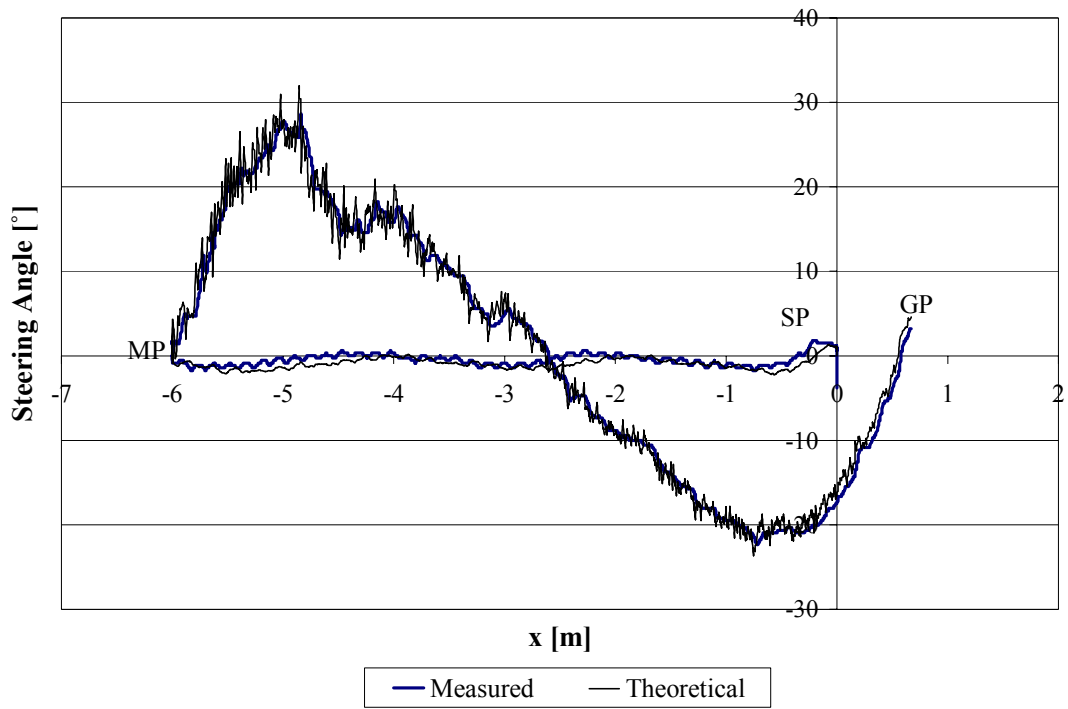
Fig. 8.7 Comparison of tractors steering angle during forward and backward travel
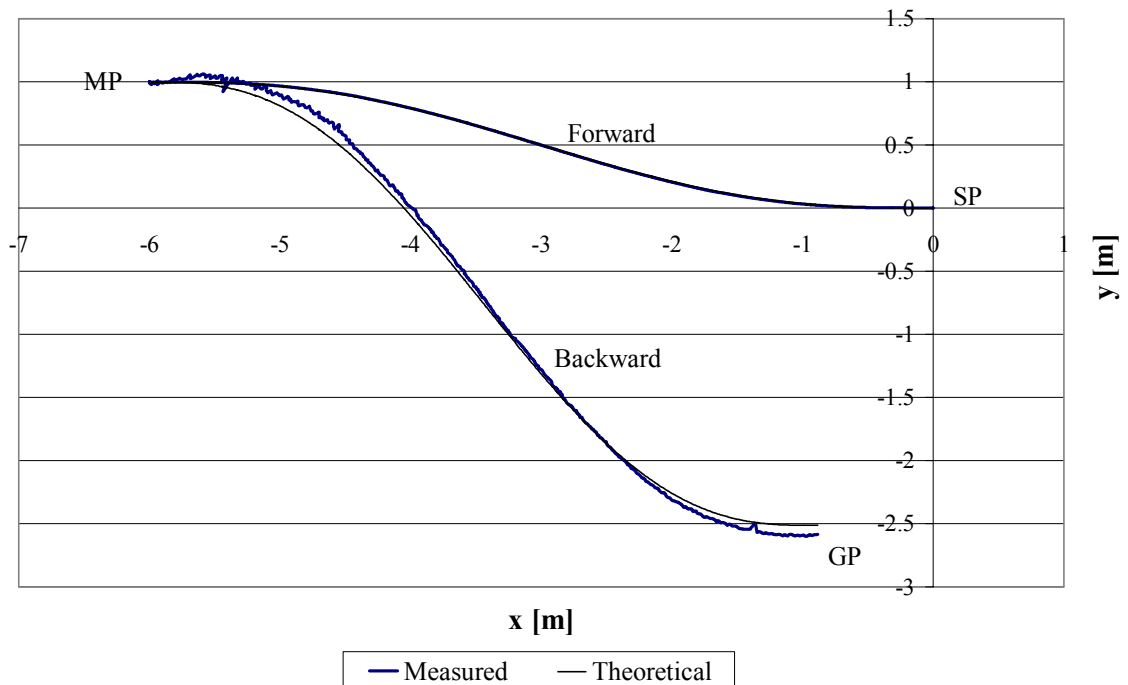
Fig. 8.8 Trajectories during forward-backward approach to the implement in wide turning
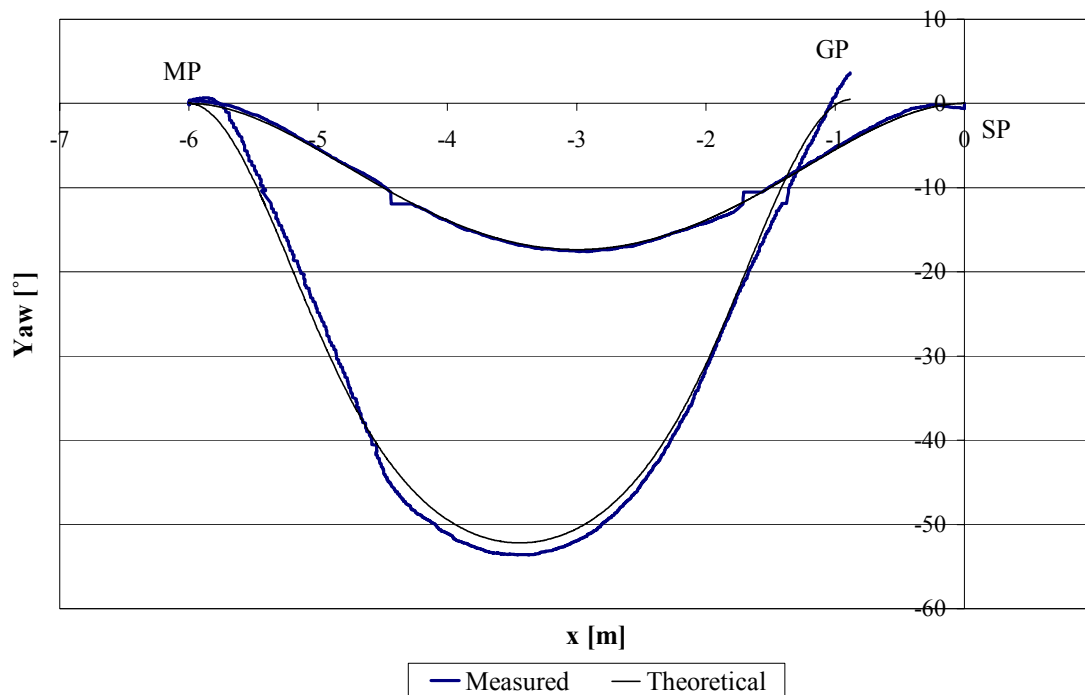
Fig. 8.9 Comparison of theoretical and measured yaw in forward-backward approach of
tractor in wide turning

Figure 8.10 shows the parking of the tractor inside the yard and Fig. 8.11 shows maneuver
using a combination of polar and Cartesian coordinates. In the forward motion (3 m, 3 m),
a 90° turn was done using the dead reckoning sensor while backward motion was
performed to park the tractor in the parking space between a combine harvester and truck.
The LRF could identify the reflector inside the yard from other objects. In the forward
movement of the 90° turn, the final x directional error was less than 3 cm and the lateral
error was less than 1 cm. The final directional error was less than 1.5°. In the Fig. 8.11,
some noisy data occurred due to the change of the coordinates from the polar to Cartesian
in the traveling course. Filter could be used to eliminate the noisy data. In the backward
motion toward the yard, final lateral error was less than 1 cm and the directional error was
less than 1° at the goal point inside the yard. Comparisons of yaw performance are shown
in Fig. 8.12; and this figure is referenced in a local path due to the change of coordinates
from the polar to Cartesian. The start-to-midpoint path planning was done in polar
coordinates, and the yaw increased up to 90°; then Cartesian path planning was executed
until the tractor arrived at the goal point. The allowable error at the final position depends
on the operational aspect.

Fig. 8.10 Parking of the tractor inside the yard
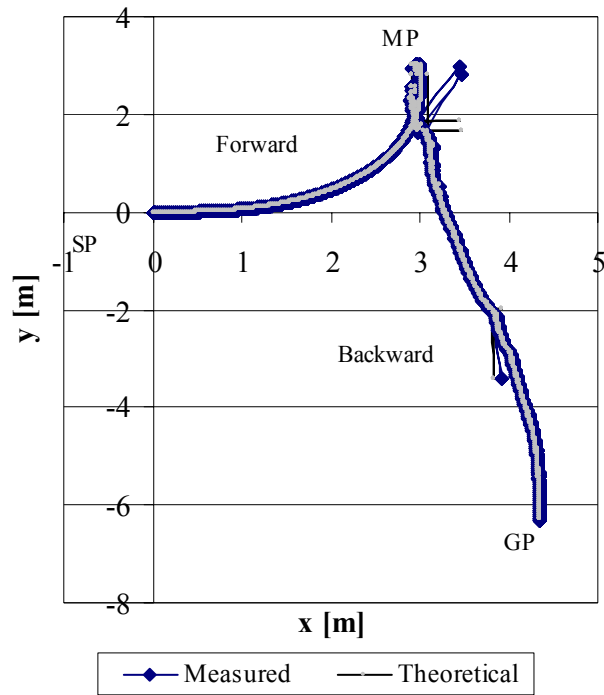
Fig. 8.11 Forward 90˚ turn in polar coordinates and backward parking in Cartesian coordinates
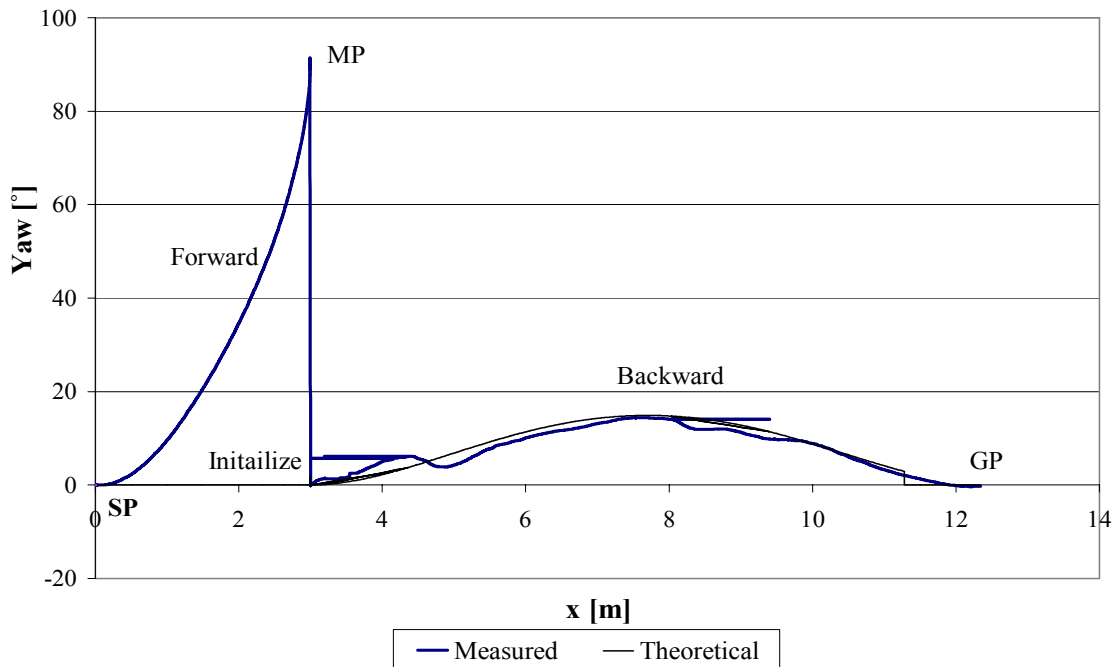
Fig. 8.12 Comparison of theoretical and measured yaw in forward 90˚ turn and backward parking of tractor in the yard

Generally, for ordinary approaching, loading of the container, fertilizer refilling, and follow-up of the vehicle requires less than 10 cm error at the target position and directional error should be less than 5°. Our developed positioning method using LRF could be able to navigate to the target position within final lateral error of 2 cm and directional error of 1°. Therefore, for general approaching at the target position, the positional accuracy was satisfactory. In view of mind to hitch the implement with the tractor at the top link position the maximum accuracy is required. In this situation, our further experiment will introduce another proximity ultrasonic sensor to guide a small distance between the target position and the top link position of the implement with the maximum accuracy to hitch the implement with the tractor using several forward-backward approaches.

The limitation behind of this study was the observable range of reflectors by the LRF. Since LRF has the field view of -50° to 50°, therefore the path planning had done based on field view of the LRF. To overcome this limitation, a 180° or 360° field view LRF could be used. In case of wide offset turning, autonomous tractor has the limitations to reach at the target position properly. This occurred due to the steering angle limitation and the slower response of the controller to support the feedback system. Moreover, the magnitude of the feedback output in the backing up motion was higher than the forward motion. To overcome the wide offset turning problem, several backward-forward approaches could help to guide the tractor at the implement position.

8.5 Conclusions

Although the automation of agricultural robots in outdoor applications is challenging, researchers are making steady efforts in this field to reduce human drudgery in agricultural operations. To contribute to this progress, attempts were made in two key areas of autonomous operations using combinations of sensors and coordinate systems: first, approaching an implement, and second, parking a tractor inside the yard. It was clear that in the broad range of demands of agricultural operation, no single device could suffice for all purposes. We need to engineer sensors for particular applications, rely on multi-sensors systems with complementary failure modes, and fuse data to maximize accuracy and reliability. The works still left is the possibility of automating coupling, using a modified quick coupler to hitch the implement with several forward-backward approaches. In addition, high accuracy GPS is needed to implement for road running with a developed positioning system to carry the implement to the field.

Chapter 9

Automatic Hitching of Implement

In agriculture, working with tractors is characterized by a frequent change of implements or tools. This coupling and uncoupling may create a risk of injury. To reduce this risk the quick couplers have been developed. However, they work properly, if the tractor can approach the implement or tool closely enough to bring the quick coupler into action. If the operator fails to drive the tractor into the catching area where the automatic couplers come into actions, the operator or another person often steps into the space between the tractor and implement to adjust the implement position and to connect the coupling elements manually. This is a situation of high risk of injury.

To ensure the safety and reduce drudgery of farmers automatic hitching of implement with the tractor is required in agricultural automation. This automatic hitching with the implement is one of the challenging works for the researchers and manufactures. In the last few years, researchers and manufacturers have placed emphasis on autonomous operations, including straight runs and turns at a row's end. Few of the study, addressed about the coupling possibility that are related with human interface (Graf and Jahns, 1996; Lang and Harms, 2002). The vision of this chapter is to concentrate on approaching an implement's top link position and hitch the implement with the autonomous tractor. Once tractor is outfitted with the appropriate implement automatically, it can ensure safety and reduce drudgery. Figure 9.1 shows some of the 3-point hitch agricultural implements, which are frequently use in agricultural operation.
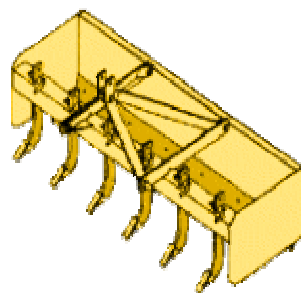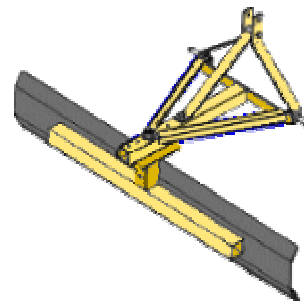
(a) Scrapper   (b) Rake
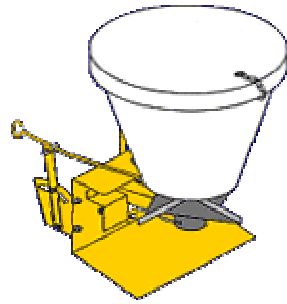
<div align="center">(c) Fertilizer applicator   (d) Digger</div>

<div align="center">Fig. 9.1 Some 3-Point hitch agricultural implements</div>

9.1 Three Pont Hitch Couplers

This is the device, which facilitates the connection of the tractor three-point linkage to the implement. American Society of Agricultural Engineer (ASAE) recommended several types of three-point hitch couplers.

9.1.1 U-Frame Coupler

This part of ISO 11001 specifies the essential dimensions for the attachment of three-point hitch implements to agricultural wheeled tractors equipped with a three-point free link hitch according to ISO 730-1, ISO 730-3 or ISO 8759-2, and a U-frame hitch coupler. The three-point hitch coupler systems constitute a special method of implement mounting. The hitch couplers are an additional component located between the three-point linkage and the implement, making it possible to hitch and unhitch from the operator's seat. Due to the special construction and function of hitch couplers, it may be necessary to vary the length of the links indicated in the referenced standards. A-frame coupler system is a one-phase implement coupler where the three-point linkage of the tractor (ISO 730-1, ISO 730-3 or ISO 8759-2) is fitted with a U-frame and the implement has the provisions to be mounted to the frame. Hitching and unhitching can be operated from the tractor operator's seat.

9.1.2 A-frame Coupler

It specifies the essential dimensions for the attachment of three-point hitch implements to agricultural wheeled tractors equipped with a three-point free link hitch according to ISO 730-1 or ISO 8759-2, and an A-frame hitch coupler. The three-point hitch coupler systems constitute a special method of implement mounting. The hitch couplers are an additional component located between the three-point linkage and the implement making it possible to hitch and unhitch from the operator's seat. Applies to category 2 of agricultural wheeled tractors as defined in ISO 730-1.

9.1.3 Link Coupler

This coupler specifies the essential dimensions for the attachment of three-point hitch implements to agricultural wheeled tractors equipped with a three-point free link hitch according to ISO 730-1 or ISO 8759-2, and a set of link couplers. The three-point hitch coupler systems constitute a special method of implement mounting. The hitch couplers are an additional component located between the three-point linkage and the implement making it possible to hitch and unhitch from the operator's seat. Link coupler applies to categories 1 to 3 of agricultural wheeled tractors as defined in ISO 730-1.

9.2 Triangle Hitch

The triangle hitch consists of three parts, two of which make up an interlocking triangle. In the Fig. 9.2, an example of triangle hitch is illustrated. The first part is triangle-shaped receivers that can be either bolted or welded onto most three-point hitch implements. The second part is the triangle-shaped tractor unit that attaches to the two lower lift arms of the tractor three-point hitch. The last part is a specially designed hydraulic cylinder, which replaces the third link. Once the triangle-shaped tractor part is aligned underneath the implement triangle-shaped receiver, a combined lifting of the tractor hitch with the correct pivoting supplied by the hydraulic cylinder allows the triangle parts to interlock. A latch, which can be released by the farmer/rancher pulling a cord while in tractor seat, secures the connection until the farmer/rancher decides to unhitch the implement.

Fig. 9.2 Example of triangle hitch

9.3 Objective

The main objective of this chapter is to enable the automatic hitching with the developed positioning method using reflector as artificial landmark.

9.4 Field Experiments for Hitching

Few trails were conducted to realize the coupling possibility with the existing system; single reflector positioning method and double reflector positioning method were implemented. The approximate position of the implement and the tractor on the grid has been illustrated in Fig. 9.3.
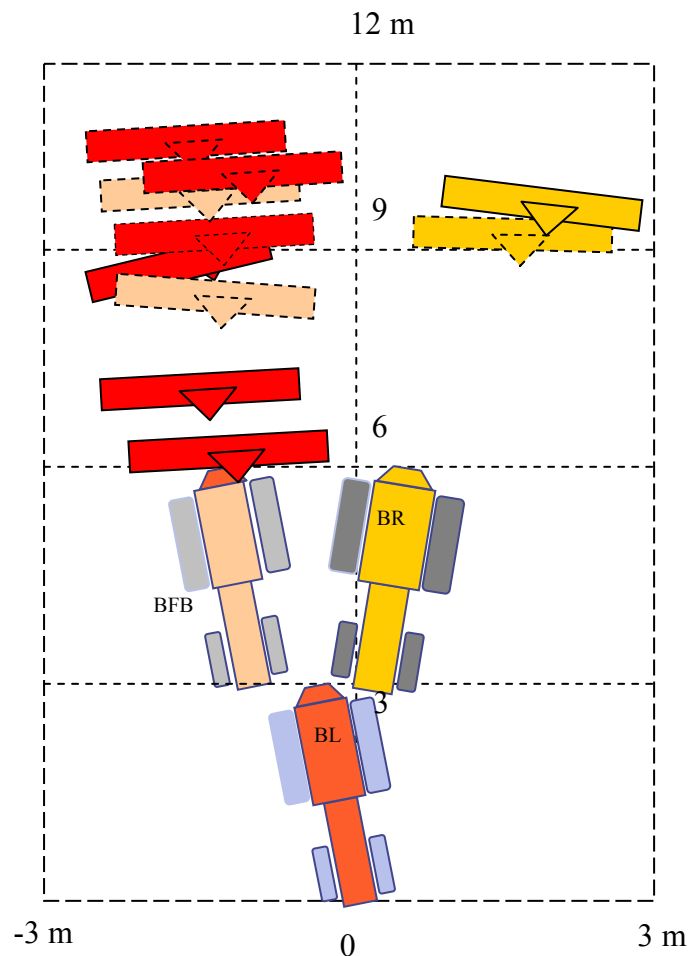
Fig. 9.3 Tractors and implement approximate position for hitching (BFB: Backward-Forward- Backward; BR: Backward Right; and BL: Backward Left. In the implements, solid line indicates success and dashed line indicates the failure in coupling)

9.5 Single Path Backward Approach for Hitching

9.5.1 Single Reflector Positioning
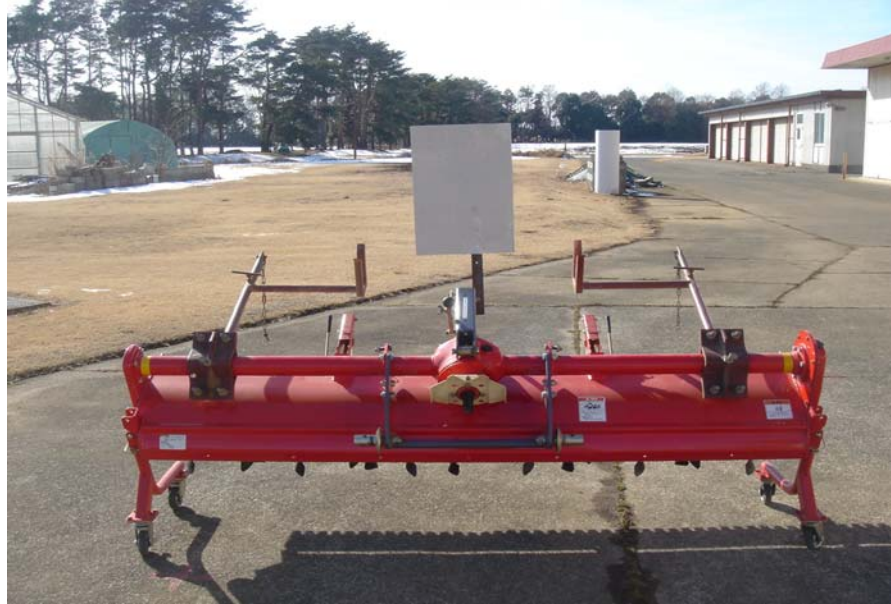
Fig. 9.4 Placement of the single reflector on the paddy harrow

Fig. 9.5 Placement of two reflectors on the paddy harrow

In the chapter 7 and 8, the positioning method, using reflector as artificial landmark was described in details. In the first reflector positioning, 35 cm x 50 cm reflector was placedon the paddy harrow as depicted in Fig. 9.4. The midpoint of the reflectors was along the centerline of the top link of the implement. Once the top link could couple by the quick coupler, which is attached with the tractor's lower links and top link, it is easy to grip the bottom link of the implement. The safe stopping distance was measured such way that the tractor could stop and raise the coupler so that top link of the coupler could grip the top link of the implement. The safe stopping distance was considered 1.54 m from the center of the rear wheel to the center of the reflector.

9.5.2 Two Reflectors Positioning

In the two reflectors positioning method, the reflectors of 22 cm x 85 cm were placed with 1 m interval on the paddy harrow. The placement-distance of two reflectors on the implement was selected by trail. It was noted that when the tractor is close to the implement then there is a possibility of loosing the reflectors due to the limitations of angular range of LRF. The reflectors were attached on the middle fixed by screw as shown in Fig. 9.5. Since the reflectors were placed 27 cm front from the position of the single reflector, thus the safe stopping distance was considered 1.27 m from the center of the rear wheel to the center of the reflector.

9.6 Sequential Paths Backward-Forward-Backward Approach for Hitching

First, the autonomous tractor approached the implement in the backward direction to the target position, and then travels forward direction 2 to 3 m and travel again backward direction to the top link position and hitches the implement. Figure 9.6 depicted the process of sequential forward-backward approach to the top link position of the implement.
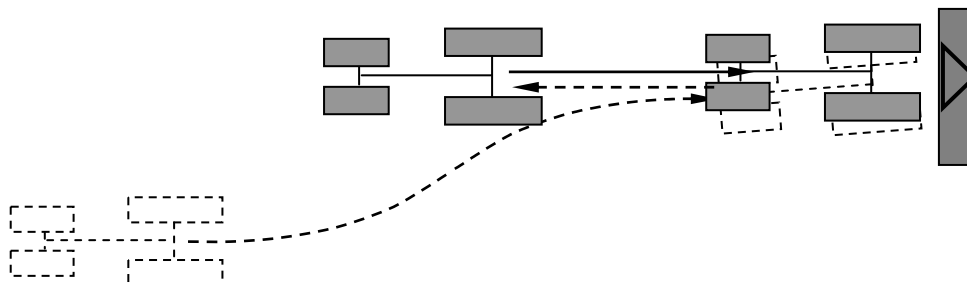
Fig. 9.6 Sequential traveling towards the implement top link position to couple the implement

Figure 9.7 shows the stages of automatic hitching of the implement using single reflector. In this case, the implement was placed on the left side of the tractor as shown in Fig. 9.3. In another trail shows in Fig. 9.8, the implement was placed on the right of the tractor, and enabled the automatic hitching using single reflector positioning method. In the Fig. 9.9, two reflectors were used to enable the automatic hitching of implement with the tractor. Figure 9.10 shows the stages of approach towards the implement for hitching. First the LRF was used for backward movement to the implement position, secondly, 2 m forward traveling was done by the dead reckoning sensor and finally backward traveling was conducted using LRF. Two reflectors positioning method was used to calculate the target position and navigate the tractor to the top link of the implement.

In the stages of automatic hitching with the implement, first, the LRF measured the relative distance between the vehicle and the implement using the reflector as landmark of the implement. Second, the current position of the tractor was taken as the origin of the coordinates ($x=0$, $y=0$, $\psi=0°$, $\delta=0°$) and final position (x_f, y_f) was set just before the implement. Third, the lower link of the quick coupler set at the lowest position automatically, and fourth a trajectory was generated that permitted the vehicle to travel from the start point to its final position. Finally, the lower link was raising and quick coupler came into action to couple the top link of the implement, and while raising the implement other bottom two link of the coupler was attached with the implement.

In the sequential traveling, the stages of approach was similar as like single path backward traveling; only the in forward traveling the dead reckoning sensor was employed. At the second backward traveling using LRF, the approach was done to hitch the implement with the tractor. In the field experiments, two trails have been conducted for sequential repeated movement as backward-forward-backward approaches. One was nearly hitched the top link but slipped in the process of hitching due to stop the tractor just 1 cm before the safe stopping distance. It was measurement error came from reflector setting on the top link of the paddy harrow. In another trail, controller had an error while the tractor was approaching from the longer distance. The first backward and forward movement was done, but at the second backward movement, the program was terminated with closing all the digital boards and tractor was stopped.

Fig. 9.7 Stages of automatic coupling with the implement using single reflector (Implement at left)

Fig. 9.8 Stages of automatic coupling with the implement using single reflectors (Implement at right)
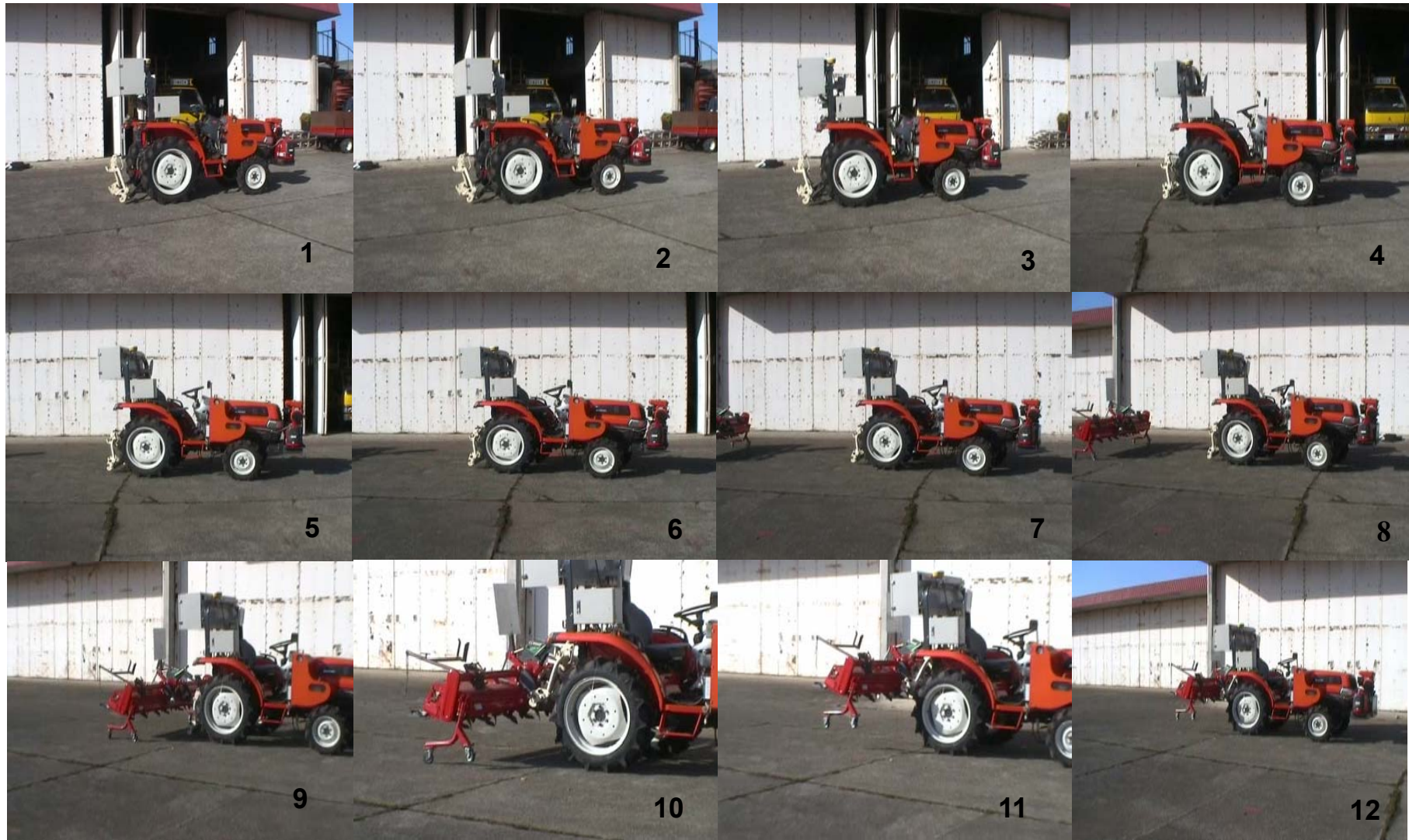
Fig. 9.9 Stages of automatic coupling with the implement using two reflectors (Implement at left)

Fig. 9.10 Stages of automatic coupling in the sequential traveling with the implement using two reflectors (Implement at right)

9.7 Results and Discussion

9.7.1 Results

The experiments were conducted on the concrete surface. In the experiments, 10 trails were done to enable to automatic hitching; out of the 10 trails, 4 trails were succeeded to enable the automatic hitching. In the single reflector positioning method, the trajectories of backward traveling is shown in Fig. 9.11 while the implement was at the right side (Fig. 9.3). The lateral error at the final point was less than 3 cm and the tractors was stopped just before the implement, and then raise the bottom link to couple the top link of the implement. The allowable range to hitch the implement is around 4 cm in laterally and 3 cm longitudinally. Figure 9.12 shows the comparison of actual and theoretical yaw angles during backward traveling for automatic coupling of the implement. At the final position, the average error was less than 2°.

Figure 9.13 shows the trajectories using single reflector positioning method for coupling the implement with the tractor while the implement was placed at the left side (Fig.9.3). In the backward movement, the response of the feedback controller was slow. The final lateral error was less than 2 cm. However, the actual trajectory obtained with the feedback control coincided with the theoretical trajectory. In the Fig. 9.14, the comparison of theoretical and actual yaw angles is shown and the directional error at the final position was less than 1°. It was observed the positioning method developed by the single reflector could able to navigate to the implement position both left side and right side, and the tractor could able to hitch the implement automatically.

Figure 9.15 shows the trajectories in the backward traveling for automatic coupling of the implement using two reflectors positioning method. In this trail, the implement was placed at the left of the tractor, and the final lateral error was less than 1.5 cm. The comparison of actual and theoretical yaw angle is shown in Fig. 9.16. The directional error at the final position was less than 0.5°. It was observed that some noise occurs during the traveling of vehicle. The possible noise source was calculation of midpoint orientation from the two reflectors, some times when there is strong wind, the vibration occurred in the reflectors, thus the exact calculation of midpoint was difficult.

The trajectory for the sequential traveling to backward-forward-backward approaches to hitch the implement is shown in Fig. 9.17. In this repeated approach, the automatic coupling was not succeeded due to noise from the autonomous system. There would be

required few trails to confirm the repeated accuracy while the orientation of the implement was worse. In each of the approach tractor initialized the position in local coordinates. Hence in the figure three sets of theoretical and actual trajectories are shown. It was observed that at the end of the traveling noises occurred due to miss of reflectors while the tractor was close to the implement. In the first trail of repeated experiment while the orientation of the implement was worse, the final lateral error was less than 6 cm in the first backward approach as depicted in the figure backward-1. The forward traveling was conducted by dead reckoning sensors, and 2 m observable range is given to move forward the autonomous tractor. At the forward movement, the lateral error at the midpoint was than 1 cm. Finally the second backward approach noted as backward-2 in the figure, was done by LRF and lateral error was less than 12 cm at the final position. The noises occurred from the controller and missed the location of reflectors while the tractor was very close to the implement.

Figure 9.18 shows the comparison of theoretical and actual yaw angle using two reflectors for backward-forward-backward approaches. In the first backward approach, the directional error was less than 3° at the final position and directional error was less than 1° at the midpoint for forward traveling of vehicle. At the second backward approaching to the implement, the directional error was less than 3°.
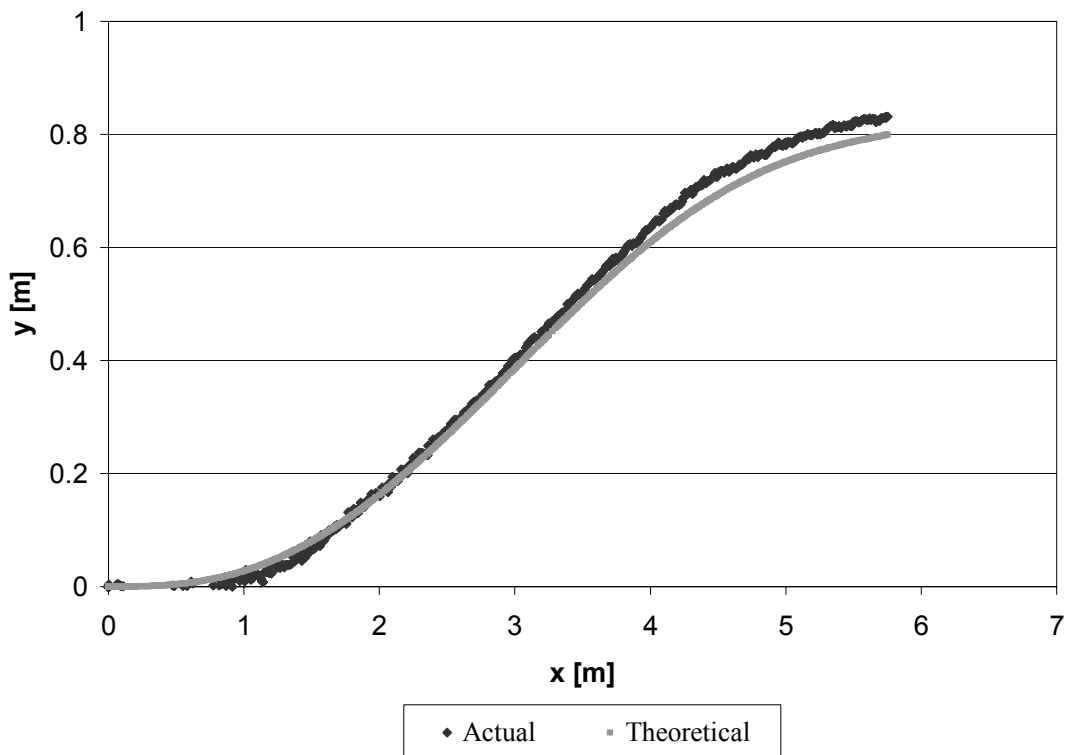
Fig. 9.11 Trajectories during backward traveling for hitching to the paddy harrow with single reflector positioning method (Implement at right)
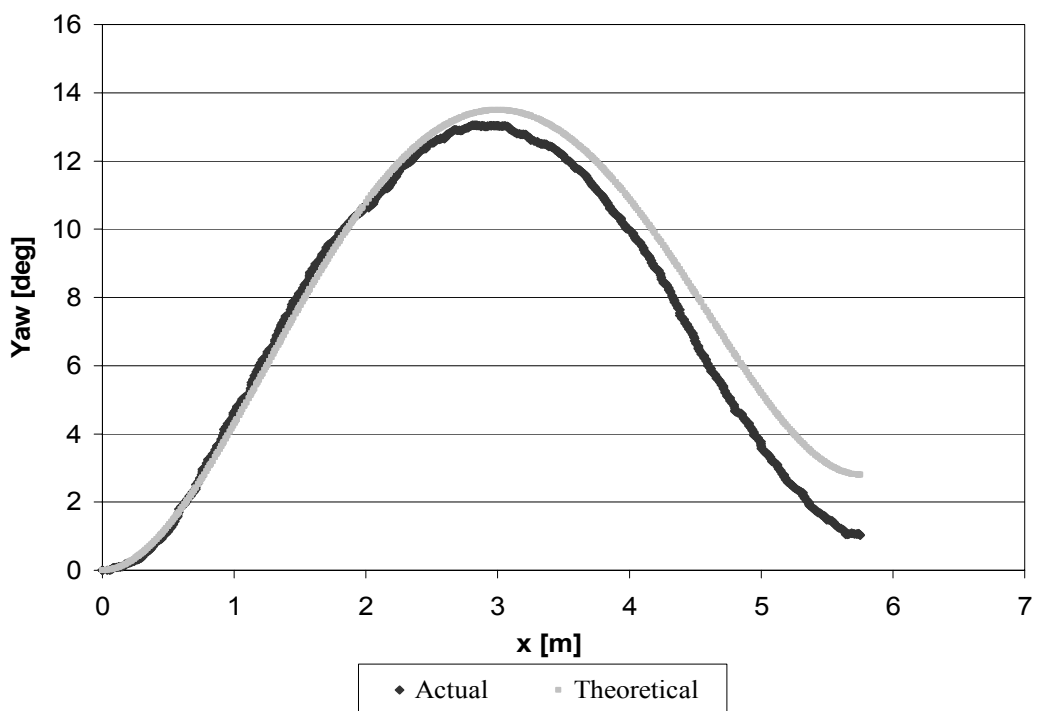
Fig. 9.12 Comparison of yaw angle during backward traveling for hitching to the paddy harrow with single reflector positioning method (Implement at right)
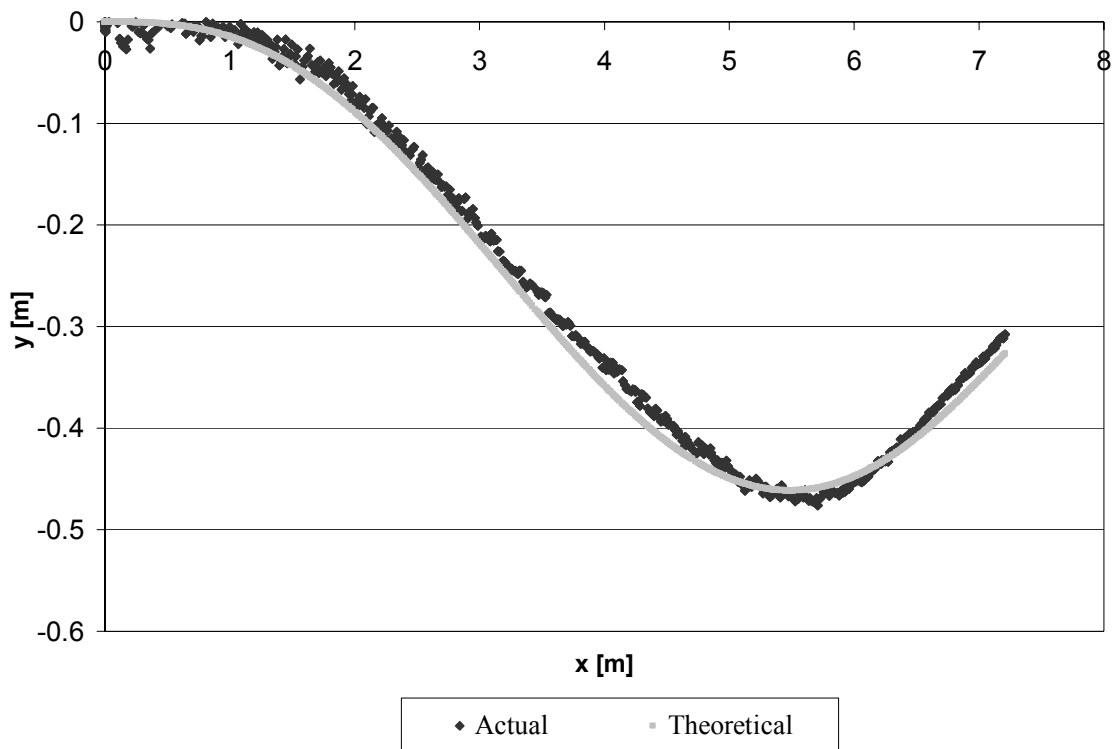
Fig. 9.13 Trajectories during backward traveling for hitching to the paddy harrow with single reflector positioning method (Implement at left)
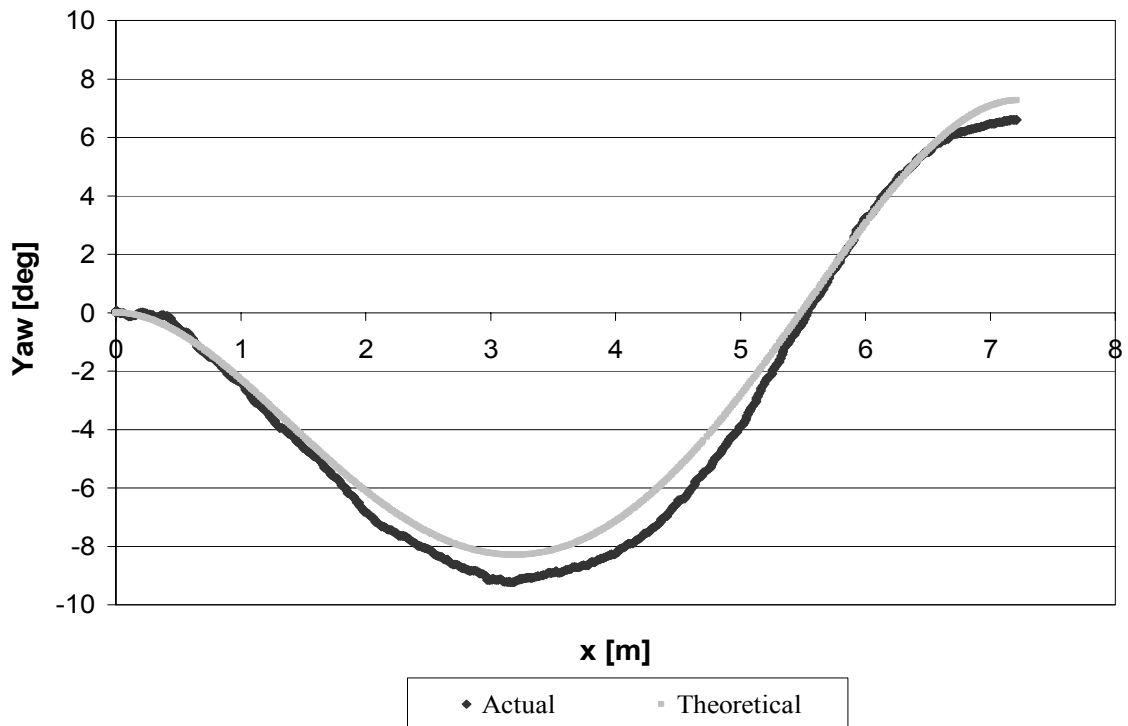
Fig. 9.14 Comparison of yaw angle during backward traveling for hitching to the paddy harrow with single reflector positioning method (Implement at left)

Fig. 9.15 Trajectories during backward traveling for hitching to the paddy harrow with two reflectors positioning method
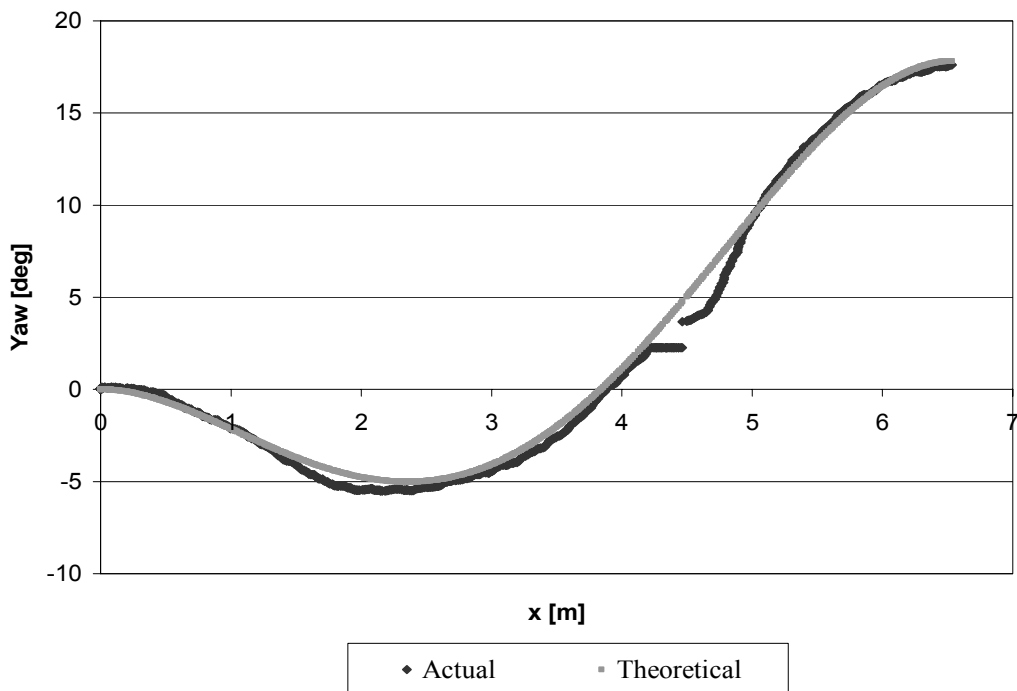
Fig. 9.16 Comparison of yaw angle during backward traveling for hitching to the paddy harrow with two reflectors positioning method
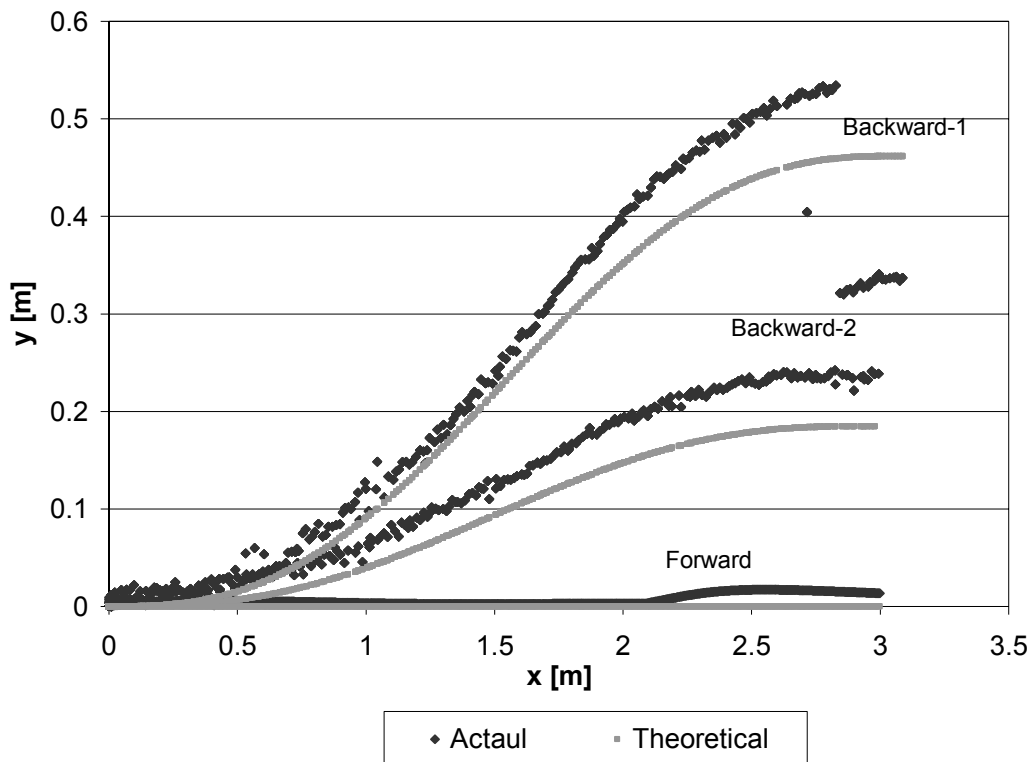
Fig. 9.17 Trajectories during backward-forward-backward traveling for hitching to the paddy harrow with two reflectors positioning method
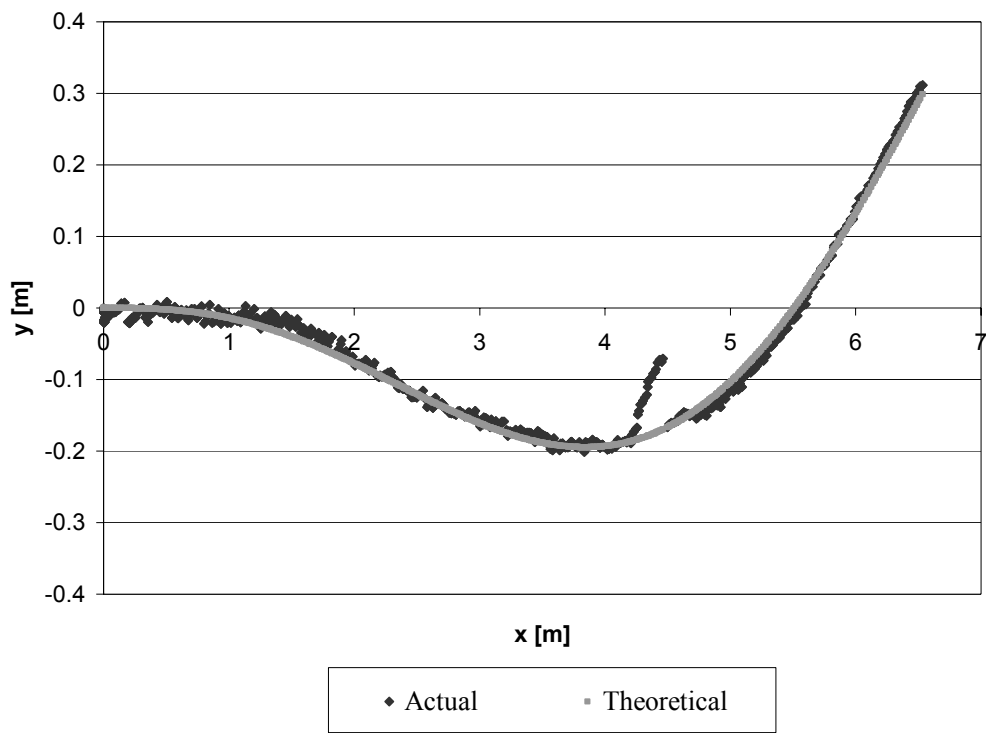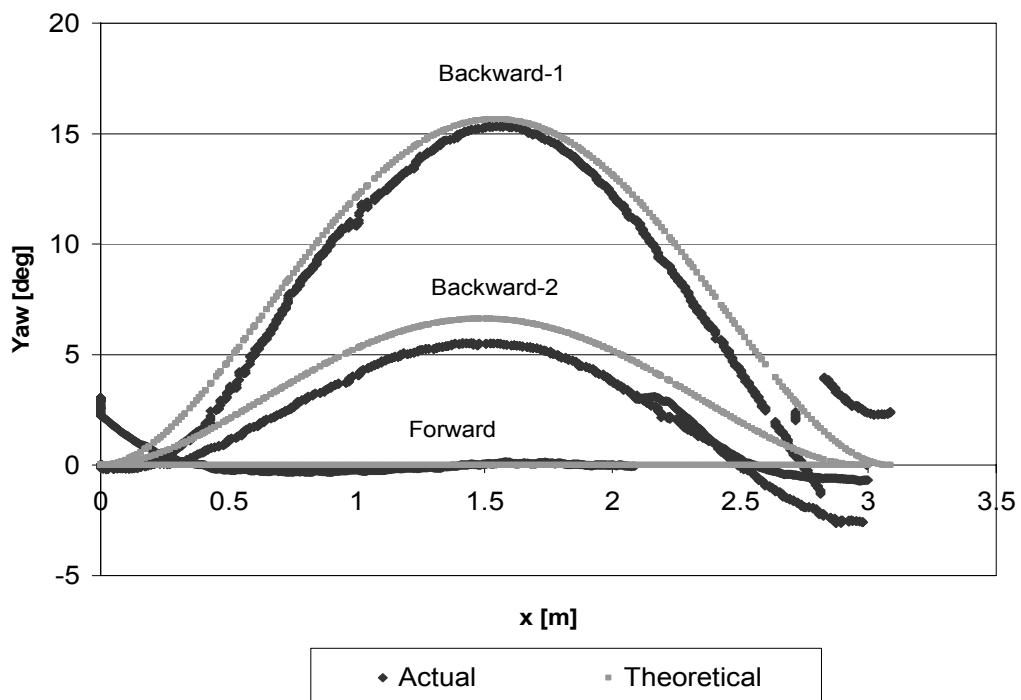

Fig. 9.18 Comparison of yaw angle during backward-forward-backward traveling for hitching to the paddy harrow with two reflectors positioning method

141

9.7.2 Discussion

In the single and two reflectors positioning methods, there is no significant difference in the navigational accuracy to hitch the implement. However, further experiments are required to come in conclusion for the number of reflectors is suitable at different orientations of implement. It was observed that two reflectors positioning has better orientation then the one reflector positioning for automatic hitching of the implement from the longer distance. On the other hand, there were noises at the end of the traveling course while the reflectors were out of the angular range. In two reflectors positioning method, within 1 m interval two reflectors were placed. When the tractor was very close to the implement, the reflectors were not visible by the LRF. Noises were occurred in these situations. In case of single reflector positioning, the reflector was always observable, even the vehicle was very close to the implement. The shortcoming of single reflector is the orientations, while the implement is very wide then it is difficult to maintain the exact orientations of the vehicle from the longer distance. In the repeated traveling to approach the implement for hitching needs to conduct several experiments. At the top link position, it was difficult to improve the accuracy from the longer distance. It was noted that the controller had the slow response in the feedback system in backward traveling.

To improve the performance of repeated traveling, additional experiment is under considerations. First consideration is the using of proximity sensor, such as ultrasonic sensor for traveling the vehicle to the closer distance between the implement and the tractor. In addition, modification of the quick coupler could enable the hitching of the implement with the tractor more easily. The quick coupler used in the experiment, had a narrow gap at the top link section, which was difficult to align exactly with the top link of the implement. With consideration of final positional error, A-frame type quick coupler may have more flexibility in automatic coupling. Some of the recent coupling method, there has two couplers, one with the implement, and other with the tractor. This type of arrangement has flexibly of coupling while a small lateral offset exists at the hitching position. Our further investigation will include more flexibility in repeated approach and A-frame type quick coupler will be used to compare the hitching performance with existing quick coupler.

9.8 Conclusions

The automatic hitching of implement with the tractor can ensure the safety during coupling of heavy implements. It is one of the most challenging works in the field of automation. To

accomplish this challenging automation, the automatic hitching of the implement was conducted, and successfully coupling was performed in some limited field conditions. Further experiments are required with the uses of proximity sensors and A-frame type quick coupler will be used to compare the hitching performance and flexibility in the allowable error range.

Chapter 10

Conclusions

This thesis attempts to address the uses of multiple sensors in the autonomous operation of agricultural vehicle. The autonomy of the autonomous vehicle is considered as the key subject of the present research. To reinforce the autonomy of the autonomous agricultural vehicle the contributions of this thesis is discussed briefly in the section 10.1. Section 10.2 suggests the areas of future work in this compelling field of research.

10.1 Summary of Contributions

The goal of our research projects is to complete the navigation process from yard to field and essential approaching requires for outfitting the implement with the tractor. To achieve this goal, the following sub sections reviewed the major contributions were performed in this thesis.

10.1.1 Robust Recognition of Landmark

The recognition of landmark is essential for approaching navigation. If the reflector can discriminate from the other objects of environment, it could function as reliable artificial landmark for robust relative positioning. The uses of the reflector bit in the LRF for coding received energy to evaluate the distance and compare this with an internal reference. The higher energy value or reflectivity indicates the reflectors from the surroundings. Least square algorithm was used to fit the line, circle and geometrical shape of the reflector to localize the position of the reflector on the x-y coordinate.

10.1.2 Development of Positioning Method for Landmark-based Navigation

The positioning method was developed with the combination of LRF and fiber optic gyroscope for the single run of autonomous tractor to approach the implement using discriminated landmark. The attempt was made to reduce the gyro to eliminate the cost involvement in autonomous operation. It was observed that in the traveling course of tractor, the vibration influenced the yaw angle, which was calculated from the geometrical relationship between LRF and the reflector.

10.1.3 Navigation of Tractor towards the Implement Position

The field experiments were carried out in which the autonomous tractor approached the implement on a concrete surface and a field covered with grasses. The results of the field experiments showed that the autonomous tractor could approach to the implement's

position within a final lateral error of 1 cm and directional error of 1˚, for the single reflector positioning method, both on the concrete surface and on the field covered with grasses. In the two-reflector positioning method, approaching the implement was done within a lateral error of 1 cm for the concrete surface and 2 cm for the field covered with grasses; the directional error was less than 1˚ for both surfaces. These results confirmed that positioning with reflectors as artificial landmarks for the LRF enabled navigation of the vehicle to the implement's position with high accuracy. The proposed positioning method could be used some frequently observable approaching, such as parking in the yard, loading and unloading of the container, fertilizer refilling.

10.1.4 Switching of Sensors and Coordinates in the Multiple Sensor-based Navigation

The switching of sensors is prerequisite to navigate an autonomous tractor in outdoor to indoor or vice versa, while one sensor is unable to localize the position of the tractor. In some of the cases, the reflector is out of the angular range of the LRF, the dead reckoning method was used until the reflector is observable in a certain distances, and afterwards LRF was used for approaching the implement with forward and backward movements of the autonomous tractor. In the navigation course, navigator paths are composed of multiple segments, and feasible segments either polar coordinates or Cartesian coordinates. While path design by Cartesian coordinates enabled such steering as parallel parking, polar coordinate-based design enabled movements attended with turns of greater than 90˚. It was confirmed by experiments that the autonomous tractor could switch the sensors and track multiple-segment paths. Experimental results during two-segment navigation (Cartesian to Cartesian) showed that the final lateral error was 2 cm and directional error was 1˚ at the goal position. Two-segment navigation (Polar to Cartesian) for parking a tractor in a yard showed a final lateral error of 1 cm and directional error of 1˚.

10.1.5 Automatic Coupling of Implement with the Autonomous Tractor

Automatic coupling is a challenging task in agricultural automation, and it could ensure the safety and reduce drudgery of farmers during the coupling with the farm implement. In prior to coupling, hitching maneuver requires high positioning accuracy at the top link position of the implement. Previous experiments confirmed the satisfactory accuracy at the implements position. The experiments were carried with a quick coupler in some limited conditions using single reflector and two reflectors positioning method. The automatic hitching was enabled successfully in both positioning methods. Further

experiment will be conducted using proximity sensors and the modification of the quick coupler with sequential repetition to approach the top link could enable the automatic coupling more easily with flexibility of errors within 3-4 cm at the hitch point.

10.2 Future Research

This section proposes several areas of this research requiring completion and extension to achieve the goal. Furthermore, the contributions of this thesis give scope to open the avenues of numerous applications in autonomous vehicle operation, which would be worthy for future research. Some of the promising directions are suggested below.

10.2.1 Automatic Coupling of Implements with A-frame coupler

The automatic coupling of the implement with the tractor using A-frame coupler will be conducted to compare the flexibility, performance, and sequential forward backward movements. Furthermore, proximity sensors can be implemented to detect the top link without any contact prior of coupling.

10.2.2 Application of VRS GPS for Road Navigation

The present single receiver GPS has not enough accuracy to enable the road navigation. The Virtual Reference System (VRS) GPS can be implemented to get the signal and corrections continuously through wireless-network. Switching of sensors among GPS, dead reckoning, and LRF will be conducted to enable the navigation from yard to field. In navigation course, the road navigation will be conducted using VRS-GPS, dead reckoning will be used for short traveling distance while GPS signal hinders by wall, roof, or trees, and LRF will be used for the essential approaching like coupling of farm implements, fertilizer refilling, loading and unloading of containers.

10.2.3 Sensor Data Fusion for Autonomous Navigation

The sensor data fusion is the promising way for the reliable navigation. The data fusion between odometry and GPS would be helpful while a sensor could not work properly, other sensor could be used for the positional information of vehicle. The extended Kalman filter will be used for data fusion among the multiple sensors.

Acknowledgements

To begin, I would like to express my profound gratitude and sincere appreciation to my academic advisor, Professor Masayuki KOIKE, for his availability, expertise and advice, motivation, and encouragement to move forward.

It is my great pleasure to express indebtedness, deepest sense of gratitude, sincere appreciation to my favorite teacher and research supervisor Associate Professor Dr. Tomohiro TAKIGAWA who introduced me to a most compelling research avenue. His kind advice, scholastic guidance, sympathetic supervision, and encouragement guided me to walk on this avenue.

I am pleased to express my cordial respect and gratitude to Professor Masayoshi SATOH and Professor Yukuo ABE, members of the advisory and thesis committee for their kind comments, advice, and suggestions during the course of this study.

I acknowledge my gratitude to the Embassy of Japan, Dhaka for selecting as a candidate for Monbukagakusho scholarship. Also thanks goes to the Ministry of Education, Culture, and Science, Japan for granting the scholarship that covered my study and stay in Japan. In this regard, gratitude is extended to Professor Seishi NINOMIYA, who introduced me with the Bioproduction and Machinery Lab, University of Tsukuba during the selection of University through the Embassy of Japan, Dhaka.

Special gratitude is expressed to Assistant Professor Akira Yoda and Dr. Hideo Hasegawa for their kind assistance and suggestions in both academic concern and daily life. In addition, special thanks should be expressed to staffs of Agricultural and Forestry Research Center, University of Tsukuba: Mr. Tsuyoshi Honma for fabricating experimental equipments, Mr. Yasuhiro Matsumoto and Mr. Akira Saitoh for their helps on maintaining the experimental vehicle.

Sincere gratitude and thanks to my seniors Dr. Zhang Qiang, Dr. Payungsak Junyusen for their great support during the course of study. Special thanks are extended to Mr. Kriengkrai Kaewtrakulpong, Mr. Wanrat Abdullakasim, Mr. Khone Sackbouwong, Ms. Porntipa Junkwon, Mr. Tatsuo Oshima, and Mr. Isizaki for their great camaraderie.

I thank my teachers and colleagues of the Department of Farm Power and Machinery and

faculty members of Agricultural Engineering and Technology, Bangladesh Agricultural University, for their cordial support during the study period.

Sincere expression of gratitude is due to my beloved parents whom I lost during my course of study in Japan. I remembered their moral support, unfailing patience and encouragement while I was away from home. I am thankful to my brothers and sister for their support and help.

Above all, all praises to acknowledge immeasurable grace and profound kindness of the Almighty Allah, the supreme ruler of the Universe to complete this research work.

References

ARNEX Navigation Systems AB, 1996. PDS, position determination system, description/specification. ARNEX Navigation Systems, Stora Badhusgatan 16, s-411 21 Goteborg, Sweden.

Astrand, B., Baerveldt, A.J., 1999. Robust recognition of plant rows, ICRAM'99. International Conference of Recent advance in Mechatronics.

Barshan, B., Durrant-Whyte, H.F., 1995. Inertial navigation system for mobile robots. IEEE Transactions on Robotics and Automation, 11(3), 328-342.

Bell, T., 2000. Automatic tractor guidance using carrier-phase differential GPS. Computers and Electronics in Agriculture, 25(2000):53-66.

Bell, T., 1999. Automatic tractor guidance using carrier-phase differential GPS. Computers and Electronics in Agriculture: Special Issue Navigating Agricultural Field Machinery.

Benson, E., Stombaugh, T., Noguchi N., Will, J., Reid., J.F., 1998. An evaluation of a geomagnetic direction sensor for vehicle guidance in precision agriculture applications. ASAE paper 983203. St.Joseph, MI.

Bloch, A., Reyhanoglu, M., McClamroch N.H., 1992. Control and stabilization of nonholonomic dynamic systems. IEEE Transactions on Automatic Control, 37(11):1746-1757.

Campion, G., d'Andre-Novel, B., Bastin, G., 1991. Controllability and state feedback stabilizability of non-holonomic mechanical systems, Advanced Robot Control, C. Canudas Wit, editor, LNCIS 162, Springer, pp. 106-124.

Dixon, J., Henlich, O., 1997. Mobile Robot Navigation, Imperial College, London Information Systems Engineering, http://www.doc.ic.ac.uk/~nd/surprise_97

/journal/vol4/jmd/

Drocout, C., Delahoche, L., Pegard, C., Cleretin, A., 1999. Mobile robot localization based on an omni directional stereoscopic vision perception system. Proceedings of the 1999 IEEE Conference on Robotics and Automation, Detroit, USA, 1329-1334.

Elfes, A., 1987. Sonar based real-world mapping navigation. IEEE Journal of Robotics Automation 3(3), 249-265.

Everett, H., R., 1995. Sensors for Mobile Robots: Theory and Applications. Natick mass: A.K. Peters, Ltd., New York, USA.

Farrel, J., A., Barth, M., 1999. The Global Positioning System and Inertial Navigation, Chapter 2. McGraw-Hill, NewYork.

Fehr, B.W., Gerrish, J.B., 1995. Vision-guided row crop follower. Appl. Eng. Agric.11 (4): 613-620.

Gerrish, J.B., Fehr, B.W., Van Ee, G.R., Welch, D.P., 1997. Self-steering tractor guided by computer-vision. Applied Engineering in Agriculture 13 (5):559–563.

Gerrish, J.B., Stockman, G.C., 1985. Image processing for path-finding in agricultural field operations. ASAE paper 85-3037, St. Joseph, MI.

Gerrish, J.B., Surbrook, T.C., 1984. Mobile robots in agriculture. In Proceedings of First International Conference on Robotics and Intelligent Machines in Agriculture. ASAE, St. Joseph, MI.pp.30-41.

Goel, P., Roumeliotis, S.I., Sukhatme, G.S., 1999. Robust localization using relative and absolute position estimates. In IEEE/RSJ International Conference on Intelligent Robots and Systems (IROS).

Graf, M., Jahns, G., 1996. Intelligent components for tractor/implement coupling, Ag.Eng. paper No. 96A-091.

Guivant, J., Nebot, E., Baiker, S., 2000. Autonomous navigation and map building using laser range sensor in outdoor applications. Journal of Robotic Systems, 17(10): 565-583.

Guo, L.S., Zhang, Q., 2005. Wireless data fusion for agricultural vehicle positioning, Biosystems Engineering, 91 (3): 261-269.

Hague, T., Marchant J.A., Tillet, N.D., 2000. Ground based sensing system for autonomous agricultural vehicles, Computer and Electronics in Agriculture, 25:11-28

Hata, S., Takai, M., Kobayasi, T., Sakai, K., 1993. Crop-row detection by color line sensor. International Proceedings of International Conference for Agricultural Machinery and Process Engineering, Seoul, Korea, Korean Society for Agricultural Machinery, 19–22.

Holmqvist, R. 1993. A laser optic navigation system for driverless vehicle. Arnex Navigation AB, ARNBL 344, p15.

ISO 11001-1:1993. Agricultural wheeled tractors and implements—Three point hitch couplers—Part 1: U-frame coupler.

ISO 11001-2:1993. Agricultural wheeled tractors and implements—Three point hitch couplers—Part 2: A-frame coupler.

ISO 11001-3:1993. Agricultural wheeled tractors and implements—Three point hitch couplers—Part 3: Link coupler.

ISO 730-1, 1994. Agricultural wheeled tractors -- Rear-mounted three-point linkage -- Part 1: Categories 1, 2, 3 and 4

ISO 8759-2:1985. Agricultural wheeled tractors—Front-mounted linkage and power take-off—Part 2: Front linkage.

Iida, M., Umeda, M., Suguri, M., 1998. Automated follow-up vehicle system for agriculture, ASAE Paper 983112, 1–9.

Inahata, T., Takigawa, T., Koike, M., Konaka, T., Yoda, A., 1999. Positioning method for agricultural vehicles with simple laser sensor, Journal of the Japanese Society of Agricultural Machinery (Part 1) 61(2):71-79.

Inoue, K., Otsuka, K., Sugimoto, M., Murakami, N., 1997. Estimation of place of tractor and adaptive control method of autonomous tractor using INS and GPS. In: Juste, F., Andrew, G., Valiente, J.,M., Benlloch, J.,V., (Eds.), Proc. of BIO-ROBOTICS 97, Gandia, Valencia, EurAgEng and IFAC, 27–32.

Ishida, M., 1998. Autonomous tractor forage production, Journal of the Japanese Society of Agricultural Machinery (in Japanese) 60(2):59-66

Jensfelt, P., Christensen, H., 1999. Laser based pose tracking. Proceedings of IEEE Conference on Robotics and Automation, Detroit, USA, 2994-2998.

Junyusen, P., Takigawa, T., Koike, M., Hasegawa, H., Bahalayodhin, B., 2005. Trajectory control for a trailer towed by an agricultural vehicle (Part 2). Journal of the Japanese Society of Agricultural Machinery, 67(2):70-76.

Keicher, R, Seufert, H., 2000. Automatic guidance for agricultural vehicles in Europe, Computer and Electronics in Agriculture, 25:169-194.

Kolmanovsky, I., McClamroch, N.H., 1995. Developments in nonholonomic control problems. IEEE Control Systems, December, 20-35.

Lang, T., Harms, H.H., 2002. A new concept for the three-point-hitch as a mechatronic system. Proceeding of conference on Automation Technology for Off-Road Equipment, Chicago, USA, pp. 246-251.

Luca, A.D., Orio lo, G., Samson, C., 1998. Feedback control of a nonholonomic car-like robot, in J. P. Laumond (Ed), Robot Motion Planning and Control, pp. 170-250, Springer, 1998.

Nagasaka, Y., Otani, R., Shigeta, K., Taniwaki, K., 1998. Autonomous vehicle guidance system in paddy field. In: AgEng Oslo, EurAgEng, 1–6.

Noguchi, N., Reid, J.F., Will, J., Benson, E., Stombaugh, T., 1998. Vehicle automation system based on multi-sensor integration, ASAE paper 983111, St. Joseph, Michigan, USA.

Nonami, K., Komatsu, M., Higuchi, H., Nakano, S., Adachi, K., 1993. Studies on automatic traveling control of riding-type rice transplanter (Part 1). Journal of The Japanese Society of Agricultural Machinery, 55 (4), 107–114 (in Japanese).

Ohno, K., Tsubouchi, T., Shigematsu, B., Maeyama, S., Yuta, S., 2002. Campus outdoor navigation of an autonomous mobile robot-RTK GPS trail and path map construction, Proceedings of the 7th Robotics Symposia, Japan, 3a31 (In Japanese).

Ollis, M., Stentz, A., 1996. First results in vision-based crop line tracking. Proceedings of the IEEE Robotics and Automation Conference, Minneapolis, MN, pp.951 –956.

Ollis, M., Stentz, A., 1997.Vision-based perception for an automated harvester. IEEE International Conference on Intelligent Robots and Systems. Vol. 3, IEEE, Piscataway, NJ, pp.1838 –1844.

O′Connor, M., Bell, T., Elkaim G., Parkinson B., 1996. Automatic steering of farm vehicles using GPS. Paper presented at the 3rd International Conference on Precision Agriculture, Minneapolis, MN, June 23–26.

O′Connor, M., Elkaim, G., Parkinson, B., 1995. Kinematic GPS for closed-loop control of farm and construction vehicles. ION GPS-95. Palm Springs, CA, September pp.12 –15.

Pinto, F., Reid. J.F., 1998. Heading angle and offset determination using principal component analysis. ASAE Paper 983113. ASAE, St.Joseph, MI.

Reid, J.F., Zhang, Q., Noguchi, N., Dickson, M., 2000. Agricultural automatic guidance research in North America. Computer and Electronics in Agriculture, 25(2000):155-167.

Reid, J.F., 1987. The development of computer vision algorithms for agricultural vehicle guidance. Unpublished Ph.D Thesis, Texas A&M University.

Reid, J.F., Searcy, S.W., 1986. Detecting crop rows using the Hough Transform. ASAE paper 86–3042, St. Joseph, MI.

Sasaki Y. 2002. Mechanization of Japanese agriculture and robotization. Special Issue: Development of agricultural robots, Farming Japan, 36(2):10-12.

Schultz, W., 1193. Traffic and vehicle control using microwave sensors, Sensors, October, 1993, 34-42.

Shmulevich, I., Zelter, G., Brunfeld, A., 1989. Laser scanning method for guidance of field machinery. Transactions of ASAE 32(2):425-430.

Stombaugh, T., Bensen E., Hummel, J.W., 1998. Automatic guidance of agricultural vehicles at high field speeds. ASAE paper 983110. St. Joseph. MI.

Sukkarieh S., Nebot E., Durrant-Whyte H., 1999. A high integrity IMU/GPS navigation loop for autonomous land vehicle applications. IEEE Transactions on Robotics and Automation, 572-578.

Sutiarso, L., Takigawa, T., Koike, M., Hasegawa, H., 2000. Trajectory control for agricultural autonomous vehicles: Part 3. A field experiment of the designed trajectory control. Journal of the Japanese Society of Agricultural Machinery, 62(6): 125-135.

Sutiarso, L., Kurosaki, H., Takigawa, T., Koike, M., Yukumoto, O., Hasegawa, H., 2002. Trajectory control and its application to approach a target: Part II. Target Approach Experiments. Transactions of ASAE, 45(4):1199-1205

Søgaard, H.T., Olsen, H.J., 1999. Crop row detection for cereal grain. In: Stafford, J.V.(Ed), Precision Agriculture '99. Sheffield Academic Press, pp 181-190.

Søgaard, H., T., 1999. Evaluation of the accuracy of a laser optic positional determination. Journal of Agricultural Engineering and Research, 74(3):275-280.

Takigawa, T., Sutiarso, L., Koike, M., Kurosaki, H., Hasegawa, H., 2002. Trajectory control and its application to approach a target: Part I. Development of Trajectory control algorithms for an autonomous vehicle. Transactions on ASAE, 45(4): 1191-1197.

Torii, T., Kanuma, T., Okamoto, T., Kitani, O., 1996. Image analysis of crop row for agricultural mobile robot. Proceedings of AGENG96, Madrid, Spain, EurAgEng, 1045–1046.

Umbach, D., Jones, K.N., 2000. A few methods for fitting circles to data. IEEE Transactions on Instrumentations and Measurement XX(Y):1-5.

Van Zuydam R., 1999. A drivers steering aid for an agricultural implement based on an electronic map and real time kinematic DGPS. Computer and Electronics in Agriculture, 24:153-163.

Will, J., Stombaugh, T., Benson, E., Noguchi, N., Reid, J.F., 1998. Development of a flexible platform for agricultural automatic guidance research. ASAE paper 983202. St. Joseph, MI.

Woodburry, N., Brubacher, M., Woodbury, J.R., 1993. Noninvasive tank gigging with frequency-modulated laser ranging, Sensors, September, 27-31.

Yoshida, J., 1996. A study on the automatic farm machine system for rice. Crop Engineering System Laboratory, Inc., Sakai, p. 148.

Yukumoto, O., Matsuo, Y., Noguchi, N., 1995. Research on autonomous land vehicle for agriculture. Proceedings of ARBIP95, vol. 1, 3–6 November 1996, Kobe University, Kobe, pp. 41–48.

Yukumoto, O., Matsuo, Y., Noguchi, N., 1997. Navigation technology for tilling robots. Robotisation of agricultural vehicles and the outline of navigation system for tilling robot. Proc. International Symposium on Mobile Agricultural Bus-System Lab and PA for the Large Scale Farm Mechanization, 18 September, Sapporo, Japanese Society of Agricultural Machinery, Omiya, pp. 59–78.

Appendix

-- **Navigator Class**---

class Tractor: virtual public Control, virtual public Handling

```
{
    private:

    public:
        int count;
        double XToGo[10], YToGo[10], OrientToGo[10];                /* PathPlaning*/
        int CMode[10], RunDir[10];
        int NumPoints, CurrentTarget;
        double Global_x, Global_y, Global_yaw;                      /* Global */
        double Local_xo, Local_yo, Local_yawo;
        double Global_x1, Global_y1, Global_yaw1;
        Tractor();
        PParaType P[2];
        CParaType C[2];
        void LocalToGlobalCoord(int);
        void GlobalToLocalCoord(int);
        void SetTarget(int,    int);
        void Pathplanning(int);
        void TheorecticalCal(int);
        void FeedbackCal(int);
        void display(int );
        void AutoControl(void);
        void EndAutoControl(void);
        void CounterConf(void);
        void SteeringCalibrate(void);
        void EncCalibrate(void);
        void yawcalibrate(void);
        void Test(void);
};
```

-- **Control Class of the Navigator**------------------------------------

class Control: virtual public Hardware,   virtual public Gyro,   virtual public Laser,   virtual public GPS

```
{
```

```cpp
    private:
        long tyreL, tyreR, th1Count;
        long tyreLbuff, tyreRbuff;
        double th1Buff, yawBuff;
        double PreviousTime, PreviousX, PreviousY;
        double MeasYaw;
    public:
        double Dead_xr, Dead_yr, Gyro_yaw;
        double Laser_xr, Laser_yr, Laser_yaw, Ls, Lo;
        double Laser_xm, Laser_ym, Laser_eta, Laser_neu;
        double Laser_xmBuff, Laser_ymBuff, Laser_etaBuff, Laser_neuBuff, ThetaInBuff,
        L_yawBuff;
        double xo, yo, yawo;
        double xo_l,   yo_l;
        double theta1, theta2, xr, yr, xh, yh, xt, yt;
        double D_xr, D_yr, D_xh, D_yh, D_xt, D_yt;
        long SAngle;
        double SCal, SMeas, SSpeed, SVolt, SCal1;
        double TimeSpent, TimeNow, TimeTotal;
        double vr, vt;
        double l, lh, lt;
        double yaw, alpha, lsyaw;
        Control();
        void BufferInitialize(void);
        void DeadReckoning(int DIR);
        void LaserPositioning(int DIR);
        void GyroLaserGpsBuff(void);
        void SpeedCalc(void);
        void ResetSpeedCalc(void);
        void CounterCheck(void);
        void Gear(int);
        void Direction(int);
        void Stop();
        void SteeringSet();
        void SteeringRead(void);
        void Steering(int);
};
```

---Hardware Class ---

class Hardware{

  protected:

    HANDLE hDioDev1;   Handle for Dio board 2503 IO control

    HANDLE hDioDev2;   Handle for Dio board 2424 IO control

    HANDLE hEncHandle1;   Handle for Encoder Counter IO control

    HANDLE hTimerHandle;   Handle for Timer board IO control

    HANDLE hAD;   Handle for ADC board IO   control

    HANDLE hDA1;   Handle for DIO board IO control

    unsigned char Dio0, Dio1, Dio2, Dio3;   4 bytes for DIO control

    int nRet, errorFlag;

    DWORD dwValue, dwData;

    ADSMPLCHREQ pSmplChReq[1];   For ADC sampling

    DASMPLCHREQ pdSmplChReq[1];   For DAC output

    int pData[1], pdData[1];

  public:

    Hardware(void);

    int BoardOpen(void);

    void BoardClose(void);

    void TimerClear(void);

    unsigned long TimerRead(void);

    void CounterInitialize(int channel,   int zphase);

    long CounterRead(int channel);

    void CounterSet(int channel);

    void CounterInitializeH(int channel);

    long CounterReadH(int channel);

    void CounterSetH(int channel);

    void DA_setH(int channel,   double volt);

    double ADCRead(int channel);

    void DACWrite(double volt,   int channel);

    long ADCDIRead(void);

    void DioOutput0(unsigned char command);

    void DioOutput1(unsigned char command);

    void DioOutput2(unsigned char command);

    void DioOutput3(unsigned char command);

    void InitDio(void);

    void Neutral(void);

```cpp
        void Forward(void);
        void Reverse(void);
        double SAngleRead(void);
        void SteerEnable(void);
        void SteerDisable(void);
        BYTE Switch(void);
        void Brake(int command);
        void ShiftSelection(int shift);
        void LinkPositionSelection(int pos);
};
```

------------------------------------Gyro Class for the Sensory data -----------------------------------

```cpp
class Gyro: virtual public SerialCom
{
    protected:
            int GyroComPort;
    public:
            double roll, pitch, G_yaw;
            Gyro();
            bool GyroCloseComPort(void);
            bool GyroOpenComPort(void);
            void GyroComSet(void);
            bool GyroRead();
            bool GyroBufferClear(void);
};
```

---------------------------------------LRF Class for the Sensory data ------------------------------------

```cpp
class Laser:virtual public SerialCom
{
    protected:
        unsigned int j;
        long num;
        int LaserComPort;
        int LaserCommandMode;
    public:
        int LaserComSpeed;              /* 0: 9600,   1: 19200,   2: 38400*/
        int LaserMeasureUnit;           /* 1: cm    10: mm*/
```

```cpp
    int LaserScanInterval;                    /* 1.0 0.5 0.25 => 100   50   25 */
    int NoOfData;
    int LaserScanNumber;
    double distance[410];
    double scan_theta[410];
    double m[410], n[410];
    int refbits[410];
    int NoOfRef;

    Laser();
    bool LaserCloseComPort(void);
    bool LaserOpenComPort(int);
    void LaserComSpeedSet(int);
    void LaserWait(int);
    bool LaserInstMode(void);                                /* Mode Setting
    bool LaserConfiguration(int);
    bool LaserChangeScanMode(int);
    bool LaserReadStart(void);                               /* Measurement
    void LaserReadRefOnce(void);
    void LaserReadStop(void);
    bool    LaserRead(int);
    unsigned int CreateCRC(unsigned char*,   unsigned int);        /* Utility
    bool LaserRespCheck(int ,    unsigned char* );
    bool LaserBufferClear(void);
    void SwitchToRefMeasMode(void);
    void MeasurmentStart(void);
    int MeasurePosture(int);
    void LaserReset(void);
    bool ReflectOnly;
    int RefNo;
    double xm[5], ym[5];
    double xmm, ymm, RefOrM, RefIncM;
    double lm3, lm1, lmeta1, lmm;
    double RefOri[5], RefInc[5], RefLength[5];              /* Only the reflector is treated
    double L_yaw,    ThetaIn;
};
```

```cpp
class GPS:virtual public SerialCom
{
    private:
        int errorFlag;
        bool GPSOpenComPort(void);                    // Basic functions
        void GPSComSet(void);
        Vector blh2ecef(double, double, double);
        Vector ecef2enu(Vector,    Vector);
        Vector ecef2blh(Vector ec);
    public:
        GPS(void);
        bool GPSBufferClear(void);
        bool GPSCloseComPort(void);
        int GPSComPort;
        int GPSRead(void);
        double UTC, Latitude, Longitude;              /* GGA * /
        char    dirLat, dirLon;
        int    QualityInd, NumSV, datum;
        double HDOP, AHeight, Geosep, AgeGPS;
        double HDOP2, PDOP, VDOP;
        char    meter1, meter2;
        char StID[10];
        int SatelliteNo[20];                          /* GSA */
        int NoOfSat;
        bool AutoMode;
        int DimMode;                                  /* VTG */
        double MDirTrue, MDirMag, SpeedKnot, SpeedKm;
        /* Functions for conversion from measured Longitude and Latiude to XYZ coodinates */
        /* Converted */
         double PositionX, PositionY, PositionZ;
         double    Lat_theta, Lon_gamma;
         void CalcEcef(void);
         void CalcXY(void);
};
```

-------------------------------------Serial Class to get the Sensory data ----------------------------------

class SerialCom

{

    protected:

      /* Buffer for serial communication */

      unsigned char szRead[4096], buff[4096], szRead1[4096], buff1[4096];

public:

    ComSetting Comconfig[NumberofPort];

    SerialCom(void);

    void sleep(long T);

    void ComconfigInt(void);

    bool InitDCB(int PortNumber);

    bool InitCommTimeOuts(int PortNUmber);

    bool SerialOpenPort(int PortNumber);

    bool SerialClosePort(int PortNumber);

    DWORD SerialWriteStrings(int PortNumber, int NumberOfBytes, char *szWrite);

    DWORD SerialReadStrings(int PortNumber, char *ReadBuff);

    bool SerialClearBuffer(int PortNumber);

    bool ComChangeConfig(int PotNumber);

};